

N00014-90-J1913

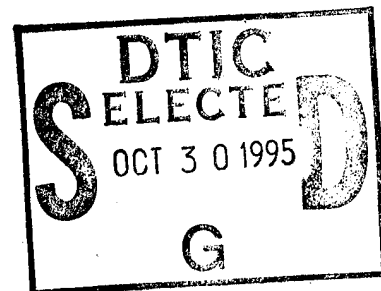
Final Report

**STUDY OF BRIGHTNESS AND CURRENT LIMITATIONS IN INTENSE  
CHARGED PARTICLE BEAMS**

For the period  
July 1, 1993 – December 31, 1994

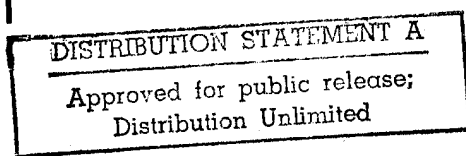
Submitted to  
Office of Naval Research

Submitted by  
Electrical Engineering Department  
and Institute for Plasma Research  
University of Maryland  
College Park, MD 20742



Principal Investigators  
M. Reiser and S. Guharay

19951027 001



**19951027 001**

**Office of Naval Research  
Arlington, Virginia**

**Per Anne Watson, she has no way of getting the  
missing pages. The reports that are sent to us is  
all that she has. When she get the pages they will  
be sent to DTIC with distribution.**

**February 27, 1996**

**DSN: 226-4108  
(703) 696-4108**

# **STUDY OF BRIGHTNESS AND CURRENT LIMITATIONS IN INTENSE CHARGED PARTICLE BEAMS**

M. Reiser and S. K. Guharay  
University of Maryland, College Park, Md. 20742

## **INDIVIDUAL RESEARCH ABSTRACT**

Our research on intense, high-brightness charged particle beams encompassed efficient generation and transport of  $H^-$  beams. The work was directed towards the development of neutral particle beams for space defense applications. Other important relevance of this work has been in the context of developing low-emittance injectors for future high-luminosity colliders. In both the cases, the present state-of-the-art of beam qualities is far from the desired level. Over the past several years, we made detailed theoretical work, both analytical and computational, on the problem of emittance growth. A 30 mA, 35 kV  $H^-$  beam was considered with the aim of transporting this highly diverging beam from an ion source over a distance of about 30 cm and transforming it into a converging beam which would match with the acceptance ellipse parameters of a high-frequency radio-frequency quadrupole accelerator (RFQ). We studied the beam dynamics in detail using simulation codes, and then designed a low-energy beam transport (LEBT) device. We included the practical constraints as much as possible in our theoretical studies; this led us to expect good performance of the LEBT. The LEBT has been built in-house.

Our work until mid January 1994 was earlier reported to ONR in the renewal proposal of this contract (No. N00014-90-J-1913) which was submitted to ONR in January 1994; the sections covering the progress report have been included in Appendix A.

During the period of mid January 1994 to December 1994 we focussed on the operation of the magnetron-type H<sup>+</sup> source; the major components of the source were earlier received from the Superconducting Super Collider Laboratory (SSCL). After a good deal of investigation of the control parameters we decided to implement some major modifications in the source for long, reliable operation. The technological "know-how" for source operation has been developed.

We are now fully equipped to run in-house experiments using the magnetron ion source facility and the LEBT system. Unfortunately, as this contract had been terminated, we are forced to leave a very important work incomplete at its final stage.

Accesion For	
NTIS	CRA&I <input checked="" type="checkbox"/>
DTIC	TAB <input type="checkbox"/>
Unannounced <input type="checkbox"/>	
Justification _____	
By _____	
Distribution / _____	
Availability Codes	
Dist	Avail and / or Special
A-1	

# STUDY OF BRIGHTNESS AND CURRENT LIMITATIONS IN INTENSE CHARGED PARTICLE BEAMS

M. Reiser and S. K. Guharay

University of Maryland, College Park, Md. 20742

## RESEARCH OBJECTIVES:

With the goal to meet the requirements of the neutral particle beam program for space defense we worked on understanding and improving the current state-of-the-art of transport and focusing of intense, high-brightness  $H^-$  beams. The main task here has been to develop an efficient low-energy beam transport (LEBT) system and satisfy a very stringent emittance budget.

We made a critical analysis of the existing schemes for beam transport and focusing. Despite significant amount of research in the past, no experimental evidence of an efficient LEBT system for high-perveance beams exists today. A generalized beam perveance of  $K = 0.003$  is considered here;  $K = 2I/I_0 \beta^3 \gamma^3$ , where  $I$  is the beam current,  $I_0$  is the characteristic current and it is 31 MA for  $H^-$  ions,  $\beta$  and  $\gamma$  are the usual relativistic notations for beam velocity and mass correction factor, respectively. Based on detailed simulation of beam dynamics we designed a 30 cm-long LEBT system consisting of six electrostatic quadrupole lenses (ESQ) and a short einzel lens. The ESQ LEBT has been constructed in-house. The main objective of our work was to perform beam transport experiments with our ESQ LEBT and compare the experimental results with simulation predictions. A cross check between experiments and simulations will shed a very important light to the present state-of-the-art.

We developed an  $H^-$  test stand facility to support the experimental work in-house.

**STUDY OF BRIGHTNESS AND CURRENT LIMITATIONS IN INTENSE CHARGED  
PARTICLE BEAMS**

M. Reiser and S. K. Guharay

University of Maryland, College Park, Md. 20742

**PROGRESS REPORT**

The progress report of our work until mid January, 1994 was submitted to ONR in the last renewal proposal; the relevant sections are included in Appendix A.

During the period of mid January to December 31, 1994 our research effort in experiments was mainly focused to the following items:

- (a) Study of  $H^-$  beams from the magnetron ion source on our in-house test stand;
- (b) Optimization of control parameters for the source operation;
- (c) Development of diagnostics.

In regard to the theoretical work, a significant progress was made towards improvement of the linear beam optics code, which solves the K-V envelope equations, for a computer-aided optimization scheme.

Our major accomplishments in experiments and theory are described below.

## A. Experiments with H<sup>-</sup> Magnetron Ion Source at Maryland

The H<sup>-</sup> ion source on our in-house test stand has been operational. A good deal of effort was made to obtain a stable discharge in the magnetron-type ion source, to run the source reliably for a long time, and to extract H<sup>-</sup> beams without any significant arcing across the extraction gap. The key elements for achieving a satisfactory operation of this surface plasma source were found to be: (a) control of cesium feed, (b) control of gas dynamics, (c) choice of the operating point on the arc current vs. arc voltage characteristics, and (d) surface conditions of the electrodes. Due to complex surface processes involved in the generation of the H<sup>-</sup> beams from surface plasma sources, the optimum operating conditions for one source can be widely different from another one if the two sources are not identical in all respects. Experiments were carried out with our ion source over a wide range of values of the control parameters to determine the optimum condition for operation of our source and also for efficient extraction of H<sup>-</sup> beams. In order to diagnose the H<sup>-</sup> beam we implemented several diagnostics, namely, toroid, Faraday cup, and phosphor screen.

Typical discharge characteristics for different operating conditions of our magnetron source are shown in Figs. 1 and 2. We noted that the best operating conditions corresponded to: cesium boiler temperature of about 115 C, hydrogen gas pressure of  $2 - 3 \times 10^{-6}$  Torr (average pressure), arc voltage of about 130 V, and arc current of about 25 A. Typical pulse shapes of the arc voltage and extracted H<sup>-</sup> current are shown in Figs. 3 and 4.

We have so far established a reliable operation for an H<sup>-</sup> beam current of about 18 mA at extraction voltage of 25 kV; the perveance of this beam is almost same as 30

mA, 35 kV beam which correspond to the input beam parameters for the LEBT design.

## **B. Theoretical Work**

A computer-aided optimization method for designing the LEBT system has been developed. In its present form, a numerical code searches for the optimal combination of a set of lens parameters when the trajectory through the entire lens system remains very close to a predetermined trajectory. The predetermined trajectory is generally chosen on the basis of minimization of some parameters which control the emittance growth. Some preliminary numerical results are shown in Figs. 5 - 7. Figures 5 and 6 are for magnetic solenoids; figure 7 corresponds to electrostatic quads. Input beam corresponded to generalized perveance of 0.01 and effective emittance of  $10^{-4}$  m rad. The optimal focusing function in each case is determined automatically through the numerical scheme which implements the aforementioned minimization principle.

**Figure Captions:**

Fig. 1 Extracted  $H^-$  current vs. arc current for various extraction voltages in the magnetron source.

Fig. 2 Extracted  $H^-$  current vs. extraction voltage for various arc voltages in the magnetron source.

Fig. 3 Pulse shapes for: extracted  $H^-$  current (top), and arc current (bottom). Horizontal scale: 10  $\mu$ s/div. Vertical scale: 5 mA/div (top), 10 A/div (bottom).

Fig. 4 Pulse shapes for: extracted  $H^-$  current (top), and arc current (bottom). Horizontal scale: 10  $\mu$ s/div. Vertical scale: 5 mA/div (top), 10 A/div (bottom).

Fig. 5 Optimal trajectory (thick line) for a magnetic solenoid lens system for  $R_i = 1$  cm and  $R_i' = 20$  mrad and  $R_f = 1$  cm,  $R_f' = -20$  mrad. The hard-edge focusing functions for the lenses are shown by dashed lines.

Fig. 6 Optimal trajectory (thick line) for a magnetic solenoid lens system for  $R_i = 2$  cm,  $R_i' = 0$  mrad and  $R_f = 1$  cm,  $R_f' = -20$  mrad. The hard-edge focusing functions for the lenses are shown by dashed lines.

Fig. 7 Optimal trajectory (thick line) for an ESQ lens system for  $R_i = 2$  cm and  $R_i' = 20$  mrad and  $R_f = 2$  cm,  $R_f' = -20$  mrad. The hard-edge focusing functions for the lenses are shown by dashed lines.

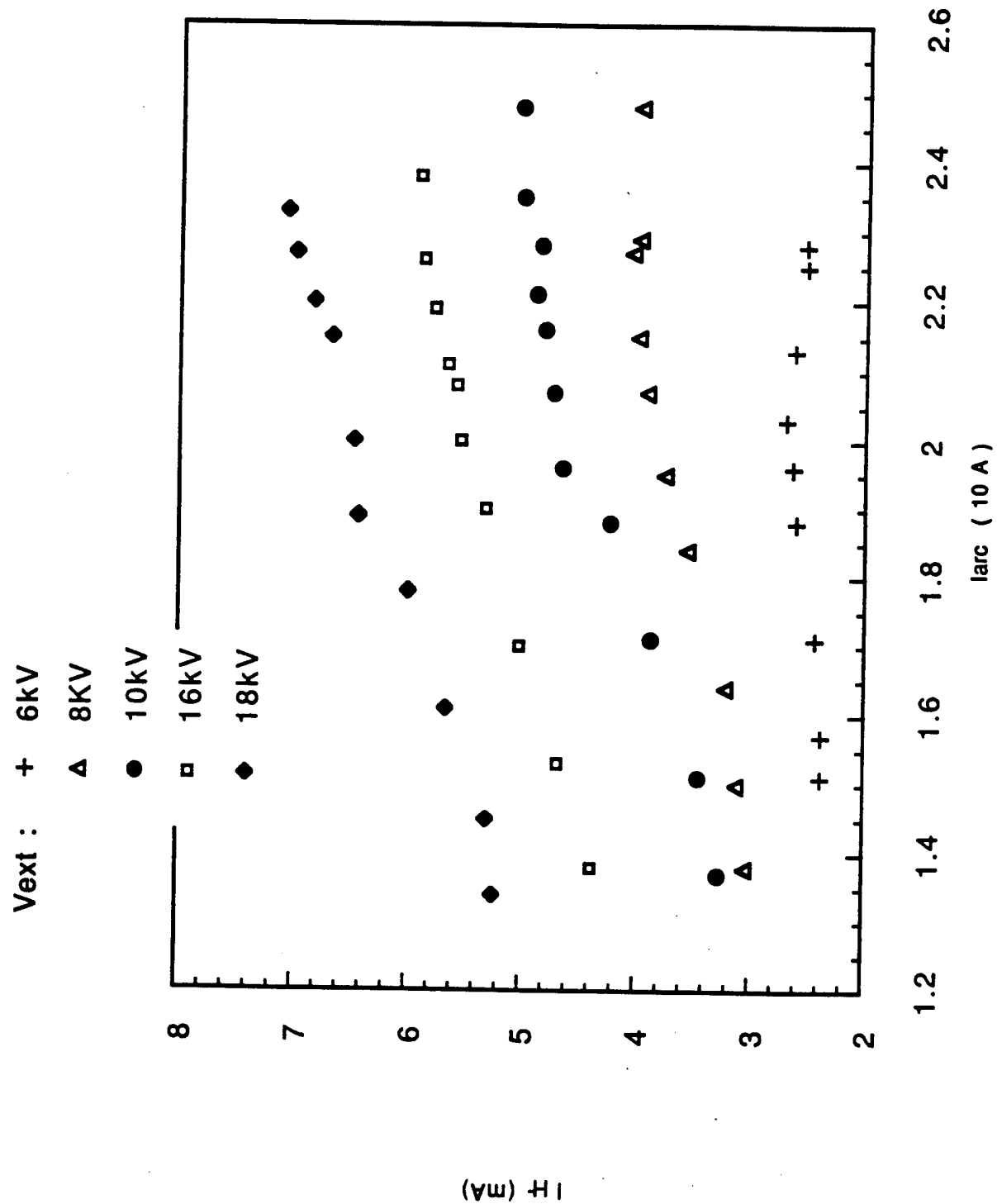


Figure 1

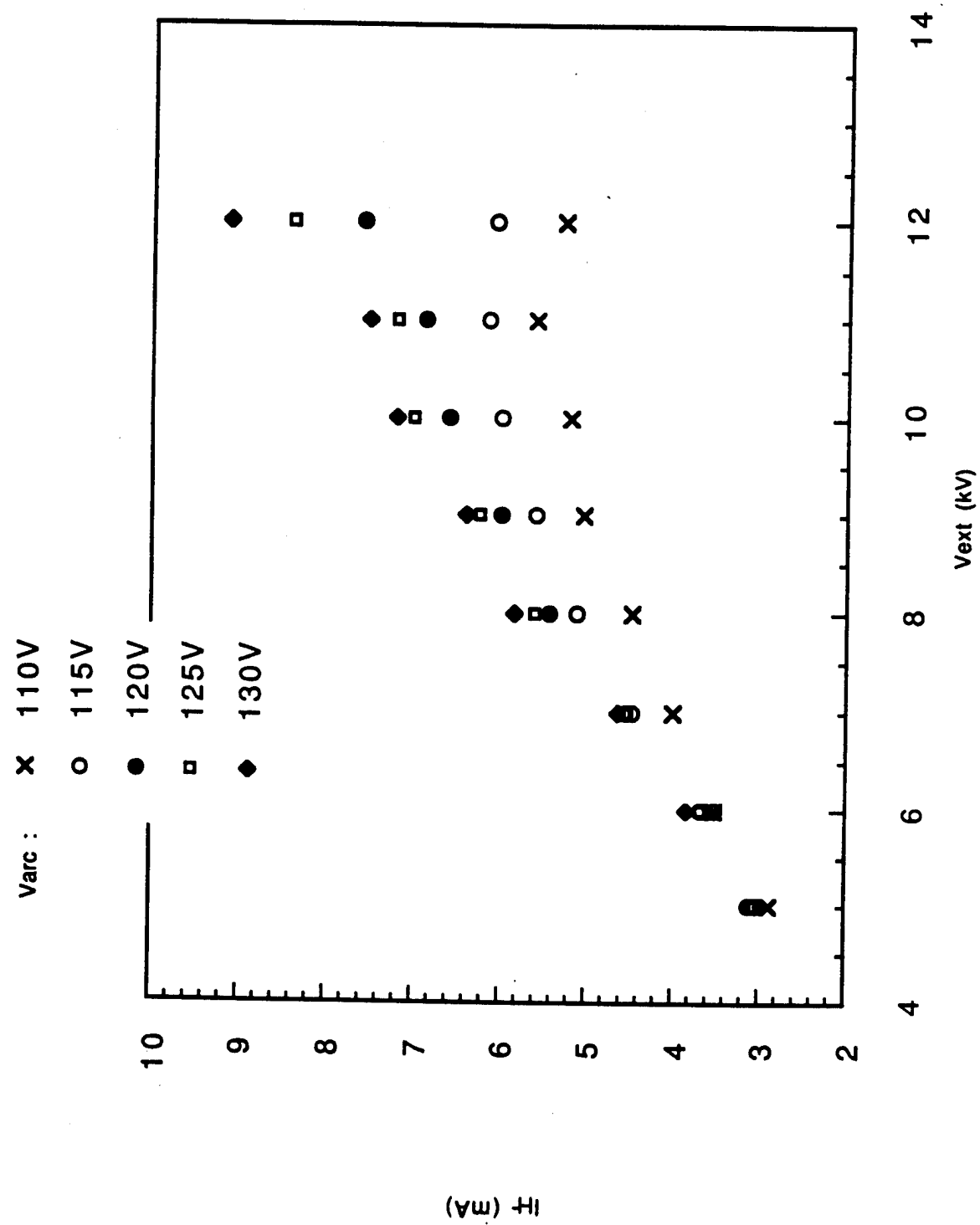


Figure 2

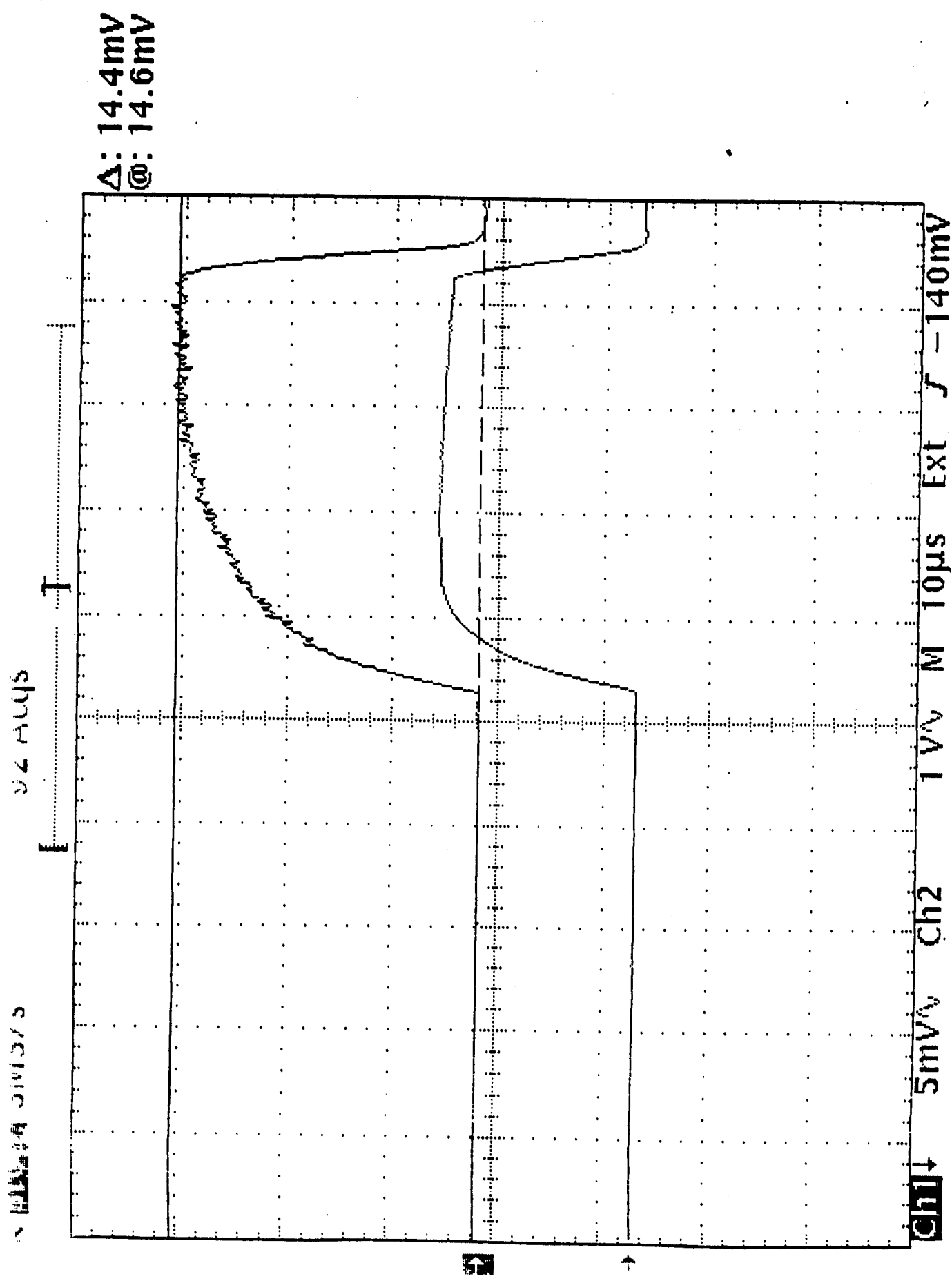


Figure 3

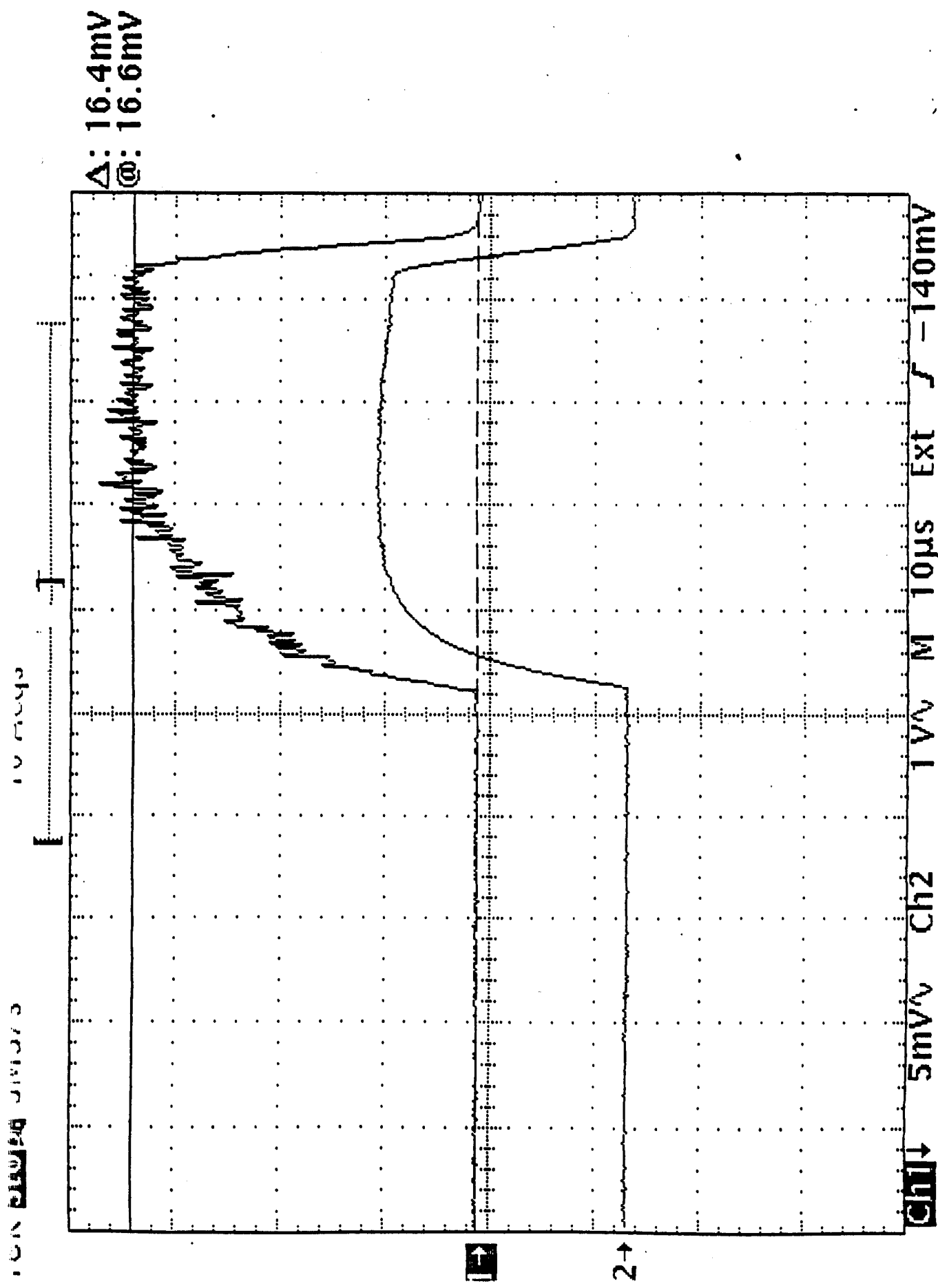


Figure 4

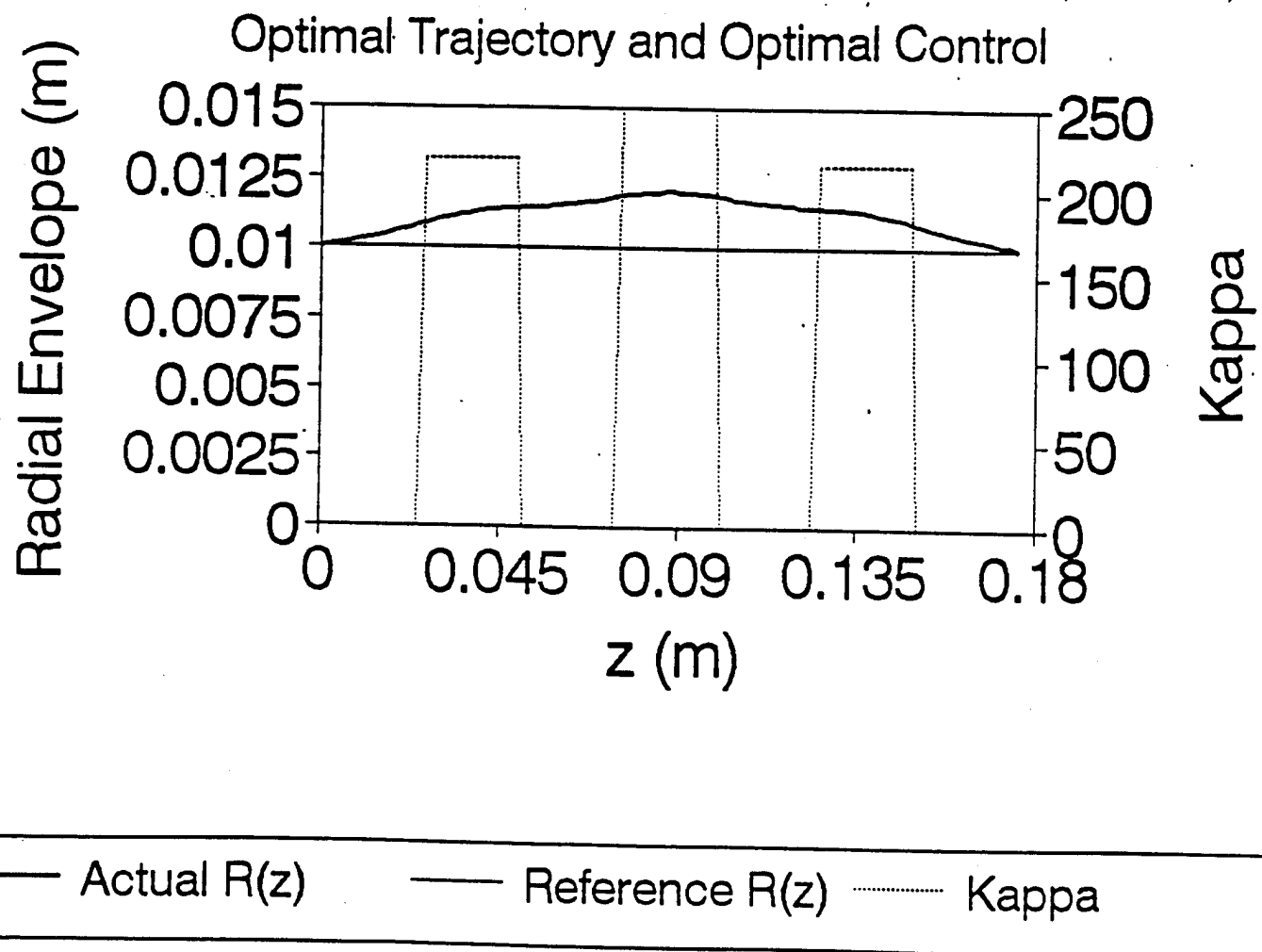


Figure 5

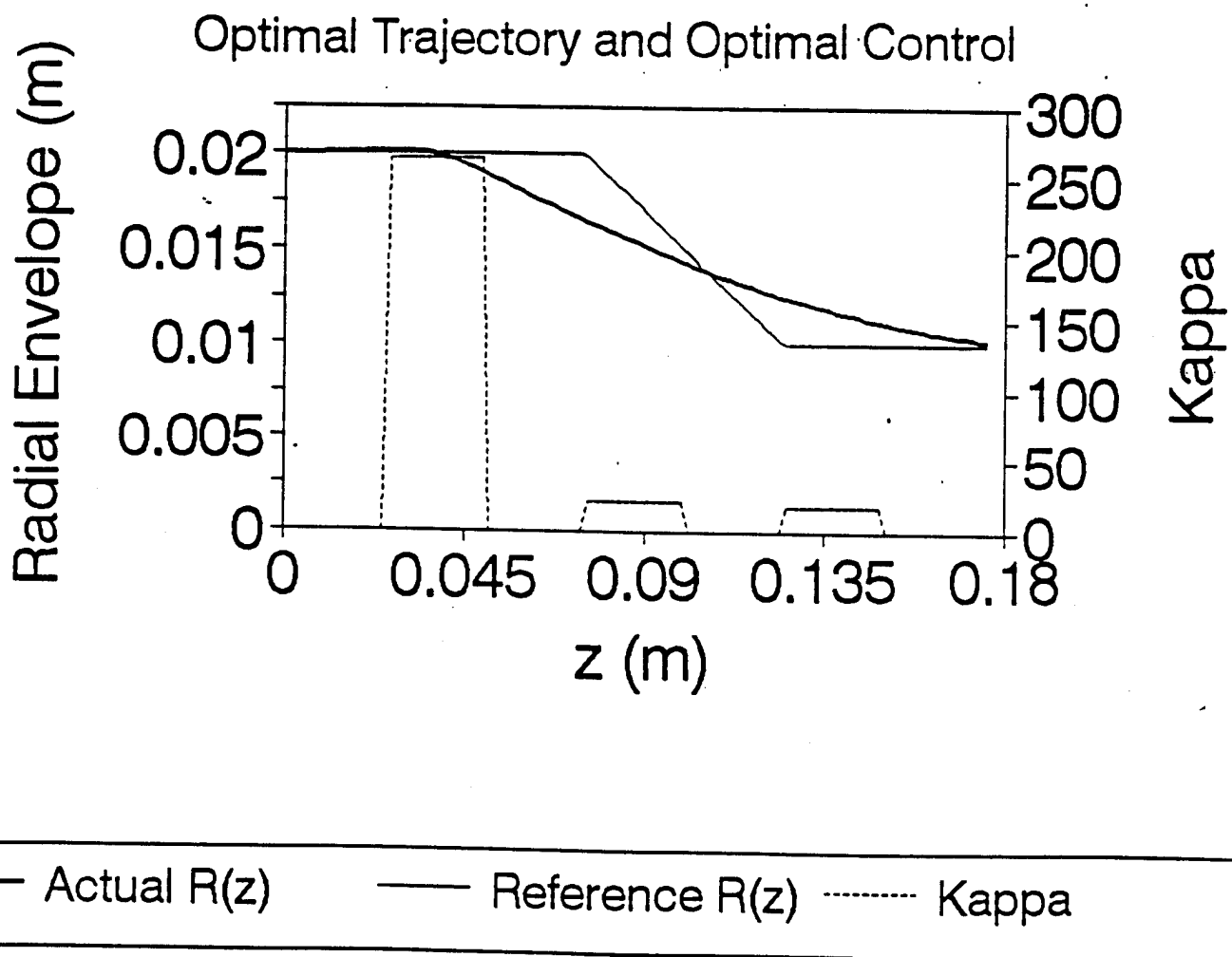


Figure 6

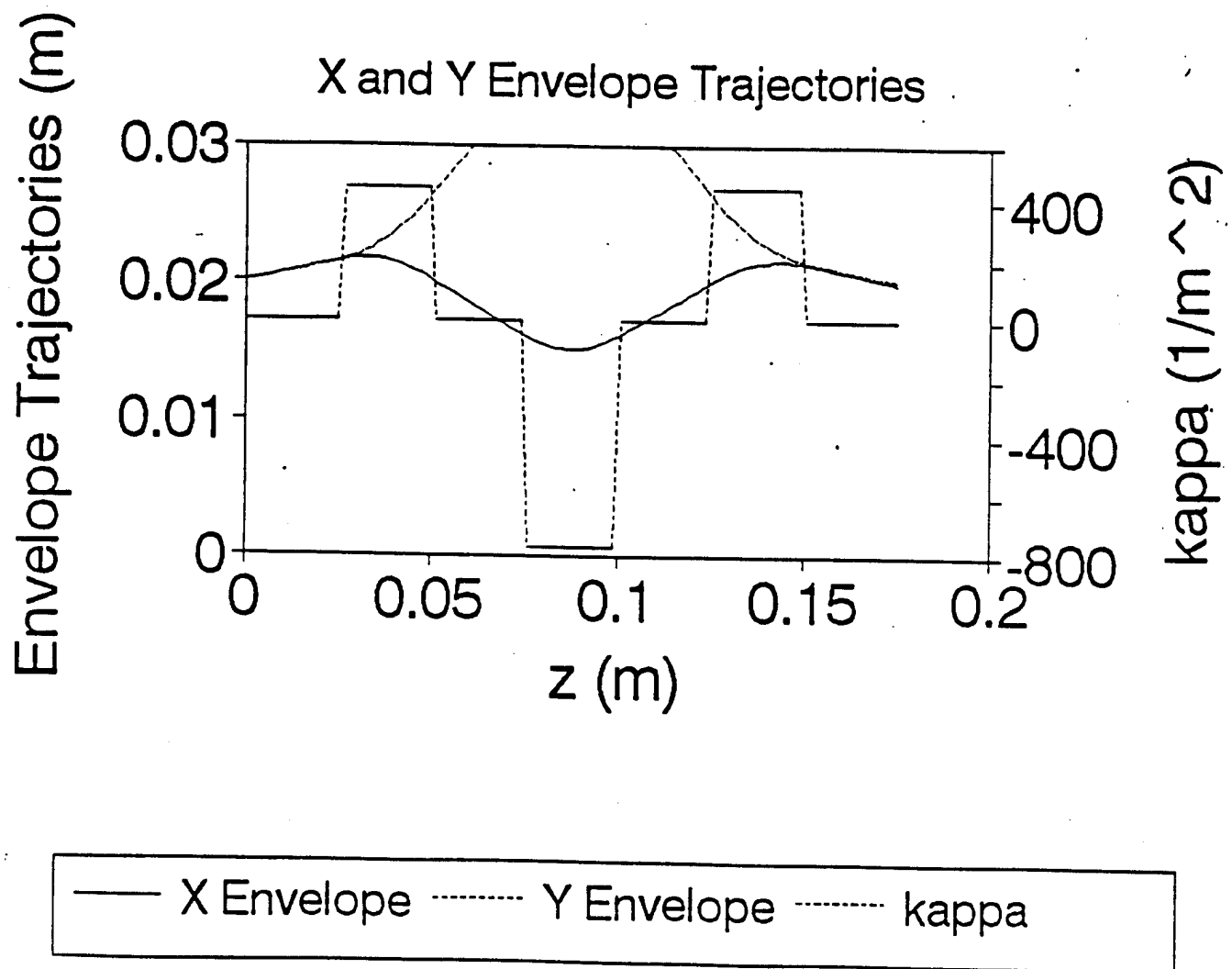


Figure 7

# **STUDY OF BRIGHTNESS AND CURRENT LIMITATIONS IN INTENSE CHARGED PARTICLE BEAMS**

**M. Reiser and S. K. Guharay**

University of Maryland, College Park, Md. 20742

## **PRESENTATIONS, PUBLICATIONS, AND INVITED TALKS**

1. S. K. Guharay, C. K. Allen, M. Reiser, K. Saadatmand and C. R. Chang, "Low energy beam transport system for  $H^-$  beams relevant to the SSC injector", in Production and Neutralization of Negative Ions and Beams, ed. J. G. Alessi and A. Hershcovitch, AIP Conf. Proc. No 287, 1994, p.672.
- \*2. S. K. Guharay, C. K. Allen and M. Reiser, "Study of beam dynamics for an intense, high-brightness  $H^-$  beam to design an efficient low-energy beam transport using ESQ lenses", Nucl. Instrum. & Meth. in Phys. Res. A **339**, 429 (1994).
3. M. Reiser, "Theory and Design of Charged Particle Beams", John Wiley & Sons, Inc., 1994.
4. C. K. Allen, S. K. Guharay, M. Reiser, "Analysis of an electrostatic quadrupole lens using the method of moments", Bulletin of the American Phys. Soc. **39**, 1047 (1994).
5. C. -H. Chen, S. K. Guharay, M. Reiser, " $H^-$  beam from a magnetron ion source and low-energy beam transport", Bulletin of the American Phys. Soc. **39**, 1047 (1994).
- \*6. S. K. Guharay, C. K. Allen, M. Reiser, K. Saadatmand and C. R. Chang, "Efficient low-energy beam transport for intense, high-brightness  $H^-$  beams in high energy accelerators: perspectives and a solution using ESQ lenses", Rev. Sci. Instrum. **65**, 1774 (1994).

7. S. K. Guharay, M. Reiser, V. Dudnikov, "H<sup>-</sup> beam based projection microlithography: a conceptual study of the beam parameters", *Rev. Sci. Instrum.* **65**, 1745 (1994).
8. S. K. Guharay and M. Reiser, "LEBT for high-luminosity colliders", *Proc. Workshop on Future Hadron Facilities in the U.S.*, July 6-10, 1994, FERMILAB-TM-1907, p.96.
- \*9. S. K. Guharay and M. Reiser, "An electrostatic LEBT for a low-emittance injector: transport and focusing of a high-brightness H<sup>-</sup> beam from a magnetron ion source", *Nucl. Instrum. & Meth. in Phys. Res. A* (submitted for publication).
10. C. K. Allen, S. K. Guharay, and M. Reiser, "Solution of Laplace's equation by the method of moments with application to charged particle transport", *Proc. Computational Accelerator Physics*, ed. R. Ryne, AIP Conf. Proc. vol. 297, 568, 1994.
- \*11. C. K. Allen, S. K. Guharay, and M. Reiser, "Optimal control of low energy particle beams", *Proc. 10 th Intern. Conf. on High Power Particle Beams*, San Diego, June 20-24, 1994, vol. 2, p. 540.

\*Copies of these papers are included in the Appendix B.

Appendix A: Progress Report until mid-January 1994  
as included in the last Research Proposal  
(January 1994)

# 1 Introduction

The problem of efficient generation and transport of intense, high-brightness charged particle beams is of crucial importance for advanced accelerator applications in basic science, energy, defense, and industry. These beams are characterized by very high peak and/or average power at full energy and very stringent requirements on beam quality (emittance, energy spread). Examples are high-current H<sup>-</sup> or proton linacs for high-energy colliders, space defense, transmutation of radioactive nuclear waste, tritium production, neutron spallation sources, or the thorium reactor scheme recently proposed by Rubbia at CERN; heavy-ion accelerators for inertial confinement fusion; electron beams for high-power microwave generation, free electron lasers, or future linear e<sup>+</sup>e<sup>-</sup> colliders. In all of these applications, the beams are dominated by space-charge effects at low energies (near the particle source) and to a lesser extent throughout much of the accelerator systems. Many important beam physics issues, e.g., maximum allowable current under optimal conditions, brightness limitations, sources of emittance dilution or beam loss in transport channels and accelerators, etc., need to be investigated through an interplay of controlled experiments, reliable computer simulations and rigorous theoretical work to enhance the present understanding and state-of-the art. Our research at the University of Maryland sponsored by ONR has as its major goal the study and development of an efficient system to transport the high-brightness H<sup>-</sup> beam from a magnetron or volume ion source and focus (match) it into a RFQ linear accelerator. All existing accelerators use space-charge neutralization by a background gas which is ionized by the beam. But this technique is highly unsatisfactory due to the empirical nature of optimizing performance, the lack of reproducibility and the poor beam quality and beam loss that often result from instabilities and nonlinear forces in the neutralization channel. By contrast, an electrostatic lens system, which suppresses space-charge neutralization, can be designed and operated with the aid of simulation codes and, in principle, its performance should be predictable and reproducible. Nonlinear forces due to fringe fields and chromatic aberrations can be issues of concern in electrostatic systems. However, with the "realistic" simulation codes at our disposal the electrostatic lens system may be designed in a way that these deleterious effects are minimized. Ultimately, we plan to compare the performance of different transport schemes experimentally on our test stand; this will be the first such effort to determine which method represents the best solution to this important problem.

$H^-$  beams offer many attractive features over proton ( $H^+$ ) beams. By charge-exchange they can be used to generate charge-neutral  $H$ -beams for space defense, fusion-plasma heating and other applications or proton beams for non-Liouvillean phase-space stacking in synchrotrons or storage rings. A further advantage of  $H^-$  beams is that the contamination by other negative ions is negligibly small (the electrons can be easily removed from the beam by a deflecting magnetic field at the source). Proton beams from hydrogen plasmas, by contrast, are usually contaminated by molecular hydrogen ions ( $H_2^+$ ,  $H_3^+$ ) and other positive ion impurities. Because of these special advantages,  $H^-$  sources are now also being considered for application in ion-beam microlithography, and a joint paper with V. G. Dudnikov on this topic will be published shortly (see paper #10 in Sec. 2.8). Our research program on high-brightness  $H^-$  beams involves experimental, computational and theoretical work on the generation and transport of the beams; the major emphasis here is on the study of the beam emittance and brightness limitations.

Over the past several years of our research under ONR sponsorship we investigated various methods of transporting high-brightness  $H^-$  beams. In the course of this work we studied the beam characteristics from different types of  $H^-$  sources, namely, the Penning-Dudnikov type, the volume ionization type, and magnetron type sources. We have determined by detailed simulation studies that an electrostatic quadrupole lens system is a good choice, especially for transporting pulsed beams (for pulse length < charge-neutralization time). We have developed a set of simulation codes with unique features to study the beam dynamics in such a lens system. Many practical features and constraints are included in our simulation codes, and the simulation predictions are expected to be reliable.

During the current two-year contract period we made the transition from theory and design studies to setting up an experimental program, as we had envisioned in our last proposal. This transition was made possible through a collaboration agreement with the SSCL - there are no funds for equipment in our current ONR contract. The SSCL had acquired two different types of  $H^-$  sources, a magnetron source and a volume source. They were interested in an independent research study like ours to determine the optimal way of transporting and matching the  $H^-$  beams from these two sources into the RFQ accelerator. By a fortunate coincidence, the beam parameters for the SSC - like those at Brookhaven and Fermilab - are very similar to the requirements for space-defense applications that we have been studying. Initially, we had planned to do experiments at the SSCL site. However,

while developing a low-energy beam transport (LEBT) system for experiments with the SSCL volume ionization source we found that the priorities of experiments at the SSCL were often in conflict with our plan and it caused significant delay in our program; also such a mode of operation was very inefficient and expensive in terms of travel time. This difficulty had been anticipated by us, and we recognized already two years ago that an in-house test facility should be developed to make real progress and to provide the best training for graduate students in this area of research. Fortunately, we were able to persuade the SSCL to ship the magnetron ion source including the vacuum system, power supplies and a substantial portion of the associated electronics to the University of Maryland. Adequate space was provided in the Institute for Plasma Research, and during the past months we have worked very hard to build up the laboratory, to assemble the  $H^-$  beam facility and to develop a control system for operating the ion source. Initial tests of the individual components have been conducted, and necessary software support to control the components remotely has been developed. At this time (mid-January, 1994) the ion source is operational, and the study on generation, extraction, and transport of  $H^-$  beams will be resumed soon.

In parallel with the assembly of the ion-source test facility we worked on the development of a new electrostatic quadrupole (ESQ) lens system designed to transport the  $H^-$  beam from the magnetron source. This ESQ system is currently being assembled, and with its completion we will have a full-scale facility to do experimental research. What we still need is some of the diagnostics such as an emittance meter, current profile monitors, etc. We have included some support in the proposed budget to develop these diagnostic systems in-house. We recruited a new outstanding graduate student, C.-H. Chen, to do his Ph.D. dissertation research with our  $H^-$  beam facility, and some additional support is required to pay his graduate research assistantship until Chris Allen who occupies the current RA position in our ONR contract, completes his Ph.D. by the end of this year.

In theoretical work we have made significant improvements to the simulation codes taking into account many practical considerations. A new code has been developed to solve the Laplace/Poisson equations on a personal computer. The code is being tested and its performance is being compared with our previous effort on using a finite difference method solution on the Connection Machine. Chris Allen, our graduate student for theory and simulation, has been working on the theoretical problem of beam transport towards his Ph.D. degree. He is expected to finish the Ph.D. work by the end of 1994. We intend to continue our work on

simulation studies by detailed comparison of the simulation predictions with beam transport experiments. In the experiments planned in our laboratory we will be able to examine the merits of the various codes and study direct comparison between simulation predictions and measurements.

Chris Allen, in his Ph.D. dissertation, is also involved in fundamental studies of the role of image forces on the longitudinal beam behavior and equilibrium of bunched beams.

There has also been major progress in the related work on the thermodynamic description of bunched beams and on the behavior of space-charge waves in electron beams.

A progress report of our recent work is presented in Sec. 2. The proposed research program is described in Sec. 3, and the estimated budget requested from ONR is given in Sec. 4.

## 2 Progress Report

### 2.1 Background and Overview

During the current two years of our research supported by ONR the characteristics of H<sup>-</sup> beams from two types of ion sources at the SSCL, namely, a volume ionization type and a magnetron type source, were studied, and suitable LEBT systems were developed through detailed simulation of beam dynamics. The crux of the problem was to develop an efficient LEBT system so that a highly diverging beam from the source could be transformed into a highly converging one to match it to the acceptance ellipse of a radio-frequency quadrupole (RFQ) accelerator. The parameters of the SSC RFQ were considered, and this required to follow a very stringent emittance budget. After detailed beam dynamics studies, we were finally successful to design an optimized LEBT system that could deliver a matched beam to the SSC RFQ. This is the first time that such good beam matching has been simulated in the context of a particular experiment. The simulation codes were simultaneously improved by incorporating many practical features that we had encountered during analysis of experimental data. Details of our work on high-brightness beam transport and focusing are described in Sec. 2.2.

As the current ONR contract does not have provisions for purchasing equipment, we had planned so far to carry out the beam transport experiments in an external laboratory

where an ion source and beam diagnostics facility could be available. In view of this some collaboration was established initially with the Los Alamos National Laboratory to use the BEAR (Beam Experiment Aboard a Rocket) test stand and later with the Superconducting Super Collider Laboratory (SSCL). However, the BEAR facility was shut down, and the priority of experimental programs at the SSCL was often found to be in conflict with our plan; this caused a significant delay in our experiments. This experience led us to put a strong effort to set up an ion source test stand in-house at Maryland. Finally, our efforts paid off, and in the summer of 1993 we received a magnetron ion source through a collaboration arrangement with the SSCL. Sec. 2.3 describes the status of the magnetron ion source and the test stand facility.

The Maryland test stand has been designed to accommodate some flexibility in terms of performing tests of a LEBT system without coupling it with the ion source, namely vacuum tests, voltage hold-off tests, etc. The LEBT system and the test results have been described in Sec. 2.4.

In theoretical work supported by this contract, Chris Allen, a graduate research assistant working towards his Ph.D. has developed a new moment-method Laplace solver to aid designing the low-energy beam transport system. This technique is expected to increase both speed and accuracy of electrostatic field calculations. The longitudinal image force on bunched beams has been calculated in cylindrical conducting tubes assuming an ellipsoidal uniform density; the geometry factor involving the bunch length and the tube radius has been shown to play an important role in the calculation of the image field. Further, the problem of particle distribution for a relativistic beam in a linear focusing system with different transverse and longitudinal temperatures has been studied taking into account the space-charge forces. Additional work on the thermodynamic equilibrium state of a bunched beam is also described there. Some details of the theoretical work have been described in Sec. 2.5. In Sec. 2.6 we will discuss some related work with electron beams. References are given in Sec. 2.7 and papers resulting from our research will be listed in Sec. 2.8.

## 2.2 High-Brightness H<sup>-</sup> Beam Transport and Focusing

After a good deal of investigation of the characteristics of various types of transport systems,<sup>1,2</sup> we decided to focus our attention on an electrostatic system, mainly the electrostatic quadrupole configuration,<sup>3,4</sup> in the context of transporting short-pulse beams (typically, pulse length  $\ll$

beam neutralization time). Our approach has been to initially develop a good understanding of the beam dynamics through simulation studies, and to build up a close link between experimental results and simulation predictions. This helped us to continuously improve upon any weak points of the simulation schemes, and it, therefore, enhanced the confidence level of simulation predictions.

As mentioned earlier, the goal of this work has been to deliver a matched beam to an RFQ in a linac section without any significant emittance dilution. As we were lately connected to the SSCL for beam transport experiments, we used the acceptance ellipse parameters of the SSC RFQ.<sup>5</sup> The matching conditions of the SSC RFQ were governed by the following Twiss parameters:  $\alpha = 1.26$ ,  $\beta = 1.86$  cm/rad,  $\tilde{\epsilon}_n = 0.2$  mm-mrad. This demanded a strong convergence of the beam from the LEBT section: beam diameter of  $\sim 2.2$  mm and slope of the beam envelope of  $\sim -90$  mrad. From an analysis of beam parameters from the source, as described in the next two sections, we determined that a combination of a 6-lens ESQ LEBT and a short einzel lens module between the ESQ and the RFQ could efficiently handle the emittance budget giving a good tunability of the LEBT. This scheme was found especially suitable for the SSC RFQ where a large drift space ( $\sim$  a few cm) was used to accommodate the mechanical structures as its front wall; however, from the beam dynamics viewpoint the drift space should be kept to a minimum to deliver a good beam to the RFQ. The LEBT system has been described in the following two sections for H<sup>-</sup> beams corresponding to (i) SSCL volume source and (ii) SSCL magnetron source.

### 2.2.1 Transport of H<sup>-</sup> Beams from a Volume Source

The emittance measurements of a 30 mA, 35 kV H<sup>-</sup> beam from the SSCL volume source have been shown as contour plots in Fig. 1. These data were taken at a distance of about 10 cm from the extraction electrode (aperture radius of the extractor = 4 mm). The beam parameters at this location were estimated as<sup>7</sup>: beam size = 2.38 cm, full divergence = 260 mrad, rms normalized emittance  $\tilde{\epsilon}_n = 0.1537$  mm-mrad. The drift space of 10-cm-long was due to an electron suppression system used to separate the electron component (initial electron-to-ion current ratio was about 40.) from the extracted H<sup>-</sup> current. Such a long drift space caused a significant blow-up of the H<sup>-</sup> beam; a shorter electron suppression system of about 5-cm-long was planned to be used.

In order to estimate the beam parameters at the extraction electrode the aforementioned

beam data at  $z = 10$  cm were used as input to a simulation code solving the K-V envelope equations. This code, developed here, included several practical considerations, e.g., space-charge effects due to the accumulation of extraneous charges (electrons and positive ions) in the neighborhood of the extraction region, plausible profiles of the extraneous charge elements, etc. Figure 2(a) shows the assumed space-charge correction factor,  $f$ , due to the electrons. Note that  $f$  was taken negative; the beam perveance  $K$  in the envelope equations

$$X'' + \kappa_x(z)X - \frac{2K}{X+Y} - \frac{\epsilon_x^2}{X^3} = 0,$$

$$Y'' + \kappa_y(z)Y - \frac{2K}{X+Y} - \frac{\epsilon_y^2}{Y^3} = 0,$$

should be multiplied by a factor of  $(1 - f)$  to include the space-charge forces due to electrons. The beam envelope upstream towards the extraction electrode (here, at  $z = 0$ ) is shown in Fig. 2(b). This suggests that the beam formed a waist close to the extraction electrode and it filled up almost the full aperture.

Using the above information of beam parameters at the extraction electrode, the characteristics of the ESQ LEBT system and the behavior of the beam through the LEBT were determined. Figure 3 shows the envelope of the  $H^-$  beam through the ESQ LEBT. It may be noted that the aperture of the ESQ lenses were about a factor of two larger than what we mentioned in our previous report to ONR; this change was necessary to accommodate the large beam at the end of the 5 cm-long electron suppressor in this experiment. The distribution of the beam particles through the ESQ LEBT was estimated using the modified PARMILA code.<sup>3</sup> Figure 4 shows the particle distribution in phase space. The output beam parameters are:  $X = 7.2$  mm,  $Y = 7.3$  mm,  $X' = -51$  mrad,  $Y' = -51$  mrad, ratio of output-to-input rms normalized emittance  $\bar{\epsilon}_{nf}/\bar{\epsilon}_{ni} \sim 1.5$ . From our simulation studies we concluded that the emittance growth was mainly due to chromatic aberrations.

Using the output beam parameters from the ESQ LEBT as input to an einzel lens, it was determined from the SNOW-2D code that the einzel lens geometry, shown schematically in Fig. 5a, satisfied the nominal matching conditions at a distance of about 3.0 cm from the front wall of the SSC RFQ without any noticeable emittance growth (Fig. 5b); the third electrode at ground potential simulated the front wall of the RFQ.

It was concluded that the LEBT system consisting of the ESQ lenses and an einzel lens could deliver a matched beam to the SSC RFQ with an emittance growth of about 50%.

### 2.2.2 Transport of H<sup>-</sup> Beams from a Magnetron Source

The emittance measurement of the H<sup>-</sup> beam from the SSCL magnetron source is shown in Fig. 6. These data were taken at 11.75 cm downstream from the extraction slit of the source; the beam diameter was about 3.5 cm, the full beam divergence was about 300 mrad, and  $\tilde{\epsilon}_n = 0.12$  mm-mrad. In the case of the magnetron source the ratio of  $e/H^-$  in the extracted current was about 1-2; hence, the space-charge effect of the electrons might not have been important. Following the method as described in the previous case (Sec. 2.2.1), the beam parameters at the extractor were estimated using the aforementioned emittance data, and it was found that  $X \sim 1.1$  mm and  $X' \sim 70$  mrad.

The existence of a 5 cm-long extraction cone had severely restricted the accessibility of the ESQ LEBT. This resulted in dealing with a very large, highly divergent beam at the input of the LEBT. The beam envelope through the ESQ LEBT has been shown in Fig. 7. It was noted from the particle simulation results that the emittance growth for the full beam current of 30 mA was quite large – a factor of about 3. Scraping off about 15% of the beam particles the emittance growth dropped to a factor of 1.5; Fig. 8 shows the phase-space distribution of the particles. The output beam parameters from the ESQ LEBT were found as:  $X = 4.7$  mm,  $Y = 4.4$  mm,  $X' = -49$  mrad,  $Y' = -48$  mrad. These results match closely with the typical input parameters of the einzel lens as discussed earlier.

Details of this work are given in reference 8.

## 2.3 Magnetron Ion Source Facility at Maryland

In the summer of 1993 a magnetron ion source system along with some supporting electronics was received in Maryland from the SSCL. While commissioning the source at Maryland the components were examined individually. Several missing components were identified, and plans for system integration were laid out. The major tasks that we performed could be identified as:

- i) The control of the full system was established through a personal computer, and necessary software was developed.
- ii) The temperature controller of the cesium oven was modified to obtain good stabilization of cesium flow.

- iii) Mechanical components were developed to interface the ion source with a diagnostic box and the LEBT system.
- iv) Some basic diagnostics (namely, a current monitor and a phosphor screen) have been installed.
- v) A special glove box unit has been set up in our laboratory to transfer cesium in a pure inert gas environment.

Figure 9 shows a few major components of the magnetron ion source. The entire system has been assembled.

## 2.4 ESQ LEBT System

A prototype ESQ LEBT system has been developed in-house. The lens parameters in Table 1 were chosen on the basis of our aforementioned simulation studies in Sec. 2.2.

While testing the earlier version of our LEBT system it was observed that a low current discharge had to be set up for a long time to achieve a stable voltage holding of the electrodes. It was noted that voltage breakdown frequently occurred between the dielectric insulating balls and the electrodes (Fig. 10) where some residual air might have been trapped. In order to avoid the gas accumulation the design of the electrodes has been modified. The ESQ LEBT has been supported in the vacuum vessel using a vacuum manipulator developed in-house. This allows to align the system in-situ. Figure 11 shows the LEBT test facility at Maryland.

Table 1: ESQ LEBT parameters.

Lens No.	Aperture radius (mm)	Electrode radius (mm)	Length (mm)	Spacing* (mm)
1 & 6	15.0	17.2	25.0	2.0
2 & 5	22.0	25.2	59.0	2.0
3 & 4	22.0	25.2	47.0	2.0

\*The spacing corresponds to the gap between the lens electrode and its neighboring ground plate (Fig. 10).

## 2.5 Theoretical Studies

Using the method of moments and fast iterative techniques a 3D Laplace/Poisson solver has been developed by Chris Allen, our graduate research assistant. This code is capable of running practical problems on an IBM PC. The formulation of the problem was based upon transforming Laplace's equation into an integral equation over a boundary surface; this reduced the dimensionality of the original system. The new problem was approximated by the method of moments to yield a matrix-vector equation. Conjugate gradient algorithm was used to solve the equation; this iterative method seemed to provide fast convergence. The code was tested with some known results, for example, to evaluate axial potential distributions of a conducting sphere and an einzel lens, etc.; the numerical results matched well with analytical expressions. Details about the computational method and analysis have been given in Ref. 9. In Ref. 10 the application of the above method to the cases of an electrostatic quadrupole lens and an ellipsoidal bunch in a grounded pipe was discussed. Figure 12 shows the computer model of the four electrodes of an ESQ lens. The single particle focusing effect (the kappa function  $\kappa(z)$ ) due to such lenses was determined from the derivatives  $dE_x/dx$  and  $dE_y/dy$  on axis. Figure 13 shows the computed data for the y-plane for the case in which the x-plane electrodes were held at -1 V. The grounding shunts used at either end of the lens (not shown in Fig. 12) caused a rapid decay of  $dE_y/dy$  outside the lens boundary.

Chris Allen, as part of his doctoral research, is also involved in fundamental theoretical studies of the equilibrium state of bunched beams and the effects of image forces. In this work, the so-called "g-factor", which relates the longitudinal space-charge electric field to the line charge density, was calculated systematically and for the first time for bunches of different aspect ratios  $a/z_m$  inside a conducting pipe of radius  $b$ . A detailed paper has been submitted for publication in Particle Accelerators,<sup>11</sup> and the results are also discussed in the book by M. Reiser, "Theory and Design of Charged Particle Beams", to be published in Spring 1994 by Wiley & Sons. A major theme of this book is a thermodynamic description of beams and the conversion of free energy into emittance growth when the beams are not in 3-D thermal equilibrium. A paper on this topic was published in Phys. Rev. Letters.<sup>12</sup>

## 2.6 Related Experiments with Electron Beams

In past work with our electron beam transport channel we had studied the transverse dynamics of space-charge dominated beams. The most notable study was the multiple-beam experiment where the merging and thermalization of five electron beamlets was investigated. During the past two years we began the systematic study of longitudinal effects in space-charge dominated bunched beams. This work was already more successful than we ever expected. Thus, to single out our accomplishment, we were able to generate, for the first time, single fast or slow waves (which usually occur as pairs) and follow their propagation through the electron bunch and the behavior at the bunch ends. Several papers of our longitudinal beam physics work have been published during 1993 including one in Phys. Rev. Letters.<sup>13</sup>

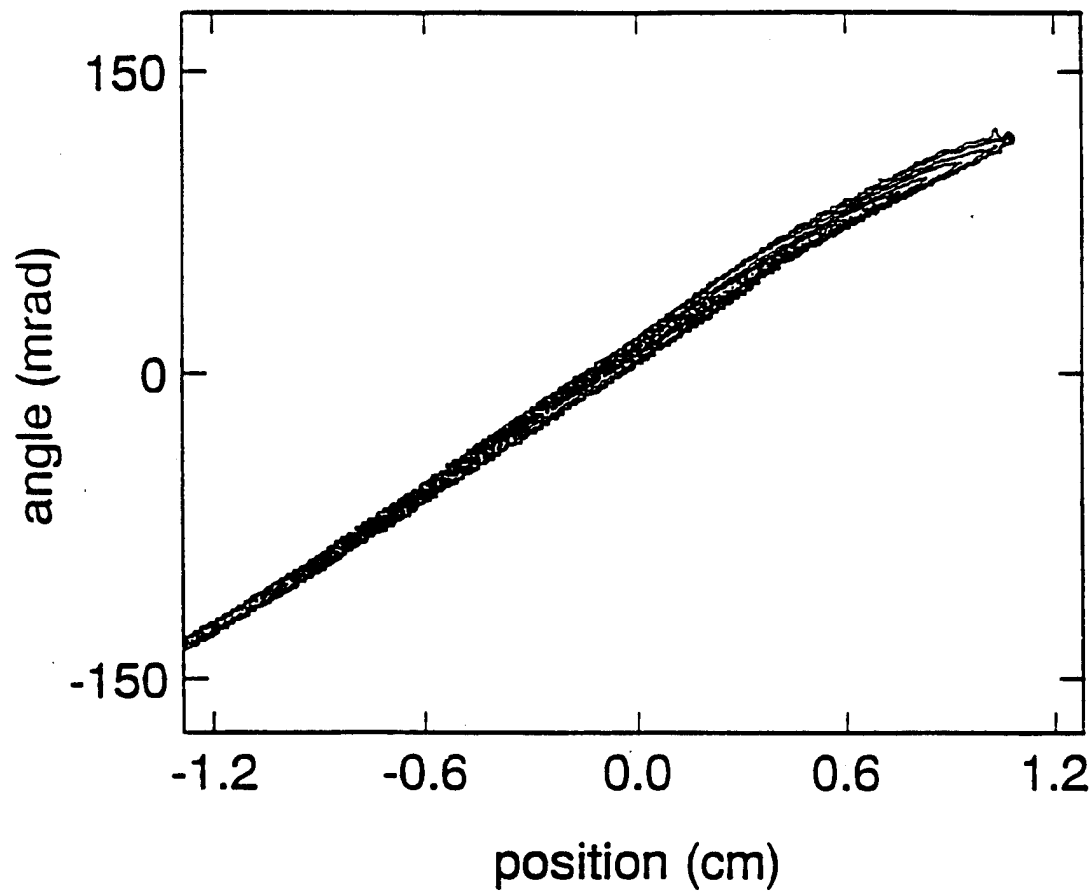
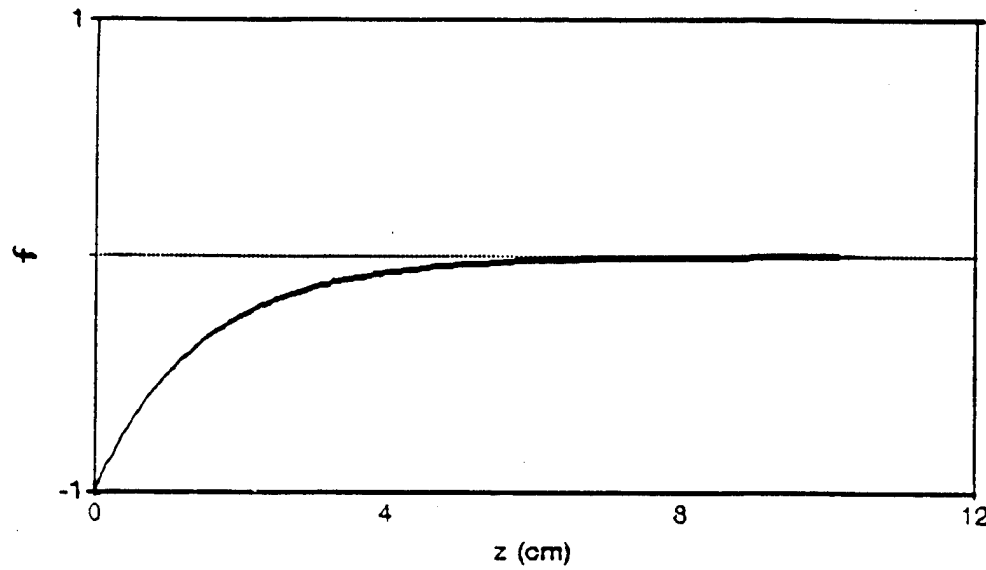


Figure 1. Contour plots of the beam from the SSC volume source at a distance of 10 cm downstream from the extractor.

## Space-charge effect of electron component



## Beam Expansion after Extraction (SSCVOL)

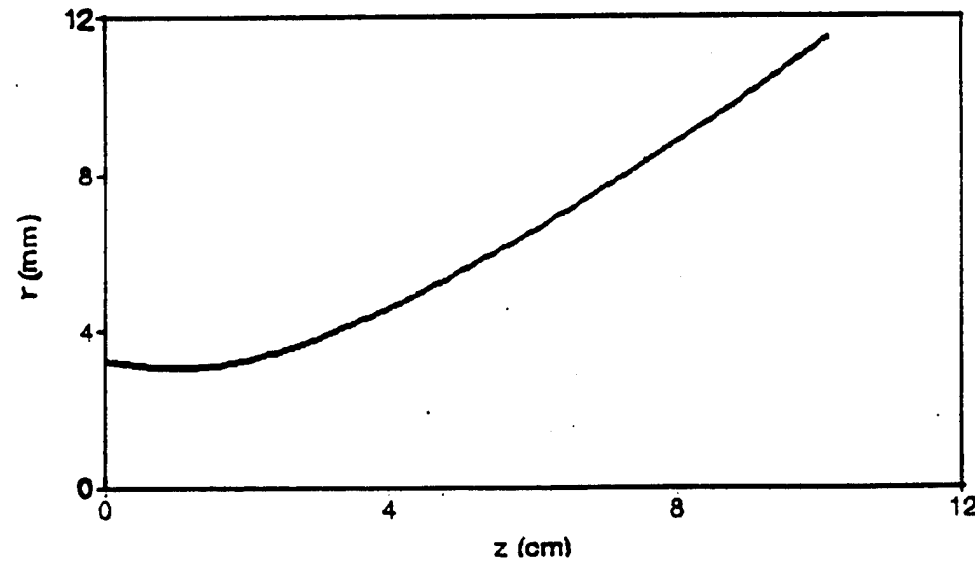


Figure 2. Estimation of beam characteristics at the extractor.

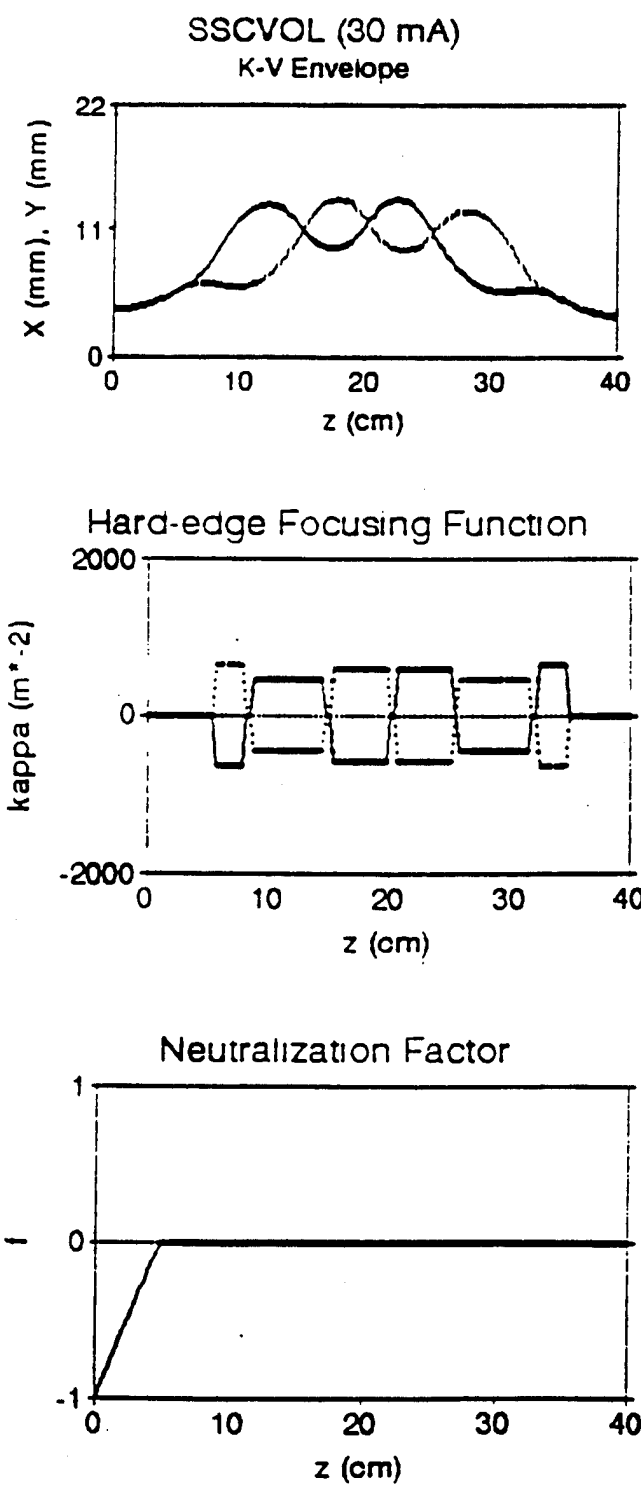


Figure 3. K-V envelope solution for an  $H^-$  beam from the volume source.

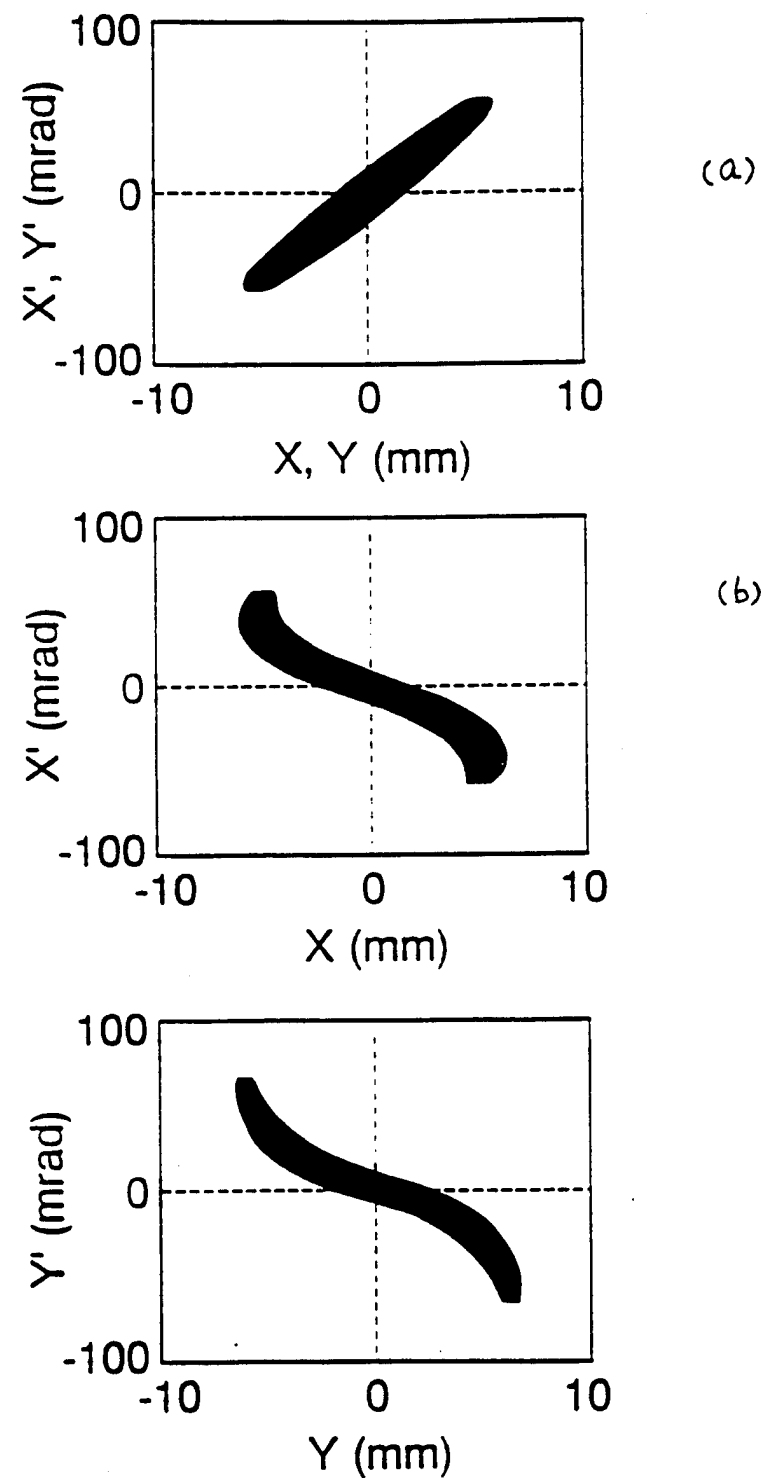


Figure 4. Particle distribution at the (a) input and (b) output of the ESQ LEBT.

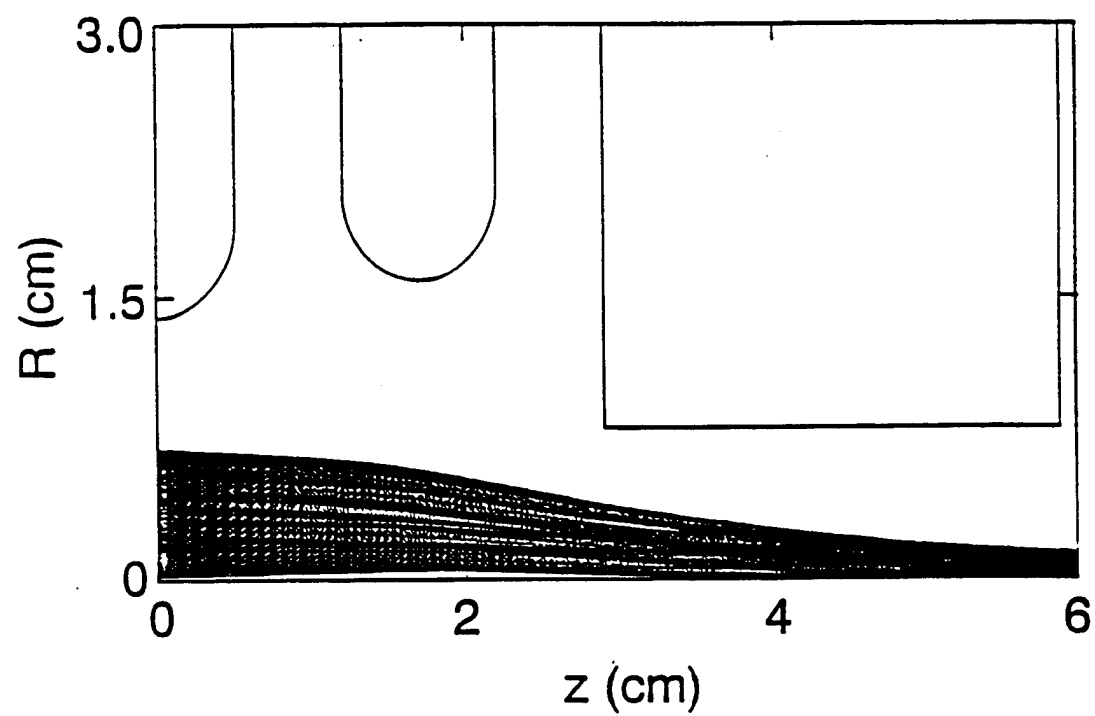


Figure 5(a). Trajectory of the beam particles through the single-stage einzel lens between the ESQ LEBT and the RFQ.

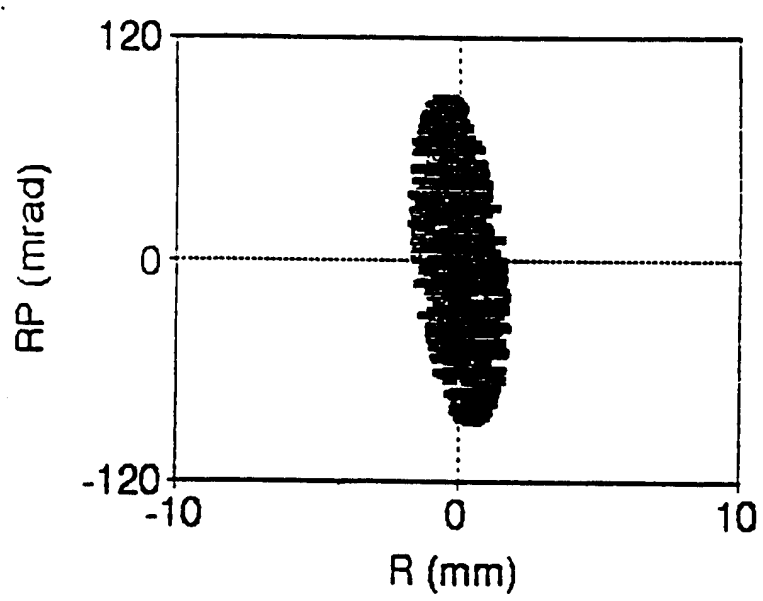
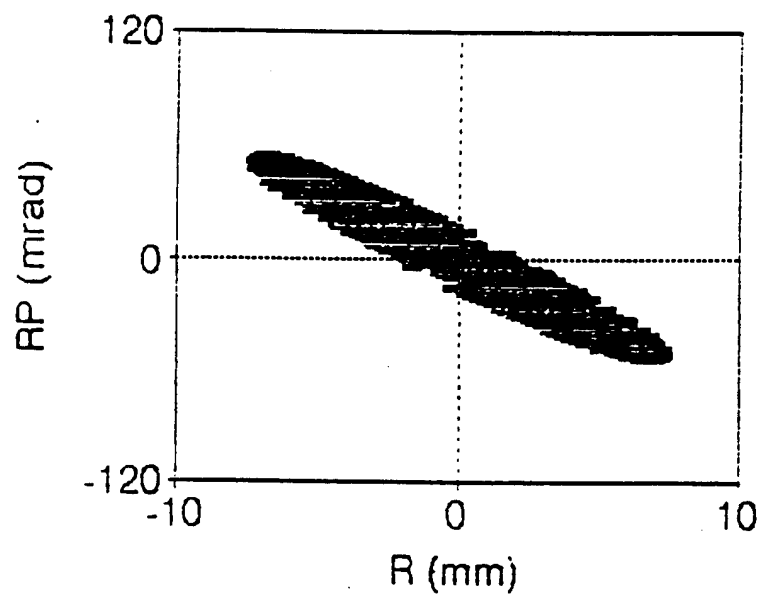


Figure 5(b). SNOW-2D results of the particle distribution; input beam (top) and output beam (bottom).

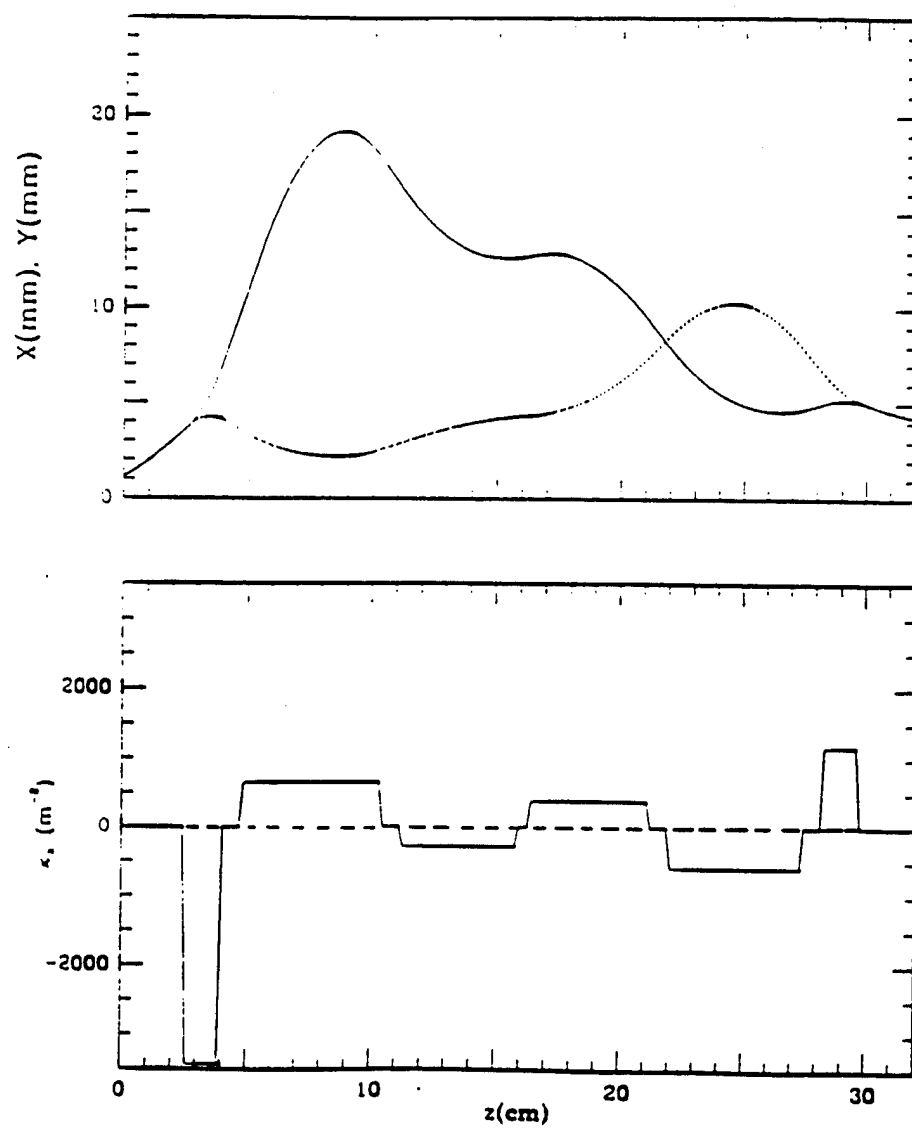


Figure 7. K-V envelope solution for an  $\text{H}^-$  beam from the magnetron source.

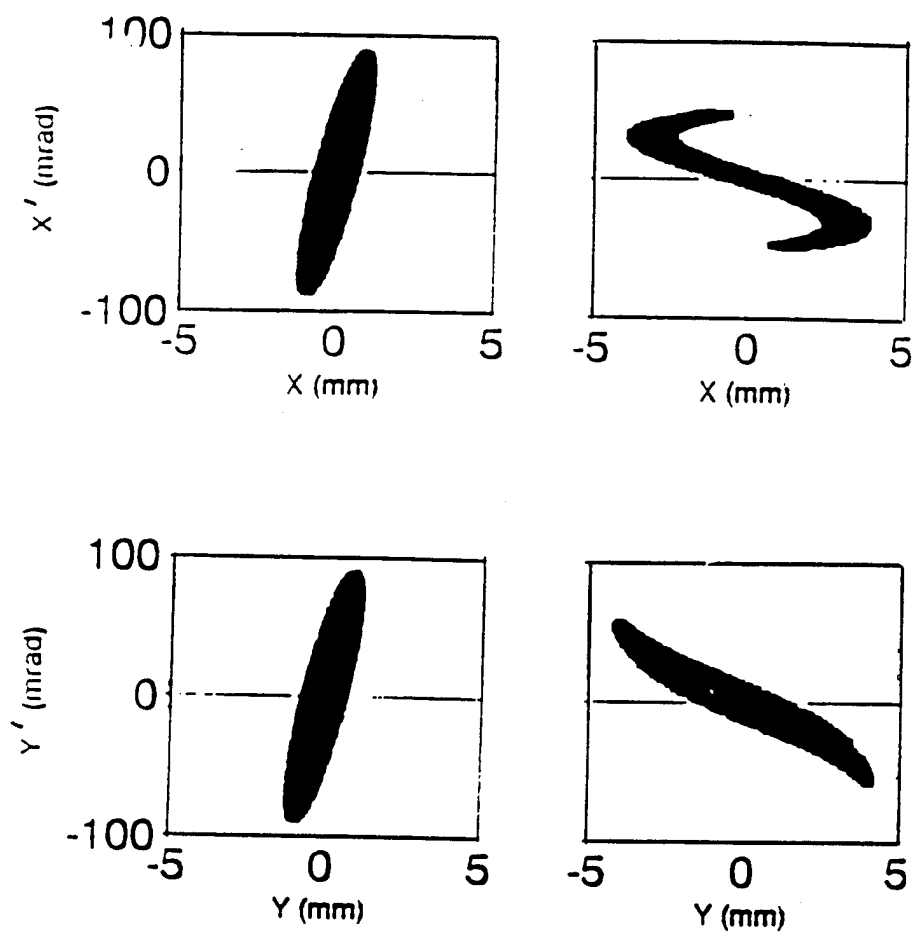


Figure 8. Particle distribution from modified PARMILA.

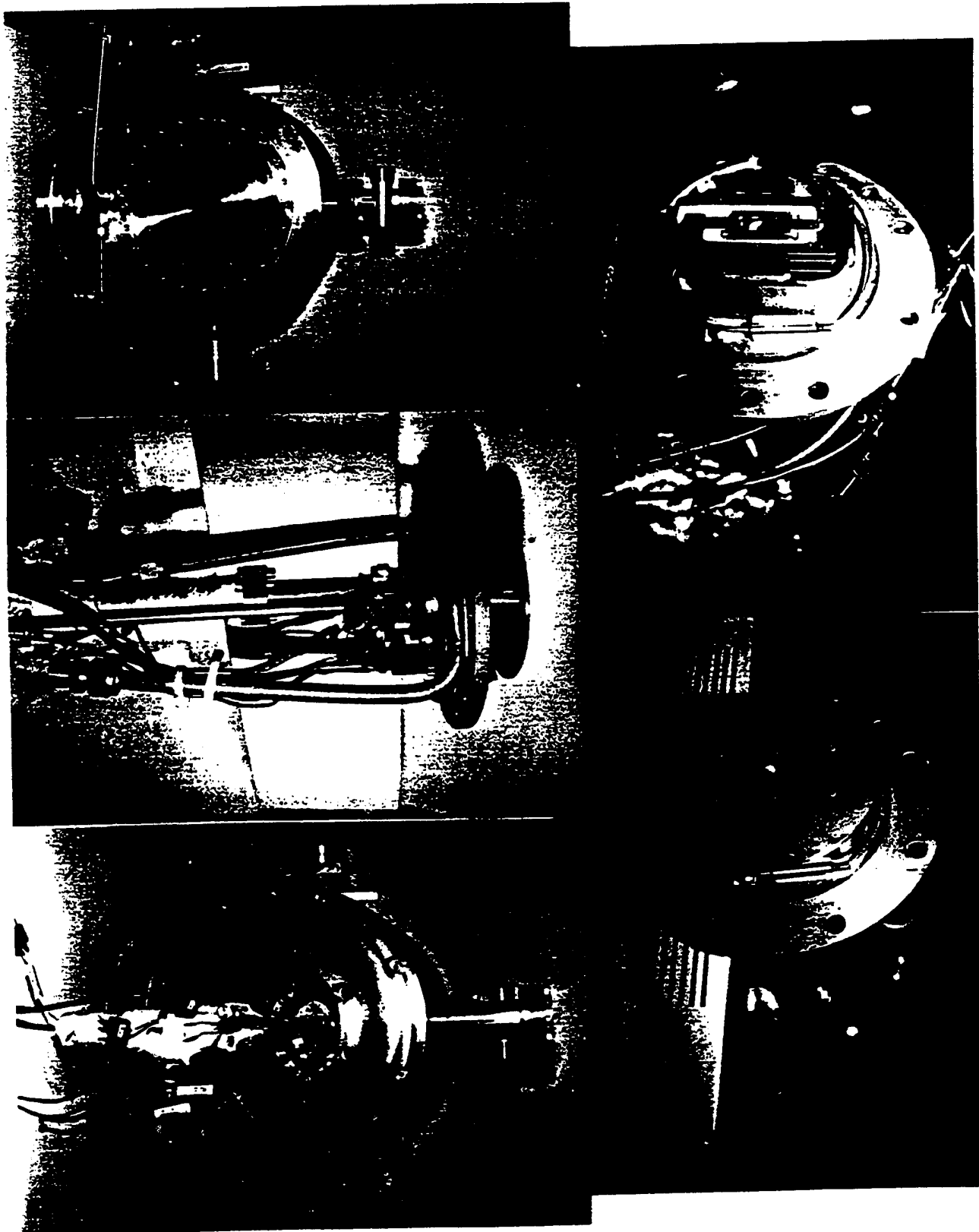


Figure 9. Magnetron source components of the test facility at Maryland.

Experimental arrangement

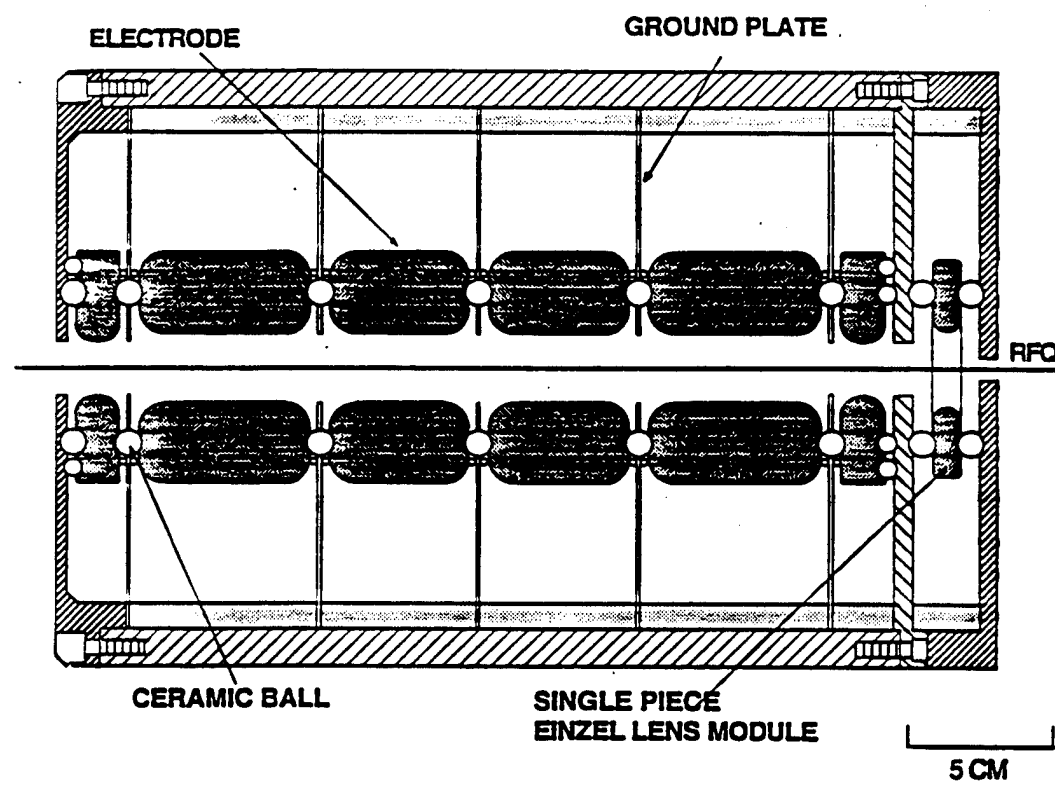


Figure 10. Schematic of the ESQ LEBT.

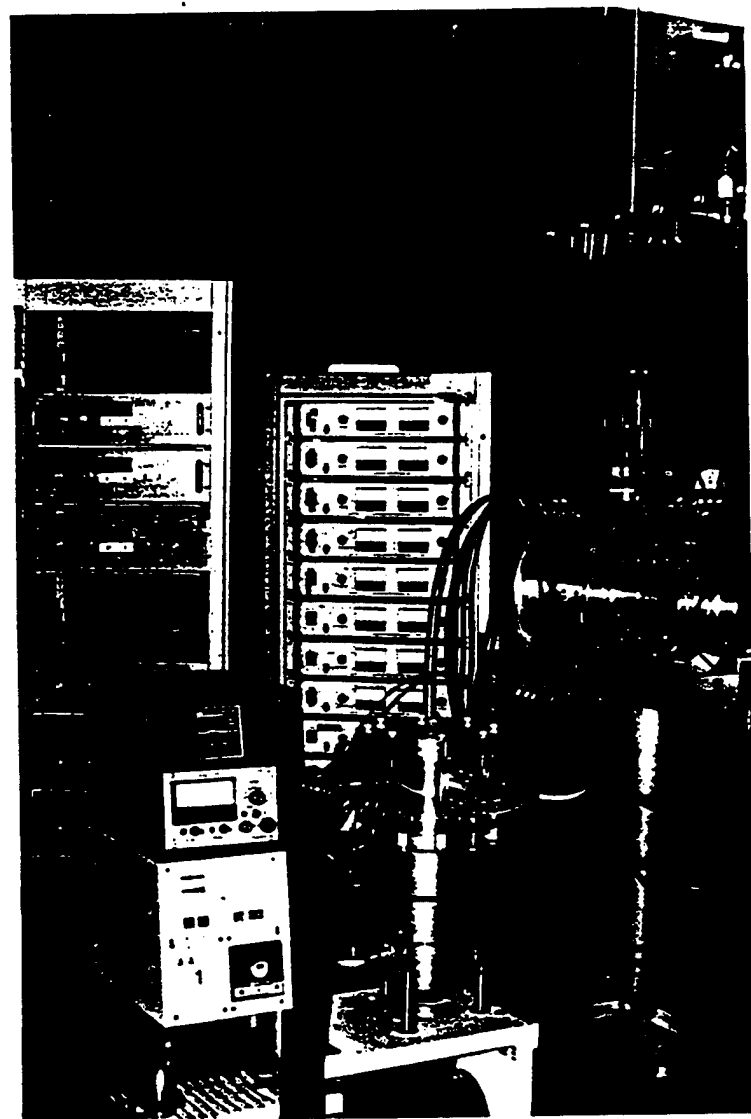


Figure 11. LEBT test facility at Maryland.

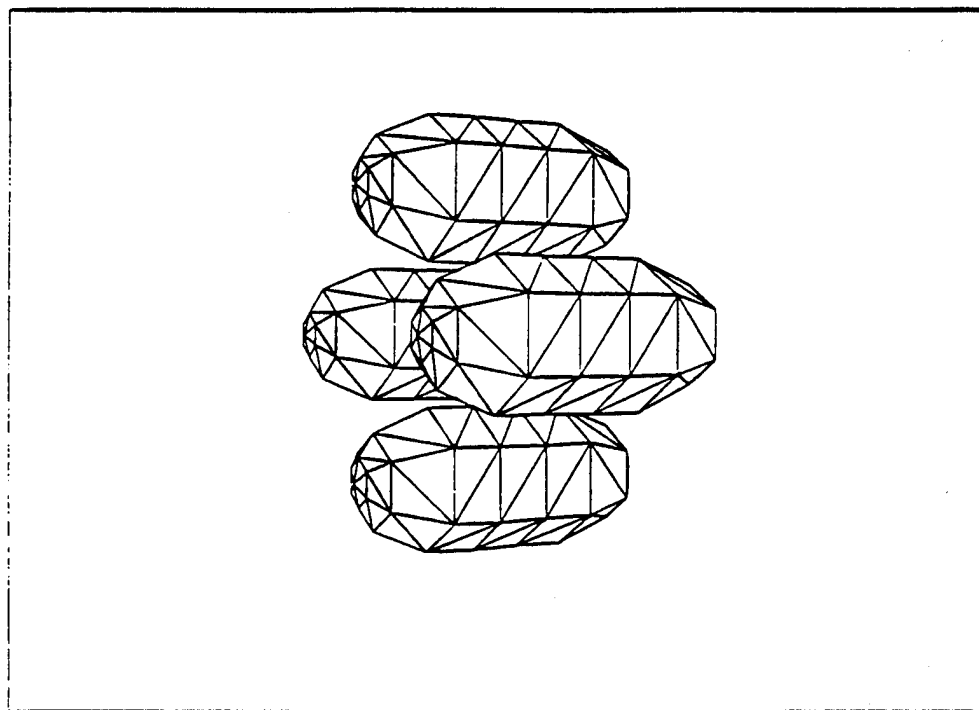


Figure 12. Triangulated ESQ lens.

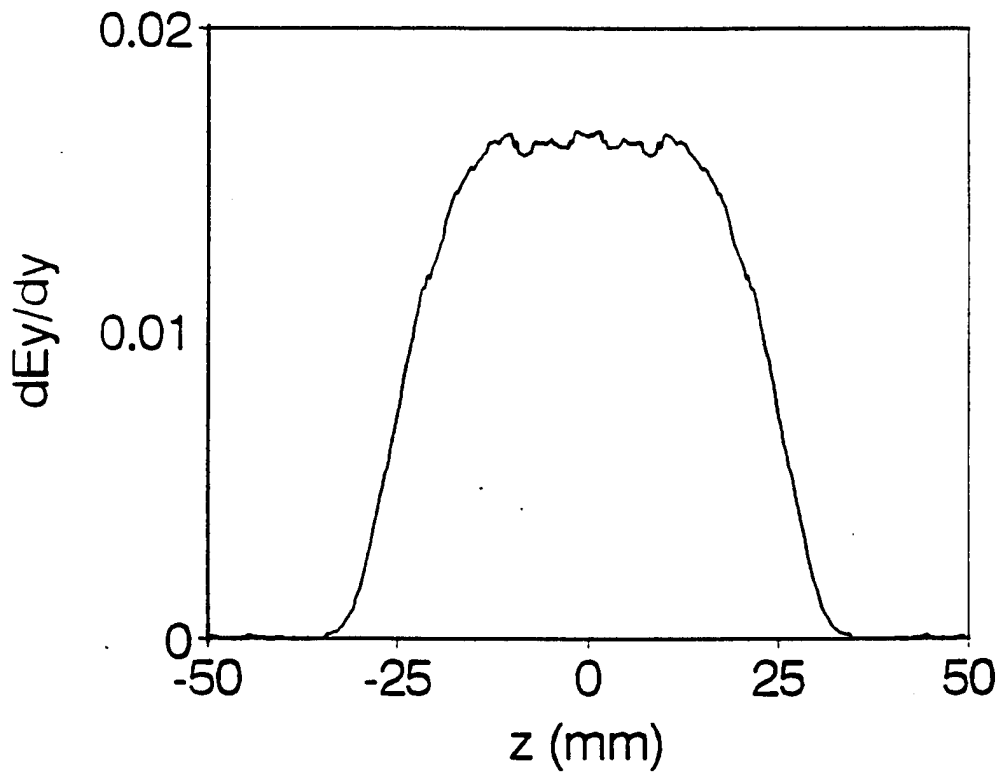


Figure 13. ESQ lens focusing function.

## 2.7 References

1. M. Reiser, Nucl. Instrum. & Methods in Phys. Res. B 56/57, 1050 (1991); Proc. 1988 Linear Accelerator Conf., 1988, p.451; IEEE Trans. Nucl. Science NS-32, 2201 (1985).
2. E. J. Horowitz, D. Chernin and M. Reiser, Phys. Fluids B 1, 1301 (1989).
3. C. R. Chang, E. Horowitz, M. Reiser, Intense Microwave and Particle Beams, SPIE vol. 1226, 483 (1990).
4. S. K. Guharay, C. K. Allen, M. Reiser, in High Brightness Beams for Advanced Accelerator Applications, AIP Conf. Proc. No. 253, 1991, p.67; Intense Microwave and Particle Beams II, SPIE vol.1407, 610 (1991); Proc. 1991 IEEE Particle Accelerator Conf., p.1961.
5. T. S. Bhatia, et al., Proc. 1991 IEEE Particle Accelerator Conf., p.1884.
6. K. Saadatmand, et al., in Production and Neutralization of Negative Ions and Beams, AIP Conf. Proc. No.287, 1992, p.448; Proc. 1993 Particle Accelerator Conf., p.2986.
7. S. K. Guharay, C. K. Allen, M. Reiser, K. Saadatmand, C. R. Chang, Review of Scientific Instrum. (accepted for publication).
8. S. K. Guharay, C. K. Allen, M. Reiser, K. Saadatmand, C. R. Chang, in Production and Neutralization of Negative Ions and Beams, AIP Conf. Proc. No.287, 1992, p.672.
9. C. K. Allen, S. K. Guharay, and M. Reiser, in Computational Accelerator Physics, AIP Conf. Proc. (to be published).
10. C. K. Allen, S. K. Guharay, and M. Reiser, Proc. 1993 Particle Accelerator Conf., p.3648.
11. C. K. Allen, N. Brown, M. Reiser, Univ. Maryland CPB Technical Rept.#93-045, Aug.10, 1993; Particle Accelerators (submitted)
12. M. Reiser and N. Brown, Phys. Rev. Letters 71, 2911 (1993).
13. J. G. Wang, D. X. Wang, M. Reiser, Phys. Rev. Letters 71, 1836 (1993).

## 2.8 Papers and Presentations Related to this Research

1. S. K. Guharay, C. K. Allen, M. Reiser, K. Saadatmand, and C. R. Chang, "Study of emittance growth and its control for a low-energy H<sup>-</sup>beam transport system," AIP Conf. Proc. on Production and Neutralization of Negative Ions and Beams, No. 287, 1992, p.672.
2. S. K. Guharay, C. K. Allen, and M. Reiser, "ESQ focusing for an intense, high-brightness H<sup>-</sup>beam: emittance growth and its remedy," Proc. 9th International Conf. on High-Power Particle Beams, Washington, D.C., 1992 , vol.II, p. 933.
3. C. K. Allen, S. K. Guharay, and M. Reiser, "Solution of LAPLACE's equation by the method of moments with application to charged particle transport," AIP Conf. Proc. on Computational Accelerator Physics (to be published).
4. S. K. Guharay, C. K. Allen, M. Reiser, K. Saadatmand, and C. R. Chang, "A compact ESQ system for transport and focusing of H<sup>-</sup>beam from ion source to RFQ," 1992 LINAC Conf. Proc., vol.1, p.338.
5. S. K. Guharay, C. K. Allen, M. Reiser, K. Saadatmand, "An ESQ lens system for low energy beam transport experiments on the SSC test stand," Proc. 1993 Particle Accelerator Conf., Washington, D.C., 1993, p.3145.
6. C. K. Allen, S. K. Guharay, and M. Reiser, "A moment method Laplace solver for low energy beam transport codes," Proc. 1993 Particle Accelerator Conf., Washington, D.C., 1993, p.3648.
7. S. K. Guharay, C. K. Allen, and M. Reiser, "Study of beam dynamics for an intense, high-brightness H<sup>-</sup>beam to design an efficient low-energy beam transport using ESQ lenses," Nuclear Instrum. and Methods in Phys. Res. A (accepted for publication).
8. S. K. Guharay, C. K. Allen, M. Reiser, "A compact, precision electrostatic quadrupole lens system for high-brightness ion beam transport and focusing," Proc. SPIE Conf. on Charged Particle Optics, San Diego, CA, 1993, SPIE vol. 2014, p. 96.
9. S. K. Guharay, C. K. Allen, M. Reiser, K. Saadatmand, C. R. Chang, "Efficient low-energy beam transport for intense, high-brightness H<sup>-</sup>beams in high energy acceler-

ators: Perspectives and a solution using ESQ lenses," Review of Scientific Instrum. (accepted for publication).

10. S. K. Guharay, M. Reiser, V. G. Dudnikov, "H beam based projection microlithography: A conceptual study of the beam parameters," Review of Scientific Instrum. (accepted for publication).
11. C. K. Allen, N. Brown, M. Reiser, "Image effects for bunched beams in axisymmetric systems", Univ. Maryland CPB Technical Rept. #93-045, Aug.10, 1993; Particle Accelerators (submitted for publication)
12. M. Reiser and N. Brown, "Thermal distribution of relativistic particle beams with space charge", Phys. Rev. Letters 71, 2911 (1993).
13. J. G. Wang, D. X. Wang, M. Reiser, "Generation of space-charge waves due to localized perturbations in space-charge dominated beams", Phys. Rev. Letters 71, 1836 (1993).
14. M. Reiser, "Theory and Design of Charged Particle Beams", Wiley Series in Beam Physics and Accelerator Technology, Wiley & Sons, to be published in Spring 1994.
15. M. Reiser, "A historical look at collective accelerators", Invited Talk, Workshop on Acceleration and Radiation Generation in Space and Laboratory Plasmas, Kardamyli, Greece, Aug.29 - Sept.4, 1993.

## Appendix B: Copies of Relevant Papers

Reprinted from

# NUCLEAR INSTRUMENTS & METHODS IN PHYSICS RESEARCH

Section A

---

Nuclear Instruments and Methods in Physics Research A 339 (1994) 429-438  
North-Holland

Study of beam dynamics for an intense, high-brightness  $H^-$  beam  
to design an efficient low-energy beam transport using ESQ lenses

S.K. Guharay \*, C.K. Allen, M. Reiser

*Institute for Plasma Research, University of Maryland, College Park, MD 20742, USA*

(Received 21 May 1993; revised form received 20 September 1993)



# NUCLEAR INSTRUMENTS AND METHODS IN PHYSICS RESEARCH

*Editor-in-Chief: Prof. Kai SIEGBAHL (Uppsala)*

## Section A: accelerators, spectrometers, detectors and associated equipment

*Editors: Prof. Kai SIEGBAHL; Secretary: Mrs. Gerd AURELIUS, tel: (18) 183557, telex: UPFYS 76263, fax: (18) 554549  
Prof. Erik KARLSSON (Uppsala)*

Manuscripts should be sent to the Editor under the address: *Institute of Physics, Box 530, 751 21 Uppsala, Sweden*

### *Editorial Board:*

**U. AMALDI (CERN)**

**H.H. ANDERSEN (Copenhagen)**

**W.A. BARLETTA (Berkeley, CA)**

**C.E. BEMIS Jr (Oak Ridge)**

**S. BRANDT (Siegen)**

**A. BRESKIN (Rehovot)**

**C.N. BROWN (Batavia, IL)**

**D. BRYMAN (Vancouver)**

**P. CARLSON (Stockholm)**

**B. DOLGOSHEIN (Moscow)**

**L.G. EARWAKER (Birmingham)**

**S. GALES (Orsay)**

**I.A. GOLUTVIN (Moscow)**

**F.S. GOULDING (Berkeley)**

**T. ISHIKAWA (Tokyo)**

**P. KIENLE (Darmstadt)**

**G.F. KNOLL (Ann Arbor)**

**H.W. KRANER (Upton, NY)**

**S. KULLANDER (Uppsala)**

**C. KUNZ (Hamburg)**

**J.W. LEAKE (Harwell)**

**J.W. MÜLLER (Sèvres)**

**W. PAUL (Bonn)**

**L.E. REHN (Argonne, IL)**

**A. RENIERI (Frascati)**

**C. ROLFS (Bochum)**

**A.M. SESSLER (Berkeley)**

**N.G. SJÖSTRAND (Göteborg)**

**A.N. SKRINSKY (Novosibirsk)**

**V.P. SULLER (Daresbury)**

**S.C.C. TING (Lexington, MA)**

**M. VAN DER WIEL (Nieuwegein)**

**WANG GANCHANG (Beijing)**

**A.A. WATSON (Leeds)**

**B. WIJK (Hamburg)**

**H. WINICK (Stanford)**

**T. YAMAZAKI (Tokyo)**

**YANG FU-JIA (Shanghai)**

### **Information to Authors**

Contributions to Section A of Nuclear Instruments and Methods in Physics Research (NIM A), written in English, French or German, and books for review may be sent either directly to Professor Siegbahn, Institute of Physics, Box 530, 751 21 Uppsala, Sweden, or to one of the members of the Editorial Board. Manuscripts and copies of figures should be submitted in *duplicate*, together with one set of good quality figure material for production of the printed figures. Short contributions of *less than 1500 words* and not subdivided into sections may be published as Letters to the Editor in a shorter time than regular articles as the proofs will normally be corrected by the Publisher.

Correspondence with the Publisher regarding articles accepted for publication or the return of corrected proofs should be addressed to: NIM A, Elsevier Science B.V., P.O. Box 103, 1000 AC Amsterdam, The Netherlands.  
Fax: (20) 5862 775; tel: (20) 5862 533/500; telex: 10704 ESPOM NL; email: nima-j@elsevier.nl

There are no page charges to individuals for publication of an article in this journal. 50 reprints of each article will be supplied free of charge. Further reprints can be ordered from the Publisher on the Order Form sent out with the proofs.

### **Subscriptions**

Nuclear Instruments and Methods in Physics Research - A (ISSN 0168-9002). For 1994, volumes 337-351 are scheduled for publication. Subscription prices are available upon request from the Publisher. A combined subscription to NIM A volumes 337-351 and NIM B volumes 83-94 is available at a reduced rate.

Subscriptions are accepted on a prepaid basis only and are entered on a calendar year basis. Issues are sent by surface mail except to the following countries where air delivery via SAL is ensured: Argentina, Australia, Brazil, Canada, China, Hong Kong, India, Israel, Japan, Malaysia, Mexico, New Zealand, Pakistan, Singapore, South Africa, South Korea, Taiwan, Thailand, USA. For all other countries airmail rates are available upon request.

Please address all requests regarding orders and subscription queries to: Elsevier Science B.V., Journal Department, P.O. Box 211, 1000 AE Amsterdam, The Netherlands, tel. +31 20 5803642, FAX: +31 20 5803598. Claims for issues not received should be made within six months of our publication (mailing) date.

### **Information for Advertisers**

Advertising orders and enquiries can be sent to the Advertising Manager, Elsevier Science B.V., Advertising Department, P.O. Box 211, 1000 AE Amsterdam, The Netherlands, tel. (20) 515 3220; fax: (20) 683 3041. UK: T.G. Scott & son, Portland House, 21 Narborough Road, Cosby, Leicestershire LE9 5TA, tel: (533) 753 333; fax: (533) 750 522, attn. Tim Blake. USA, Canada: Weston Media Associates, Daniel S. Lipner, P.O. Box 1110, Greens Farms, CT 06436-1110, USA, tel. (203) 261 2500, fax: (203) 261 0101.

Elsevier Science B.V.: All rights reserved. No part of this publication may be reproduced, stored in a retrieval system or transmitted in any form or by any means, electronic, mechanical, photocopying, recording or otherwise, without the written permission of the Publisher, Elsevier Science B.V., Copyright & Permissions Department, P.O. Box 521, 1000 AM Amsterdam, The Netherlands.

*Special regulations for authors* - Upon acceptance of an article by the journal, the author(s) will be asked to transfer copyright of the article to the Publisher. This transfer will ensure the widest possible dissemination of information.

*Special regulations for readers in the USA* - This journal has been registered with the Copyright Clearance Center, Inc. Consent is given for copying articles for personal or internal use, or for the personal use of specific clients. This consent is given on the condition that the copier pays through the Center the per copy fee stated on the first page of each article for copying beyond that permitted by Sections 107 or 108 of the US Copyright Law. The appropriate fee should be forwarded with a copy of the first page of the article to the Copyright Clearance Center, Inc., 21 Congress St., Salem, MA 01970, USA. If no code appears on an article, the author has not given consent to copy and permission to copy must be obtained directly from the author. All articles published prior to 1981 may be copied for a per copy fee of US \$2.25, also payable through the Center. (N.B. For review journals this fee is \$0.25 per copy per page.) This consent does not extend to other kinds of copying, such as for general distribution, resale, advertising and promotion purposes, or for creating new collective works. Special written permission must be obtained from the Publisher for such copying.

No responsibility is assumed by the Publisher for any injury and/or damage to persons or property as a matter of products liability, negligence or otherwise, or from any use or operation of any methods, products, instructions or ideas contained in the materials herein. Although all advertising material is expected to conform to ethical standards, inclusion in this publication does not constitute a guarantee or endorsement of the quality or value of such product or of the claims made of it by its manufacturer.

*US mailing notice* - Nuclear Instruments and Methods in Physics Research - A (ISSN 0168-9002) is published semimonthly with one additional issue in February, April and August, and with two additional issues in January and March (total 31 issues) by Elsevier Science B.V., Molenwerf 1, P.O. Box 211, 1000 AE Amsterdam, The Netherlands. Annual subscription price in the USA is US \$5435 (valid in North, Central and South America only), including air speed delivery. Second class postage paid at Jamaica, NY 11431.

**USA POSTMASTERS:** Send address changes to Nuclear Instruments and Methods in Physics Research - A. Publications Expediting, Inc., 200 Meacham Avenue, Elmont NY 1103. Airfreight and mailing in the USA by Publication Expediting.

Published semimonthly

Printed in The Netherlands

# Study of beam dynamics for an intense, high-brightness $H^-$ beam to design an efficient low-energy beam transport using ESQ lenses

S.K. Guharay \*, C.K. Allen, M. Reiser

*Institute for Plasma Research, University of Maryland, College Park, MD 20742, USA*

(Received 21 May 1993; revised form received 20 September 1993)

With an aim of transporting an initially diverging high-perveance (generalized beam perveance  $2I_b/I_0\beta^3\gamma^3 = 0.003$ ), high-brightness (normalized brightness  $\sim 10^{11} A/(m \text{ rad})^2$ )  $H^-$  beam and finally focusing it without any significant emittance dilution, a detailed simulation scheme has been set up incorporating the various nonlinear forces due to the beam and the external focusing elements, e.g., due to space charges, geometrical and chromatic aberrations. The analysis is done following a particular hierarchy to identify the mechanism of emittance growth; this procedure is used to optimize the lens parameters. A combination of six electrostatic quadrupole lenses is configured to deliver a satisfactory solution. The estimated emittance growth is a factor of about 1.6, and this is mainly due to chromatic aberrations. A relatively small group of particles is found to be responsible for the emittance growth. The analysis highlights a number of important issues, e.g., sensitivity to the beam distribution, beam current, lens misalignments, etc. An ESQ LEBT system with some novel features in terms of compactness and mechanical rigidity is developed, and its essential characteristics are described.

## 1. Introduction

The study of high-brightness charged particle beam transport has great relevance in many modern applications. In today's and next generation's high energy colliders, e.g., Tevatron, SSC, NLC, etc., one of the vital requirements is to achieve luminosity of colliding charged particle beams of order  $10^{31} \text{ cm}^{-2} \text{ s}^{-1}$  or higher; this demands that beam brightness also be very high [1].  $H^-$  beams, with normalized brightness of  $\geq 10^{12} A/(m \text{ rad})^2$ , are required in space defense for generation of intense particle beams to probe any foreign objects. The importance of high intensity, high-brightness beams is also evident in heavy-ion fusion (HIF), free electron lasers, etc., and of late, in an attractive scheme for radio-active waste transmutation [2]. The recent trends of ion-beam related research in accelerators and fusion reveal that major activities have been initiated with  $H^-$  beams due to their merits over proton beams:

(a) Given a phase-space area, the intensity of an  $H^-$  beam can be enhanced significantly by adapting the

principle of non-Liouvillian stacking. This is particularly useful in modern accelerators.

(b) The charge-exchange cross section at energy  $\geq 100 \text{ keV}$  is much higher for  $H^-$  beams; hence,  $H^-$  beams are used for the development of high-energy neutral beams in magnetic fusion research and also in space defense.

During its long travel through the various components in an accelerator, the characteristics of an ion beam are significantly determined by its behavior in the early stages, e.g., extraction optics in the ion source and subsequently, the low-energy beam transport (LEBT) section. The crux of the problem is to obtain a high quality beam (usually defined by the beam emittance) from an appropriate ion source with minimum distortions due to aberrations and nonlinear forces, and to preserve its quality, as much as possible, in the transport and acceleration chain. This article focuses on the LEBT section as a systematic study on this part is still missing, particularly in relevance to transport and focusing of space-charge dominated, high-brightness  $H^-$  beams.

The LEBT section isolates the first stage of acceleration, e.g., a radio-frequency quadrupole accelerator (RFQ), from an ion source providing a buffer space for

\* Corresponding author.

differential pumping; also, it presents a clean, matched beam to an RFQ. The gas focusing scheme, usually supplemented by magnetic quadrupoles or solenoidal magnets, has been mostly used as a LEBT system [3-5]. The advantage of the scheme is that the experimental hardware is simple, and it is capable of handling large beam current,  $\geq 100$  mA. However, this scheme is not well suited to beam-pulses shorter than the gas neutralization time, typically  $\geq 50$   $\mu$ s. Also, due to the complex nature of atomic and molecular processes involved, it is difficult to set up accurate computer simulation models and obtain reliable predictions *a priori*. Thus our understanding of this approach remains at a qualitative level, and there is some ambiguity in the definition of the control parameters in experiments. One of the most impressive applications of the gas focusing scheme has been in the context of the BEAR (Beam Experiment Aboard a Rocket) accelerator program at Los Alamos [4]. Results on the sensitivity of beam parameters to variations of the gas pressure suggest that reproducible operation of such a scheme is very difficult. The other LEBT schemes include radio-frequency quadrupole (RFQ) lenses [6] and electrostatic lenses [7-12], e.g., einzel lens, electrostatic quadrupole (ESQ) lens, and helical electrostatic quadrupole (HESQ) lens. Until now, the utility of RFQ lenses has been least explored. In the category of electrostatic lenses, einzel lenses are commonly used. The conventional einzel lenses have a drawback in that plasmas may build up in the field-free region, rendering the system susceptible to beam-plasma instabilities. Anderson's "ring" lens version appears to be free from this problem [8]. The einzel lenses require power supplies close to the beam voltage, typically  $\sim 30$  kV for a 35 kV beam; the ESQ lenses have an edge over the einzel lenses in this respect. Several practical factors, e.g., tuning with low-voltage power supplies (typically  $< 10$  kV), elimination of any field-free region, and ease of computer modeling, make the ESQ system a very attractive choice as a LEBT. Reiser [13] reported briefly a comparative study of the aforementioned LEBT schemes. It is understood that in spite of a good deal of research involving LEBT systems, a systematic study of beam dynamics and optimization of LEBT parameters has not been made in the context of transporting intense, high-brightness  $H^-$  beams. In order to obtain insight into the problem and advance the present state-of-the art of LEBT systems, detailed simulation studies should be first made, and the simulation predictions be compared with experimental results. In a recent article Bru enumerated a beam transport program in which all the forces are considered linear [14]. The present article addresses in detail for the first time the beam dynamics issues relevant to designing an ESQ LEBT for intense, high-brightness  $H^-$  beams incorporating the various nonlinear effects due to aberrations,

fringe-fields, etc.; a special emphasis is given here to understanding emittance growth and methods to control it. Typical beam parameters of a Penning-Dudnikov type ion source are considered in which the generalized beam permeance  $K = 0.003$  and normalized beam brightness  $B_n \sim 10^{11}$  A/(m rad)<sup>2</sup>. Here,  $K$  is defined as the ratio of  $2I_b/I_0\beta^3\gamma^3$ , where  $I_b$  is the beam current,  $I_0$  is the characteristic current ( $3.1 \times 10^7$  A for  $H^-$  beam),  $\beta = v/c$ ,  $\gamma = (1 - \beta^2)^{-1/2}$ .

Some key physics issues on emittance growth in an ESQ LEBT and its control are investigated in detail. The simulation scheme is developed in steps. A linear beam optics code is written to integrate the well-known K-V envelope equations. The lens parameters are approximated from this analysis. A 3D Laplace solver maps the equipotentials of the lens system, and the fringe fields are evaluated. Several articles have dealt with fringe fields [15-20]. Following the method of Matsuda and Wollnik [19], the effect of the fringe fields is included here in a particle simulation code, which essentially is a modified version of the well-known PARMILA code [21]. The evolution of emittance through the ESQ LEBT channel is determined from the modified PARMILA code. This simulation scheme is iterated until a satisfactory solution is obtained. The analysis is made here in the context of transporting an initially round (radius = 1 mm), diverging (slope = 20 mrad at the full beam radius) 30 mA, 35 kV  $H^-$  beam over a length of about 30 cm and transforming it into a round (radius  $\sim 1$  mm), converging (slope  $\sim -40$  mrad) beam. The control parameters of an ESQ lens can be simulated reasonably well, and this permits to delineate an in-depth investigation of the various sources of emittance dilution. This study thus establishes a strong foundation for designing an efficient LEBT system. Some comments are made on the development of the LEBT system and its experimental tests; details are beyond the scope of this paper and these issues will be reported elsewhere.

Section 2 pertains to the beam dynamics. Some characteristic features of the LEBT system are given in Section 3. Section 4 includes conclusions.

## 2. Beam dynamics through the ESQ LEBT

### 2.1. Linear beam optics calculations

The study of beam dynamics in an ESQ LEBT system is developed from a rather simple, idealistic model in order to set up the lens parameters grossly. Afterwards, the simulation is done including various practical features, e.g., real geometry of the electrodes, fringe fields, aberrations, etc. First, a beam optics code, which includes a linear external focusing force, here a hard-edge type, in the K-V envelope equations

is used; this integrates the following coupled equations by fourth-order Runge–Kutta method and gives the behavior of the beam envelope.

$$X'' + \kappa_x(z)X - \frac{2K}{X+Y} - \frac{\epsilon_x^2}{X^3} = 0,$$

$$Y'' + \kappa_y(z)Y - \frac{2K}{X+Y} - \frac{\epsilon_y^2}{Y^3} = 0.$$

$\epsilon_x$  and  $\epsilon_y$  are the  $x$  and  $y$  components of the unnormalized beam emittance, respectively. The focusing function due to the externally applied force is  $\kappa = V_q/(V_b R_q^2)$ , where  $V_q$  is the applied voltage on the quadrupole,  $V_b$  is the beam extraction voltage, and  $R_q$  is the aperture radius of the quadrupole. The derivatives are taken with respect to  $z$ , which follows the direction of propagation of the beam. The amplitude of the beam envelope,  $X(z)$  and  $Y(z)$ , is determined using certain values of the input beam parameters and an assumed configuration of the lens geometry. In the case of any gas accumulation in the channel, which may occur at the interface between an ion source and a LEBT, the above equations are solved with the beam perveance term  $K$  multiplied by  $(1 - \gamma^2 f)$ ;  $f$  is the charge neutralization factor and  $\gamma = (1 - \beta^2)^{-1/2}$ .

In order to validate the results predicted by the linear beam optics code, the various nonlinear contributions, namely due to aberrations, fringe fields and image effects, are to be minimized. The following constraints control the nonlinear effects [22].

(i) If the maximum beam excursion is not allowed to exceed 10% of the length of a quadrupole  $l$ , spherical aberrations may be kept at low level.

(ii) To reduce chromatic aberrations, the change in the beam energy due to the quadrupole focusing field should be less than about 5% of the total beam energy  $qV_b$ .

(iii) The image field may be neglected if the maximum excursion of the beam envelope remains within 75% of the quadrupole aperture radius  $R_q$ .

The following empirical relationship is satisfied to avoid any voltage breakdown [27]

$$d(\text{cm}) > 1.4 \times 10^{-3} V^{3/2} (\text{kV}),$$

Table 1  
Estimated  $\text{H}^-$  beam parameters

Beam current $I_b$	30 mA
Beam voltage $V_b$	35 kV
$v/c = \beta$	$8.6 \times 10^{-3}$
Generalized beam perveance $K = 2I_b/I_0\beta^3\gamma^3$	$3 \times 10^{-3}$
Initial rms normalized emittance $\epsilon_n \pi$	$0.069 \pi \text{ mm mrad}$
Initial beam radius $a$	1 mm
Initial divergence of beam envelope at $r = a$	20 mrad

Table 2  
ESQ lens parameters

	Lens Number		
	1&6	2&5	3&4
$R_q$ (mm)	8.00	12.00	12.00
$l$ (mm)	15.00	59.00	47.00
$L$ (mm)	6.00	6.00	6.00

where  $d$  is the interelectrode spacing and  $V$  is the voltage difference.

Due to limited accessibility in the neighborhood of the beam extraction region, it is difficult to obtain a reliable knowledge of beam parameters at the extraction point; this introduces some ambiguity in the initial values of the beam parameters which are given as input to the code. Usually measurements are made at a distance of about 10 cm downstream from the extraction slit and the data are interpolated using some simulation model to predict beam parameters at the extraction point. Table 1 lists the estimated values of the  $\text{H}^-$  beam parameters corresponding to the Penning–Dudnikov source used in the BEAR experiment, when the nominal emittance data [24] measured at a distance of 10.6 cm downstream from the extraction aperture have been used.

The desired solution is obtained after several iterations, when the lens parameters (e.g., aperture and dimensions of the individual lenses, spacing between the lenses, and number of lens elements) are adjusted at each step. As mentioned earlier, the beam envelope is constrained at each stage through the LEBT system so that distortions due to aberrations and image effects are minimized. The LEBT system has been thus configured using a set of six ESQ lenses. The geometrical parameters of the lenses are given in Table 2. Here  $l$  is the length of an electrode and  $L$  is the separation between adjacent lenses. Note that the geometrical parameters of lenses 1 and 6, 2 and 5, and 3 and 4 are identical; thus two mirror-image triplets are cascaded in the LEBT.

Fig. 1 shows the K–V envelope solution (top figure), when the input beam parameters correspond to Table 1 and a hard-edge type focusing function (bottom figure),  $\kappa(z)$ , is assumed. The voltages on the three sets of similar lenses (1 and 6, 2 and 5, and 3 and 4) are, respectively, 7.825, 3.875, and 3.820 kV. The envelope parameters of the output beam (designated by subscripts f) at two locations are given in Table 3 to elucidate the nature of focusing; the downstream location at  $z = 287$  mm corresponds to the end of the last lens in the LEBT. These results suggest that the ESQ LEBT system can deliver a converging, round beam to the next stage, typically an RFQ in the linear accelerator section, and the beam will be well matched if the

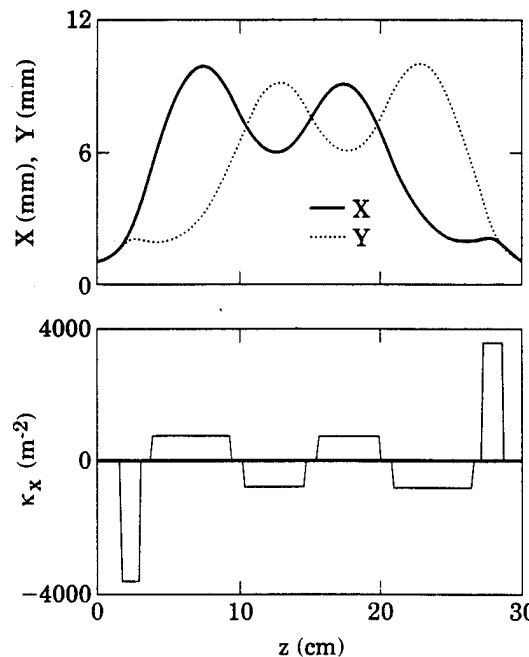


Fig. 1.  $X$  and  $Y$  are the amplitudes of the beam envelope in  $x$  and  $y$  directions;  $z$  is the direction of propagation.  $\kappa_y = -\kappa_x$ . Note that  $X$  (and  $Y$ ) = 12 mm corresponds to the maximum aperture of the electrodes.

RFQ entrance is very closely ( $< 1$  cm) coupled to the last lens of the LEBT.

An intriguing feature in the present LEBT is that the combination of the four lenses (number 1, 2, 5, and 6) is used to transform the diverging input beam into a converging one, while the other two lenses (number 3 and 4) act as a FODO transport section providing an adequate length of the LEBT. The FODO section may be cascaded to obtain any desired length of the LEBT.

### 2.2. 3D field mapping and evaluation of fringe fields

The exact geometry of the lens system is used, and the equipotentials are mapped solving the 3D Laplace equation. Cylindrical electrodes with some shaping of the end faces following Laslett [25] and Dayton et al. [26] are used, when the field is expected to be quadrupolar within about 90% of the lens aperture. In

Table 3  
Beam parameters at the output end of the LEBT

$z$ (mm)	$X_f$ (mm)	$Y_f$ (mm)	$X'_f$ (mrad)	$Y'_f$ (mrad)
293.0	1.39	1.37	-53.1	-53.7
302.0	1.03	1.00	-24.0	-24.3

order to minimize interference between two adjacent lenses [27], a grounded plate is inserted between the lenses. Following the notations of Matsuda and Wollnik [19], the potential distribution  $\phi$  can be expressed as

$$\phi(x, y, z) = \frac{k(z)}{2} (x^2 - y^2) - \frac{k''(z)}{24} (x^4 - y^4) + \dots,$$

up to the fourth order, while the electrostatic field components are governed by

$$E_x(x, y, z) = -k(z)x + \frac{k''(z)}{6}x^3 + \dots,$$

$$E_y(x, y, z) = k(z)y - \frac{k''(z)}{6}y^3 - \dots,$$

$$E_z(x, y, z) = 0 - \frac{k'(z)}{2}(x^2 - y^2) + \dots,$$

up to the third order. The first term in the above expressions represent the field components of a pure quadrupolar field; the fringe field, which has a nonlinear behavior, contributes due to the second derivative term in  $k$  for  $E_x$  and  $E_y$ , and is governed by  $k'$  for  $E_z$ . The function  $k(z)$  is determined from the equipotentials. This result in conjunction with the values of the beam amplitude components giving  $x$  and  $y$  at various  $z$ -locations from Fig. 1 is used to evaluate a comparative estimate of the main field and the fringe field which the beam envelope is expected to encounter in our particular design. Figs. 2a, 2b, and 2c show the field components, respectively, in  $x$ ,  $y$ , and  $z$ -directions; Fig. 3 shows the effective magnitude of the field components. It is evident that the contribution of the correction terms due to the fringe field is very localized over a small region towards the edges of each lens in the ESQ LEBT, and the main field significantly dominates. This suggests that geometrical aberrations may not be serious in the present ESQ system.

### 2.3. Beam dynamics calculations and analysis of sources of emittance growth

The results from the above two steps of analysis are used in a particle simulation code, PARMILA, to study the beam dynamics in further details. This code essentially pushes particles using a chain of transfer matrices, where the matrix elements are characterised by the factors governing the motion of the beam, e.g., space charge, drift space, lens elements, etc. This code adapts the following key points.

(a) The space-charge force is calculated assuming the beam as an ensemble of typically 5000 ring-like macroparticles. The macroparticles follow certain dis-

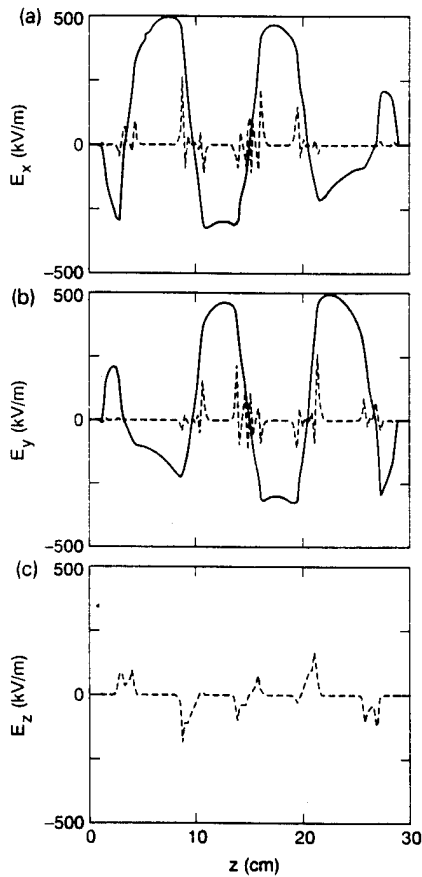


Fig. 2. 3D LAPLACE results of the field components: (a)  $E_x$ , (b)  $E_y$ , and (c)  $E_z$ . Solid line: pure quadrupole field; dashed line: fringe field. The field components are calculated using the  $x$  and  $y$  values of the beam amplitude components at various  $z$  as used in Fig. 1.

tributions in both configuration and phase spaces, e.g., K-V, waterbag, semi-Gaussian, Gaussian, etc.

(b) The electrostatic field due to the lens is decomposed into two parts: a main field of hard-edge type

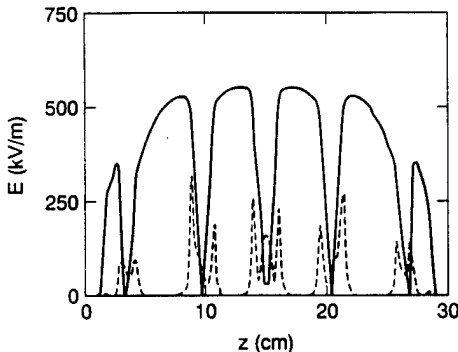


Fig. 3. Effective magnitude of the fields. Solid line: quadrupole field; dashed line: fringe field.

within the lens region, and fringe fields outside this ideal boundary. In order to get a realistic evaluation of the hard-edge boundary which can effectively represent the quadrupolar field component of a lens, an equivalent length is defined as

$$l_{\text{eff}} = \frac{1}{\kappa_0} \int_{z_2}^{z_1} \kappa(z) dz,$$

where  $\kappa_0$  is the peak value of  $\kappa$  in the flat-top region as shown in Fig. 2,  $z_1$  and  $z_2$  correspond to the zero-crossing locations of  $\kappa(z)$  on the immediate two opposite ends of a lens. A set of integrals involving  $\kappa(z)$ , as prescribed by Matsuda and Wollnik [19], is used to model the force due to the fringe field. This force is applied at the ideal hard-edge boundary, and the shifts and bends of the particle motion due to fringe fields are incorporated in the PARMILA code [22].

(c) The trajectory of the macroparticles is followed systematically with due considerations of field distributions over a cross-section of the beam. The energy conservation law is followed to tackle this problem

$$\frac{1}{2}mv_0^2 + eV_0 = \frac{1}{2}mv(r)^2 + eV(r).$$

where  $v_0$  and  $v(r)$  denote, respectively, the velocity of particles on the axis (this is equal to  $(2eV_b/m)^{1/2}$ ) and at an arbitrary location  $r$ , and  $V_0$  and  $V(r)$  correspond to the electrostatic potential due to the lens at the respective locations.

Fig. 4 shows the behavior of the particle distribution at the output of the ESQ LEBT when a K-V type distribution of the input beam particles is assumed. The distortions in the output beam are due to nonlinear effects, and this leads to some emittance growth. In this particular example, the emittance growth is a factor of about 1.6. The ellipses composed from the Twiss parameters for the output beam show a very similar nature in the two orthogonal planes; these ellipses are drawn using the effective emittance  $\epsilon = 4\bar{\epsilon}$  due to Lapostolle [29]. The corresponding characteristic beam parameters are:  $X_{\text{max}} = 1.6$  mm,  $Y_{\text{max}} = 1.3$  mm,  $(X_{\text{max}})' = -41.7$  mrad, and  $(Y_{\text{max}})' = -39.2$  mrad; a better matching of the parameters in the two orthogonal planes may be fortuitous. Various other types of distributions, e.g., waterbag, semi-Gaussian, Gaussian, have been also considered. The particle distribution of the output beam in its configuration space is shown in Fig. 5 for the various distributions. A small group of particles ( $\leq 5\%$ ) is detached from the dense core group in the case of semi-Gaussian and Gaussian distributions; these particles are essentially lost from the system as their location corresponds to the boundary of the electrodes. The rapid blow-up of the beam for a non-KV distribution (semi-Gaussian or Gaussian) may be an artifact of excess energy in tail particles of the

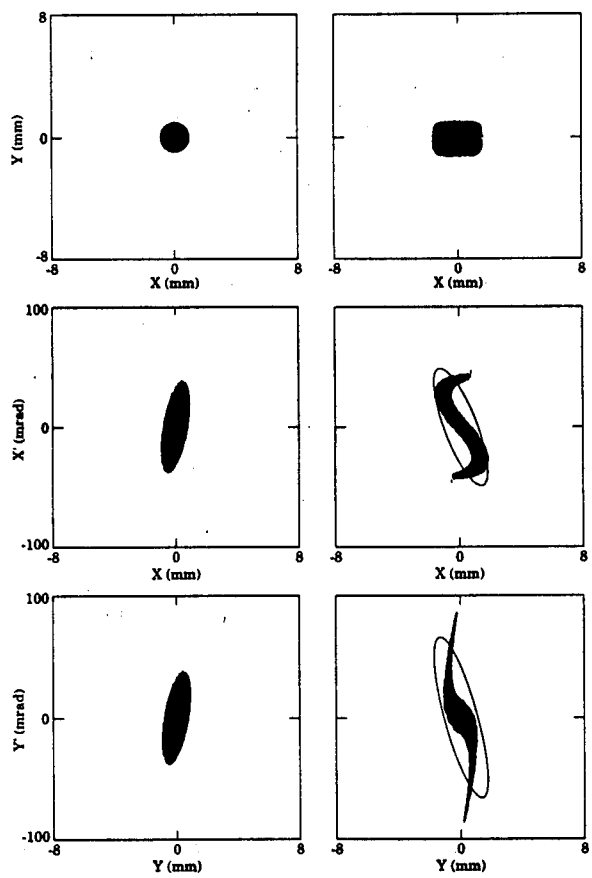


Fig. 4. Particle distribution in the output beam (right column) of the ESQ LEBT for a K-V type input beam (left column). Note that  $X$  (and  $Y$ ) = 8 mm corresponds to the aperture of the first and last lenses.

distribution function. For the sake of comparison of the beam behavior in the two extreme cases, the output beams are shown in Fig. 6 for K-V and Gaussian (with the tail cut off at  $4\sigma$ ) distributions of the input beam. The phase-space area occupied by the core group of particles seems to be similar in the two cases. The emittance of the output beam will practically follow the dynamics of a K-V type input beam if distribution is tailored to a low-temperature beam. As a K-V type distribution is commonly used in the literature for basic analysis of beam dynamics and also, it seems to represent well the beam distribution particularly in the case of a space-charge dominated, high-brightness beam [28], we have extended our analysis assuming a K-V type distribution of the input beam.

The evolution of emittance growth, as the beam propagates through the ESQ LEBT, is shown in Fig. 7. It is noted that the emittance is primarily enhanced at the second lens in the  $x$ -plane and at the fifth lens in the  $y$ -plane. This result conforms to the previous findings from the linear beam optics code when large beam

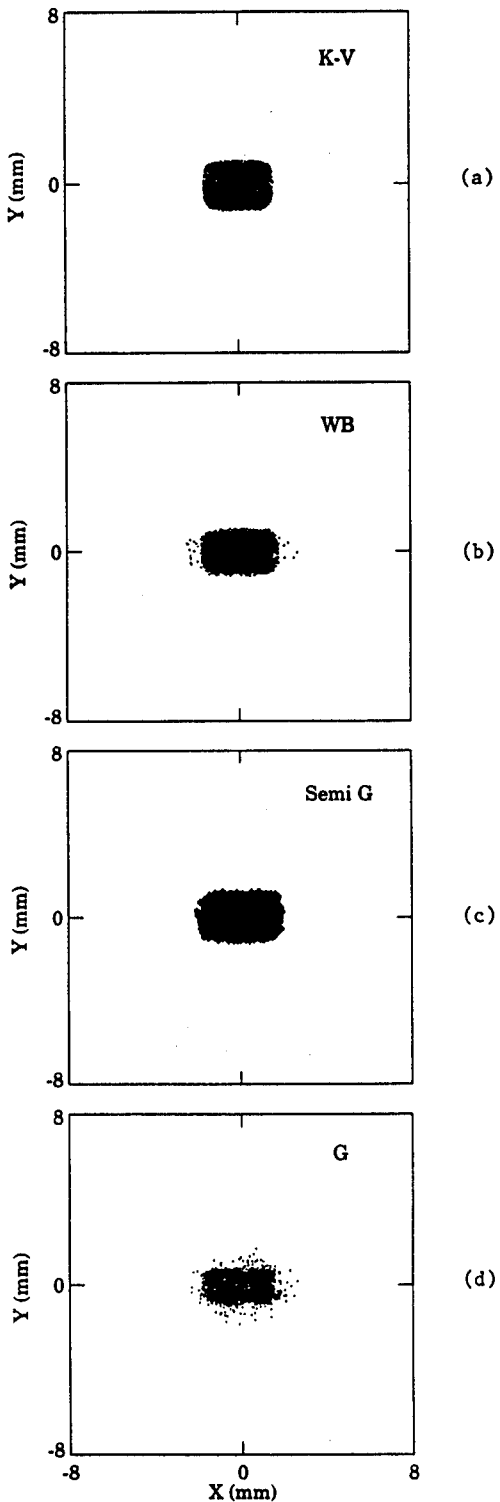


Fig. 5. Configuration-space geometry of the output beam for various input distributions: (a) K-V, (b) waterbag, (c) semi-Gaussian, and (d) Gaussian.

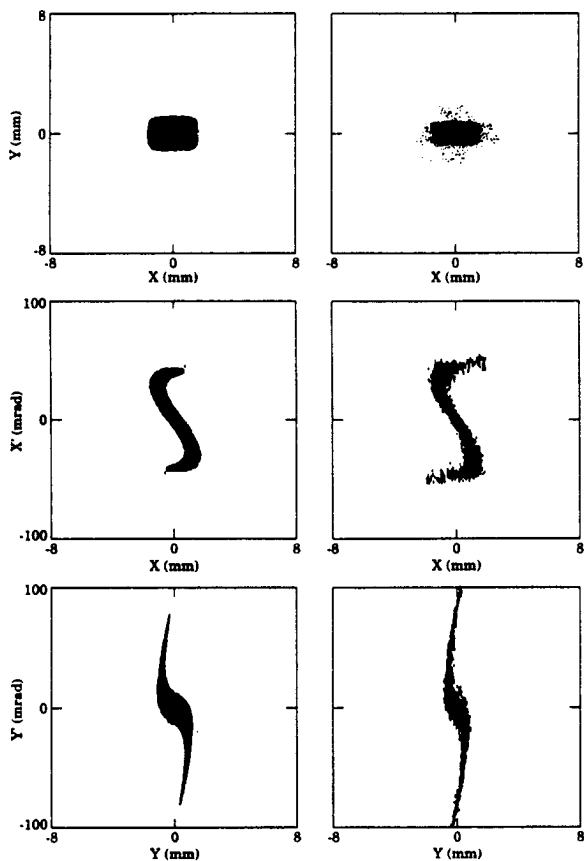


Fig. 6. Comparison of phase-space distribution of the particles in the output beam for K-V (left column) and Gaussian (right column) input distributions.

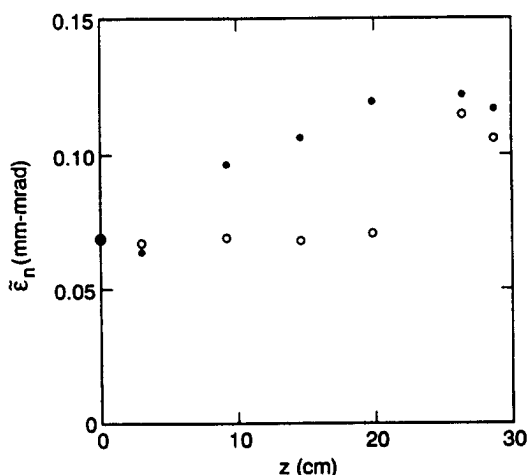


Fig. 7. Spatial evolution of rms emittance through the ESQ LEBT. The emittance values are plotted at the end of each lens in the LEBT. Solid circle: x-plane emittance; open circle: y-plane emittance.

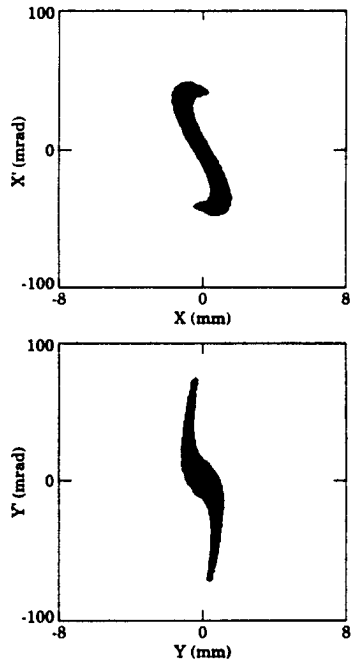


Fig. 8. Phase-space distribution of particles in the output beam when 4% of the beam is intercepted by two beam scrapers.

excursions (Fig. 1) have been noted at the aforementioned two lens elements; nonlinear effects act strongly when the amplitude of the beam envelope is large. In our simulation studies it is possible to diagnose the principal contributors to emittance growth and reject some of the unwanted group of particles by using appropriately shaped ground plates between the lenses as beam scrapers, and thus the emittance growth may be controlled. Fig. 8 shows an emittance growth by a factor of about 1.5 only when two beam scrapers are introduced: one in front of the second lens and the other in front of the fifth lens; about 4% of the beam particles is rejected here. This seems to be an easy way to control emittance of the output beam.

In an effort to further understand the effect of nonlinear forces, the architecture of the simulation code is made appropriately to evaluate the contribution of various factors piecewise, i.e., term by term. First, the transverse energy of all the beam particles is numerically maintained at a constant value through the entire LEBT. Fig. 9 shows the output beam distribution. It is evident that the output beam is free from any major distortions. The emittance growth is estimated to be reduced by more than 90%. This suggests that the chromatic aberration is the principal contributor to emittance growth in the present case. Turning the fringe-field terms off in the simulation, it is noted that the emittance growth is reduced very insignificantly.

This indicates that geometrical aberrations do not play a major role here.

The sensitivity of output beam parameters with variation of beam voltage, beam current, injection error has been studied. Using the linear beam optics code it is noted that the beam parameters do not change noticeably for a  $\pm 1\%$  change of quad voltage (from the ideal setpoint) on all the lenses simultaneously. Similar insensitivity is noted for variation of beam current (ideal = 30 mA) within a few milliamperes. The effect of an injection error is studied using PARMILA. With the variation of the amount of off-centering of the input beam, the qualitative nature of the phase-space distribution of the output beam remains almost invariant, while the beam centroid shifts coherently. A translational off-centering by 1 mil ( $= 0.0254$  mm) at the input causes an off-centering of the beam by about 3 mil at the output of the LEBT; this

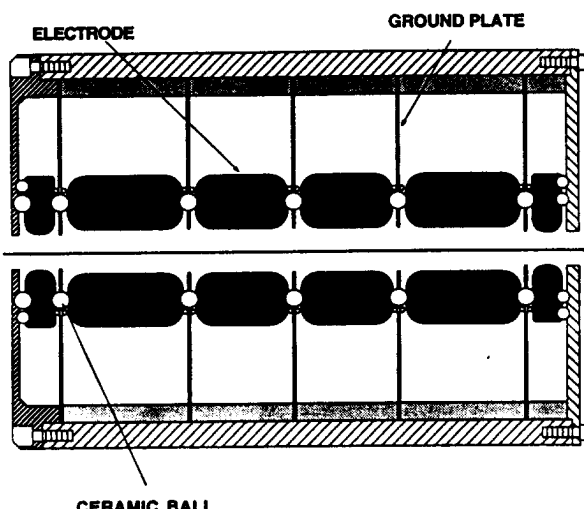


Fig. 10. Schematic layout of the ESQ LEBT.

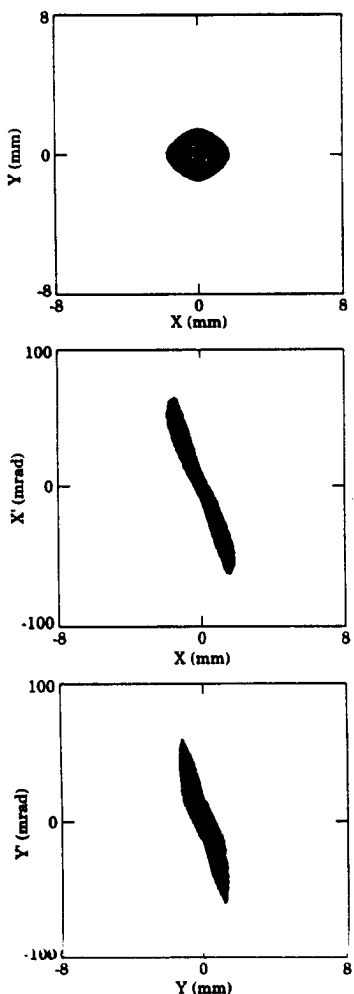


Fig. 9. Particle distribution in the output beam when all the particles are assumed to be transported with the same energy (35 kV).

also introduces an angular error of the beam centroid by about 1.5 mrad. An on-centered input beam with an error in the injection angle by 1 mrad shows an off-centering of the output beam by about 2 mil; the error in the angle does not change appreciably through the LEBT channel.

### 3. Development of the ESQ LEBT apparatus

The aforementioned guidelines are used to develop an ESQ LEBT system. Fig. 10 shows a schematic of the LEBT system developed in-house at Maryland. The principal elements of the ESQ LEBT are: (i) six quadrupole lenses, (ii) ground plates between the lenses, and (iii) precision ceramic insulating balls. The four electrodes of each lens are machined out of a single piece of finished cylindrical aluminium rod. The dimensional accuracy of each electrode is measured to be within  $\pm 0.2$  mil (average) of the designed value. The aluminium ground plates are 2 mm thick. Ceramic balls are used to develop an adjustment-free, self-aligned lens assembly. Two sets of precision balls with tolerance in sphericity within  $\pm 0.025$  mil are used. Larger balls of  $3/8$  in. diameter are used between two opposing electrodes of adjacent lenses; smaller balls of  $1/8$  in. diameter are placed between the electrodes of a quadrupole and its neighboring ground plate. The ceramic balls are hidden in the shadow of the electrodes in order that they remain mostly obscured to the field of the propagating beam. The entire lens assembly is mounted in a cylindrical housing, which is installed in a large vacuum vessel.

Voltage hold-off tests have been conducted on the lens assembly. With gradual conditioning of the surface of the electrodes by allowing some low-level corona

discharges, the lens system could finally be driven at high voltage (up to about  $\pm 14$  kV) without any noticeable breakdown. This insures practicability of the present ESQ lens design.

#### 4. Conclusions

This article addresses the problems of designing an efficient low-energy beam transport system, particularly in relevance to space-charge dominated, high-brightness  $H^-$  beams. Although several researchers used ESQ LEBT systems in the past and showed some interesting results, the input beam parameters were not as severe as considered in the present case in terms of space-charge forces, beam divergence, etc.; further systematic study of beam dynamics has thus been missing. An emphasis is given here on simulation studies to examine some beam physics issues critically. This approach lays a foundation to develop an efficient LEBT system; especially, the role of the various nonlinear forces on emittance dilution is studied in depth.

The lens assembly is designed following several iterations of the numerical scheme so that the lens geometry is optimized as much as possible. Typical beam characteristics of a high-brightness  $H^-$  source, Penning-Dudnikov type (as used in the BEAR experiment [4]), are used in the analysis with an aim of transporting a space-charge dominated, diverging beam from the source over a length of about 30 cm, and yield a converging beam at the end without significantly deteriorating the intrinsic emittance of the beam. The beam dynamics is studied in detail using a particle simulation code, which enables us to study the influence of various factors in determining the emittance growth, e.g., nonlinear effects due to chromatic aberrations and fringe fields, various types of distributions of the beam, sensitivity of various control parameters, etc.

The main contributor to emittance growth in the ESQ LEBT is found to be chromatic aberrations. It is shown in the simulations that particles responsible for enhancing the emittance growth can be identified and subsequently, they are rejected by carefully using two intermediate ground plates as beam scrapers. Thus the emittance growth can be controlled without sacrificing the beam current appreciably. In the case of the  $H^-$  beam from the Penning-Dudnikov type source the nominal emittance growth through the ESQ LEBT system is estimated to be a factor of about 1.6, while this factor is reduced to about 1.5 by rejecting only 4% of the beam particles. Such a modest value of emittance growth attributes merit to the particular design of the ESQ LEBT.

The ESQ LEBT system developed in-house at Maryland has some uniqueness in its mechanical assembly. The entire system is self-aligned and it is very

rugged mechanically. Each component is fabricated with a dimensional tolerance close to the designed value. Results on voltage hold-off tests of such a compact system are encouraging; no noticeable breakdown events occur up to a voltage level of about  $\pm 14$  kV.

Beam transport experiments are planned using the ESQ LEBT. Details of the experimental work and further studies on beam dynamics will be reported elsewhere.

#### Acknowledgements

This work is supported by the United States Office of Naval Research. The authors acknowledge valuable discussions with Dr. P.G. O'Shea of Los Alamos National Laboratory.

#### References

- [1] D.A. Edwards and M.J. Syphers, AIP Conf. Proc. on High-Brightness Beams for Advanced Accelerator Applications, eds. W.W. Destler and S.K. Guharay, No. 253 (1991) p. 122.
- [2] R.A. Jameson, *ibid.*, p. 139.
- [3] J.G. Alessi, J.M. Brennan and A. Kponov, *Rev. Sci. Instr.* 61 (1990) 625.
- [4] P.G. O'Shea et al., *Nucl. Instr. and Meth. B* 40/41 (1989) 946.
- [5] J. Klabunde, P. Spädtke and A. Schönlein, *IEEE Trans. Nucl. Sci.* NS-32 (1985) 2462.
- [6] D.A. Swenson et al., *Proc. Linear Accelerator Conf.*, Albuquerque, 1990, p. 39.
- [7] C.R. Chang, *Proc. Linear Accelerator Conf.*, Albuquerque, 1990, p. 399.
- [8] O.A. Anderson et al., AIP Conf. Proc. on Production and Neutralization of Negative Ions and Beams, ed. A. Hershovitch, No. 210 (1990) p. 676.
- [9] W. Chupp et al., *IEEE Trans. Nucl. Sci.* NS-30 (1983) 2549.
- [10] S. Okayama, *Nucl. Instr. and Meth. A* 298 (1990) 488.
- [11] Y. Mori et al., *Proc. Linear Accelerator Conf.*, Ottawa, 1992, p. 642.
- [12] D. Raparia, AIP Conf. Proc. on Production and Neutralization of Negative Ions and Beams, ed. A. Hershovitch, No. 210 (1990) p. 699.
- [13] M. Reiser, *Nucl. Instr. and Meth. B* 56/57 (1991) 1050.
- [14] B. Bru, *Nucl. Instr. and Meth. A* 298 (1990) 27.
- [15] H. Wollnik and H. Ewald, *Nucl. Instr. and Meth.* 36 (1965) 93.
- [16] H. Matsuda and H. Wollnik, *Nucl. Instr. and Meth.* 77 (1970) 40.
- [17] H. Matsuda and H. Wollnik, *Nucl. Instr. and Meth.* 77 (1970) 283.
- [18] T. Sakurai, T. Matsuo and H. Matsuda, *Int. J. Mass Spectrom. Ion Processes* 91 (1989) 51.
- [19] H. Matsuda and H. Wollnik, *Nucl. Instr. and Meth.* 103 (1972) 117.

- [20] L. Sagalovsky, Nucl. Instr. and Meth. A 298 (1990) 205.
- [21] G. Boicourt and J. Merson, Los Alamos National Lab. Report LA-UR-90-127 (1990); and references therein.
- [22] C.R. Chang, Ph.D. Thesis, Univ. Maryland, 1989.
- [23] R. Keller, AIP Conf. Proc. on High Current, High Brightness and High Duty Factor Ion Injectors, No. 139 (1985) p. 1.
- [24] P.G. O'Shea, private communication.
- [25] L.J. Laslett, Lawrence Berkeley Report No. HI-FAN-137.
- [26] I.E. Dayton et al., Rev. Sci. Instr. 25 (1954) 485.
- [27] H. Wollnik, Optics of Charged Particles (Academic Press, 1987).
- [28] I. Kapchinskij, private communication.
- [29] P.M. Lapostolle, IEEE Trans. Nucl. Sci. NS-18 (1971) 1101.

**An electrostatic LEBT for a low-emittance injector: transport and focusing of a high-brightness  $H^-$  beam from a magnetron ion source**

**S. K. Guharay and M. Reiser**

**Institute for Plasma Research**

**University of Maryland**

**College Park, MD. 20742**

**U.S.A.**

**Abstract**

In the context of developing an efficient low-energy beam transport (LEBT) system for a low-emittance injector the problem of transport and matching of a 30 mA, 35 kV  $H^-$  beam from a magnetron-type ion source is studied; the analysis is done incorporating important experimental constraints. A 30 cm-long LEBT, consisting of six electrostatic quadrupole lenses and a short einzel lens, is designed. Its control parameters are optimized to achieve a solution which matches with the acceptance of a small-aperture radio-frequency quadrupole (RFQ) accelerator. The results of beam dynamics calculations are discussed, and the key issues for emittance growth and its control are acknowledged.

## I. Introduction

In high-energy physics a major thrust of work is currently laid on the development of a high-luminosity ( $\sim 10^{34} \text{ cm}^{-2}\text{s}^{-1}$ ) collider. In this context, the Fermi National Laboratory (FNAL) recently organized a workshop to examine the present state-of-the-art in accelerator research and to identify the bottlenecks. Analyzing the emittance budget through the accelerator chain of a conceptual high-luminosity collider it has been recognized [1] that one of the major problems remains in relation to transport and matching in the section comprising the ion source, the LEBT, and the RFQ accelerator; a good handshake among these three components of the injector needs to be established. Experimental results with  $\text{H}^+$  beams [2, 3] reveal that a significant part of the beam from an ion source is lost in the low-energy section of an accelerator primarily due to mismatch and large emittance growth. This calls for a strong research and development program to design and build an improved injector which can satisfy the stringent requirements of a high-luminosity collider. In this context, the design considerations of the Superconducting Super Collider (SSC) [4] may be referred. The beam current in the collider was taken as 25 mA during a macropulse. In order to achieve this goal, a 30 mA, 35 kV  $\text{H}^+$  beam with rms normalized emittance typically in the range of about 0.12 - 0.18  $\pi \text{ mm mrad}$  was considered from an ion source. The acceptance ellipse of the SSC RFQ restricted the input rms normalized emittance (transverse) to 0.2  $\pi \text{ mm mrad}$ . These parameters, along with the practical constraints due to mechanical structures in the interfacing regions, often pose a challenge to design an efficient LEBT system. In transporting a 30 mA, 35 kV  $\text{H}^+$  beam from a volume source the experimental results with two einzel lenses at the SSC Laboratory [5] showed a large emittance growth - a factor of about 2.5 in the vertical plane and about 5.0 in the horizontal plane; the transmission through the RFQ was about 65%. In this context, we reported the beam dynamics calculations

for an alternative hybrid LEBT system consisting of six electrostatic quadrupole (ESQ) lenses in a compact configuration and one short einzel lens; a matched beam solution for the full beam current of 30 mA was obtained and the emittance growth was estimated to be a factor of 1.6 only [6]. The different LEBT schemes for the SSC Laboratory were reported in a recent article [7].

In the present article, we have studied the problem of transport and focusing of a 30 mA, 35 kV  $H^-$  beam from a magnetron-type ion source which is commonly used in many laboratories [2,8]. Here, the generalized beam perveance is  $K = 2I/(I_0 \beta^3 \gamma^3) = 0.003$ , and the normalized beam brightness is  $B_n = 2I/(\pi^2 \epsilon_n^2) \sim 10^{12} \text{ A}/(\text{m rad})^2$ ;  $I$  is the beam current,  $I_0$  is the characteristic current for  $H^-$  beams = 31 MA,  $\beta$  and  $\gamma$  are the usual relativistic notations, and  $\epsilon_n$  represents four times rms normalized emittance. It may be noted that the characteristics of the  $H^-$  beam from a magnetron source are quite different from the volume source case which we had studied earlier [6]. In the magnetron case, the beam from the source is usually much smaller (radius  $\sim 1.0\text{-}1.25 \text{ mm}$ ) than in the volume source case (radius  $\sim 4\text{-}6 \text{ mm}$ ), and the beam divergence is large (typically, the slope of the envelope  $\sim 50\text{-}70 \text{ mrad}$ ). Hence, it is difficult in the present circumstances to achieve a satisfactory solution for the beam optics, especially while matching the beam to a small aperture RFQ (SSCL-type). The crux of the present problem is to study the beam dynamics with the goal to achieve an optimal solution for the LEBT parameters and to evaluate the criticality of various controlling factors from a practical viewpoint. Nonlinear effects due to space-charges, fringe fields, and chromatic aberrations are included in our study of the beam dynamics.

In Section 2 we have described the context of the experiment, beam dynamics calculations and the characteristics of the LEBT system. Discussions and conclusions are given in Section 3.

## 2. LEBT for matching H<sup>+</sup> beams from a magnetron source into an RFQ

### 2.1. Experimental constraints

The input parameters of a LEBT are defined by the characteristics of the beam from the source, and its output beam parameters are governed by the acceptance ellipse of the RFQ. Ideally, the LEBT should be coupled as close as possible to the extraction point of the ion source, and simultaneously, it should be interfaced with the RFQ with a minimum drift space. In this context the two important practical constraints are imposed by: (a) the length (D) of the extraction cone (Fig.1), and (b) the drift space between the LEBT and the RFQ match point.

In the context of experiments with short, pulsed beams (pulse width of  $\sim 50 \mu\text{s}$  typically) we have chosen mainly ESQ lenses to develop the LEBT system. The merits of the ESQ lenses have been discussed elsewhere [9,10]. As a starting point of our design studies, the characteristic parameters of a 30 mA, 35 kV beam at the tip of the extraction cone are taken as: beam radius = 1.25 mm, slope of the beam envelope = 50 mrad, rms normalized emittance  $\pi \tilde{\epsilon}_n = 0.12 \pi \text{ mm mrad}$ . These values reasonably conform to the emittance measurements at the SSC Laboratory [11]. Furthermore, following the SSCL design the beam parameters at the RFQ match point are taken as: beam radius = 1.3 mm, slope of the beam envelope = -89 mrad, rms normalized emittance  $\pi \tilde{\epsilon}_n = 0.2 \pi \text{ mm mrad}$ ; the match point was considered at a distance of about 3 cm downstream from the front of the RFQ structure.

### 2.2. Beam dynamics calculations

The simulation architecture follows a hierarchy of beam dynamics calculations. First, a linear beam optics code, which solves the Kapchinskij-Vladimirskij (K-V) envelope equations assuming a hard-edge model of the external focusing force, is used to determine the basic

geometry of the lenses. This interactive code is run several times to optimize the lens parameters, namely, lens aperture, electrode dimensions (length and radius), location, and voltage. Second, the electrostatic field distributions are calculated by a 3D Laplace solver on the Connection Machine. The end faces of the cylindrical electrodes are shaped following Laslett [12] and Dayton et al. [13] to minimize the fringe fields, and a ground plate is inserted between the two neighboring lenses to reduce their mutual interference [14]. The details of the electrode boundary are included in our 3D field calculations. Finally, the results from the previous two steps are used in a 2½D particle simulation code, modified PARMILA [15], to determine the phase-space distribution of the beam particles and to estimate the beam emittance through the LEBT. The details of the computational scheme have been described elsewhere [9].

We note from our simulation studies that the combination of six ESQ lenses in Fig.2 has an attractive feature: the phase transformation is controlled essentially by the lenses 1, 2, 5, and 6, while the intermediate two lenses (3 and 4) provide an additional length for transport. This argument will be evident as we will go through the analysis in the subsequent sections; the importance of the einzel lens will also be revealed later.

### 2.2.1 Considerations for designing an efficient focusing optics

This section highlights on the critical role of the drift space, when the limitations posed by of the practical components, mainly due to the extraction cone, are analyzed. This study leads us to develop a strategy for satisfying the extreme matching criteria in the present problem.

Using the source beam parameters as discussed in Sec. 2.1, the beam envelope through the ESQ LEBT, which is described in Table 1, is obtained from the linear beam optics code as in Fig. 3(a). Here, the length of the extraction cone is taken as  $D = 5.0$  cm, and an additional drift

space of 6 mm is kept for mechanical coupling between the extraction cone and the first lens of the LEBT. Fig. 3(b) shows the hard-edge focusing function used in the envelope calculations, and the focusing function calculated from the 3D Laplace solver is shown in Fig. 3(c). The focusing function in Fig. 3(b) is  $\kappa = V_q / (V_b R_q^2)$ , where  $V_q$  is the voltage applied on the electrodes of a quadrupole lens,  $V_b$  is the beam voltage, and  $R_q$  is the aperture of the quadrupole lens. The qualitative nature of the focusing functions in Figs. 3(b) and (c) appears similar. The fringe fields are evaluated from the field distributions in Fig. 3(c), and these are incorporated in our particle simulation code following the prescriptions of Matsuda and Wollnik [16]. Assuming the input particle distribution to be K-V type as in Fig. 4(a), the phase-space distribution of particles at a distance of 2.2 cm from the last ESQ lens is obtained as in Fig. 4(b) and (c). This result shows an emittance growth by about a factor of 5, and the output beam does not satisfy the RFQ's matching condition. The enhanced emittance growth is due to the large beam excursions (more than 80% of the quadrupole aperture) and the resulting nonlinear contributions.

The above analysis is repeated for a shorter extraction cone with  $D = 2.5$  cm. The envelope solution in this case is shown in Fig. 5. The phase-space distribution of the particles at a distance of 3.2 cm from the last ESQ lens is shown in Fig. 6. Here the beam size is  $\sim 2.6$  mm, the beam convergence is  $\sim -39$  mrad, and the rms normalized emittance is  $\pi \tilde{\epsilon}_n = 0.36 \pi$  mm mrad; the emittance growth is a factor of about 3. The beam quality is comparatively better in this case, and the output beam remains convergent farther downstream from the last lens. This points to the sensitivity of the beam optics to the length of the extraction cone.

### 2.2.2 LEBT for matching with the RFQ

The results in the previous section suggest that the characteristics of the output beam from the ESQ LEBT do not satisfy the required matching condition for the RFQ. The underlying complexity of the present problem is analyzed below, and an effort is made to obtain a satisfactory solution.

When a divergent beam from a source, with the beam size =  $X_i$  and the angle of divergence =  $X_i'$ , is transformed into the same size but a convergent beam with angle of convergence =  $-X_f'$ , the power of the lens  $P$  can be obtained, in the thin lens approximation, from the beam transformation matrix as

$$P = (X_f' - X_i') / X_i.$$

Thus, to achieve further focusing of the beam in Sec. 2.2.1 and to satisfy the RFQ matching condition, the power ( $P$ ) of the ESQ lenses should be increased. This will cause further emittance dilution. The complexity of the present matching problem can be reduced by cascading a short einzel lens section to the ESQ LEBT as shown in Fig. 2. In this situation, a much less stringent requirement is imposed on the ESQ LEBT section. The output beam from the ESQ LEBT should be now matched appropriately to the input of the einzel lens which provides the final focusing. A similar approach was adapted earlier while dealing with  $H^-$  beams from a volume source [6]. It was found that for the einzel lens geometry given in Table 2, the output from the ESQ LEBT was required to satisfy the following conditions: beam radius of  $\sim 7.5$  mm, and slope of  $\sim -50$  mrad. We will follow this scheme and determine the ESQ lens voltages in the context of the current problem.

In order to achieve the aforementioned output beam parameters at a distance of  $\sim 1$  cm from the last lens of the ESQ LEBT so that this beam can be appropriately coupled to the einzel

lens section, the corresponding beam envelopes through the ESQ LEBT are obtained as in Fig. 7(a); here, the hard-edge focusing function is shown in Fig. 7(b). The length of the extraction cone is taken as  $D = 2.5$  cm. The phase-space particle distribution of the output beam is shown in Fig. 8(a) and (b) corresponding to the x- and y-planes, respectively. The output beam parameters are obtained as: effective beam radius = 7.8 mm, slope = -43.6 mrad, and rms normalized emittance  $\pi \tilde{\epsilon}_n = 0.29 \pi$  mm mrad. The evolution of the beam emittance (solid rectangles) through the ESQ lenses are shown in Fig. 9; correspondingly, the ratio of the quad voltage at the beam edge to the on-axis beam voltage (35 kV) is plotted (open rectangles). This voltage ratio is a measure of the chromatic aberrations. A pair of data points (solid and open rectangles) for a particular z-location corresponds to the results at the end of a lens, and these data are plotted in sequence with lens number 1 as the first set of points. It is important to note that the lenses 2, 3 and 4 contribute to the emittance growth; in all of these cases, the quad-voltage at the beam edge is more than 5% of the on-axis beam voltage. This suggests that the emittance growth is primarily due to the chromatic aberrations. We have evaluated that a relatively small group of particles mainly causes the emittance growth. More than 85% of the beam particles occupy a phase-space area which contributes to an emittance growth by a factor of about 1.6 only; the rms normalized emittance is estimated to be about  $\pi \tilde{\epsilon}_n = 0.2 \pi$  mm mrad. Fig. 10(a) and (b) show the phase-space distribution of this desired group of beam particles. The distortions appear to very modest here. We have repeated the analysis assuming a semi-Gaussian distribution of the input beam particles; the results are similar.

Next, the beam from the ESQ LEBT is transported through the einzel lens. The input beam parameters for the einzel lens are obtained from the characteristics of the effective ellipse describing the output beam (Fig.8) from the ESQ LEBT. These data are used in SNOW-2D code

[17]. Fig. 11 shows the trajectory of the beam through the einzel lens. No additional emittance growth of the beam is noted in the einzel lens section, and the beam is matched to the RFQ.

### 3. Discussions and conclusions

The present work sheds light on developing a low-emittance injector for future high-luminosity colliders. In this regard, the transport and matching problems in the ion source-LEBT-RFQ section have been studied. This problem involving a high-brightness, high-perveance  $H^-$  beam (generalized beam perveance  $K = 0.003$ ) turns out especially complex when the practical constraints are included in the beam dynamics calculations. After a good deal of simulation run we have optimized the LEBT parameters. We found that about a 30 cm-long electrostatic LEBT system, composed of a combination of six ESQ lenses in a compact configuration and a short einzel lens, offers a very satisfactory solution. This system is designed for matching a highly divergent 30 mA, 35 kV  $H^-$  beam from a magnetron-type ion source into a small aperture RFQ (SSCL-type). The full beam shows an emittance growth by a factor of about 2.5 in the entire LEBT; about more than 85% of the beam carrying a current of about 26 mA has the final rms normalized emittance of about  $0.2 \pi \text{ mm mrad}$ , and its beam characteristics match with the Twiss parameters of the RFQ at the match point. The emittance growth of the beam is primarily due to chromatic aberrations. It is learned that the drift-space in a transport line should be avoided as far as possible, especially in the case of handling a space-charge dominated beam. We have shown that in the context of our particular experiment, the length of the extraction cone in the magnetron source should be kept short -- with in 2.5 cm. Also, the 3.0 cm-long drift space in front of the RFQ match point introduces a strong constraint; a shorter distance is desired.

Some notable features of the present LEBT system are:

- (i) An adequate buffer space between an ion source and an RFQ can be provided for differential pumping, and hence, for a clean operation of the RFQ.
- (ii) An optimized combination of the first-order (ESQ lenses) and the second-order (einzel lens) focusing elements allows to satisfy extreme matching requirements without any significant emittance dilution.
- (iii) Tuning can be done by adjusting low-voltage power supplies of the ESQ lenses.
- (iv) Beam steering can be done by coupling a dipole field to the ESQ lenses.
- (v) As the same LEBT system was found to yield a very satisfactory solution for  $H^-$  beams from a volume source [6], the current design owns the merit of accommodating a good range of input conditions. A similar approach using a combination of ESQ lenses and a "ring" lens was found effective in experiments with a rather low-perveance beam [18].

The ESQ LEBT system has been developed, and we plan to start experiments on our test stand with a magnetron-type ion source.

#### **Acknowledgements**

This work is supported by the U.S. Office of Naval Research. The authors thank Dr. K. Saadatmand of the SSC Laboratory for some valuable information on the magnetron beam parameters, and Dr. C. R. Chang for his assistance in running the SNOW code. Also, we acknowledge the support of Dr. L. W. Funk of the SSC Laboratory for establishing a test stand at Maryland with the SSCL magnetron ion source.

References:

- [1] Proc. Workshop on Future Hadron Facilities in the US, Bloomington, IN, July 6-10, 1994 (to be published).
- [2] J. G. Alessi, J. M. Brennan and A. Kponov, Rev. Sci. Instr. 61 (1990) 625.
- [3] P. G. O'Shea, D. L. Schrage, L. M. Young, T. J. Zaugg, M. T. Lynch, K. F. McKenna and L. D. Hansborough, Nucl. Instr. and Meth. B40/41 (1989) 946.
- [4] "Site-specific conceptual design", Superconducting Super Collider Laboratory Rept. SSCL-SR-1056, July 1990.
- [5] K. Saadatmand, J. E. Hebert and N. C. Okay, Rev. Sci. Instr. 65 (1994) 1173.
- [6] S. K. Guharay, C. K. Allen, M. Reiser, K. Saadatmand and C. R. Chang, Rev. Sci. Instr. 65 (1994) 1774.
- [7] D. Raparia, F. Guy, K. Saadatmand and W. Funk, Rev. Sci. Instr. 65 (1994) 1457.
- [8] C. W. Schmidt and C. D. Curtis, BNL 50727, p.123.
- [9] S. K. Guharay, C. K. Allen and M. Reiser, Nucl. Instr. and Meth. A 339 (1994) 429.
- [10] M. Reiser, Nucl Instr. and Meth. B56/57 (1991) 1050; Proc. H<sup>+</sup> Ion Source for High Energy Accelerators Workshop, Dallas, TX, May 5-8, 1992.
- [11] K. Saadatmand, private communication.
- [12] L. J. Laslett, Lawrence Berkeley Report No. HI-FAN-137.
- [13] I. E. Dayton, F. C. Shoemaker and R. F. Mozley, Rev. Sci. Instr. 25 (1954) 485.
- [14] H. Wollnik, Optics of Charged Particles (Academic Press, 1987).
- [15] C. R. Chang, Ph.D. Thesis, Univ. Maryland, 1989.

- [16] H. Matsuda and H. Wolnik, Nucl. Instr. and Meth. 103 (1972) 117.
- [17] J. E. Boers, Sandia National Lab. Report No. SAND 79-1027, 1980.
- [18] O. A. Anderson, L. Soroka, J. W. Kwan and R. P. Wells, Proc. 2nd European Particle Accelerator Conf., Nice, France, June 12-16, 1990, LBL Report-28962.

TABLE 1. ESQ lens parameters.

Lens No.	Aperture radius (mm)	Electrode radius (mm)	Length (mm)	Spacing (mm)
1 & 6	15.0	17.2	25.0	2.0
2 & 5	22.0	25.2	59.0	2.0
3 & 4	22.0	25.2	47.0	2.0

The electrode radius is 1.1468 times the aperture radius to minimize nonlinear fields [13]. The spacing indicates the gap between an ESQ lens and its neighboring ground plate.

TABLE 2. Einzel lens parameters

Aperture radius of the center electrode (mm)	Thickness of the center electrode (mm)	Spacing (mm)
17.0	10.0	7.0

The spacing indicates the gap between the center electrode (at high voltage) and its neighboring ground electrodes.

## Figure Captions

Fig.1 Schematic diagram of a magnetron ion source.

Fig.2 Schematic diagram of the LEBT system.

Fig.3 (a) Amplitude of the beam envelope, (b) hard-edge focusing function, Kappa (The slope of the vertical connecting lines is a plotting artifact.), and (c) focusing function from the 3D Laplace solver. The solid and dashed lines correspond to the results in the x- and y-planes, respectively. These results correspond to the length of the extractor cone  $D = 5.0$  cm. Note that the maximum beam excursion is close to the aperture (22 mm) of the lenses 2, 3 and 4.

Fig.4 Distribution of particles in phase space. (a) The input beam at the tip of the extraction cone. The output beam at 2.2 cm downstream from the last ESQ lens: (b) distribution in the x-plane, (c) distribution in the y-plane. Here,  $D = 5.0$  cm.

Fig.5 Amplitude of the beam envelope. Here,  $D = 2.5$  cm.

Fig.6 Phase-space distribution of the output beam at 3.2 cm downstream from the last ESQ lens: (a) in the x-plane, (b) in the y-plane. Here,  $D = 2.5$  cm. The input beam corresponds to Fig. 4(a).

Fig.7 Envelope solution for matching the ESQ output to the input of the einzel lens. (a) Amplitude of the beam envelope, and (b) hard-edge focusing function, Kappa. Solid line: x-plane; dashed line: y-plane.

Fig.8 Phase-space distribution of the output beam at 1.0 cm downstream from the last ESQ lens:  
(a) in the x-plane, (b) in the y-plane. Here,  $D = 2.5$  cm. The input beam corresponds to Fig. 4(a).

Fig.9 Evolution of rms normalized emittance through the ESQ LEBT (solid rectangles). Ratio of the quad voltage (V-quad) at the beam edge to the on-axis beam voltage (open rectangles).

Fig.10 The output beam at 1.0 cm downstream from the last ESQ lens when about 14% beam particles are excluded. All other conditions are same as in Fig. 9. Phase-space distribution (a) in the x-plane, (b) in the y-plane.

Fig.11 Particle trajectories through the einzel lens.

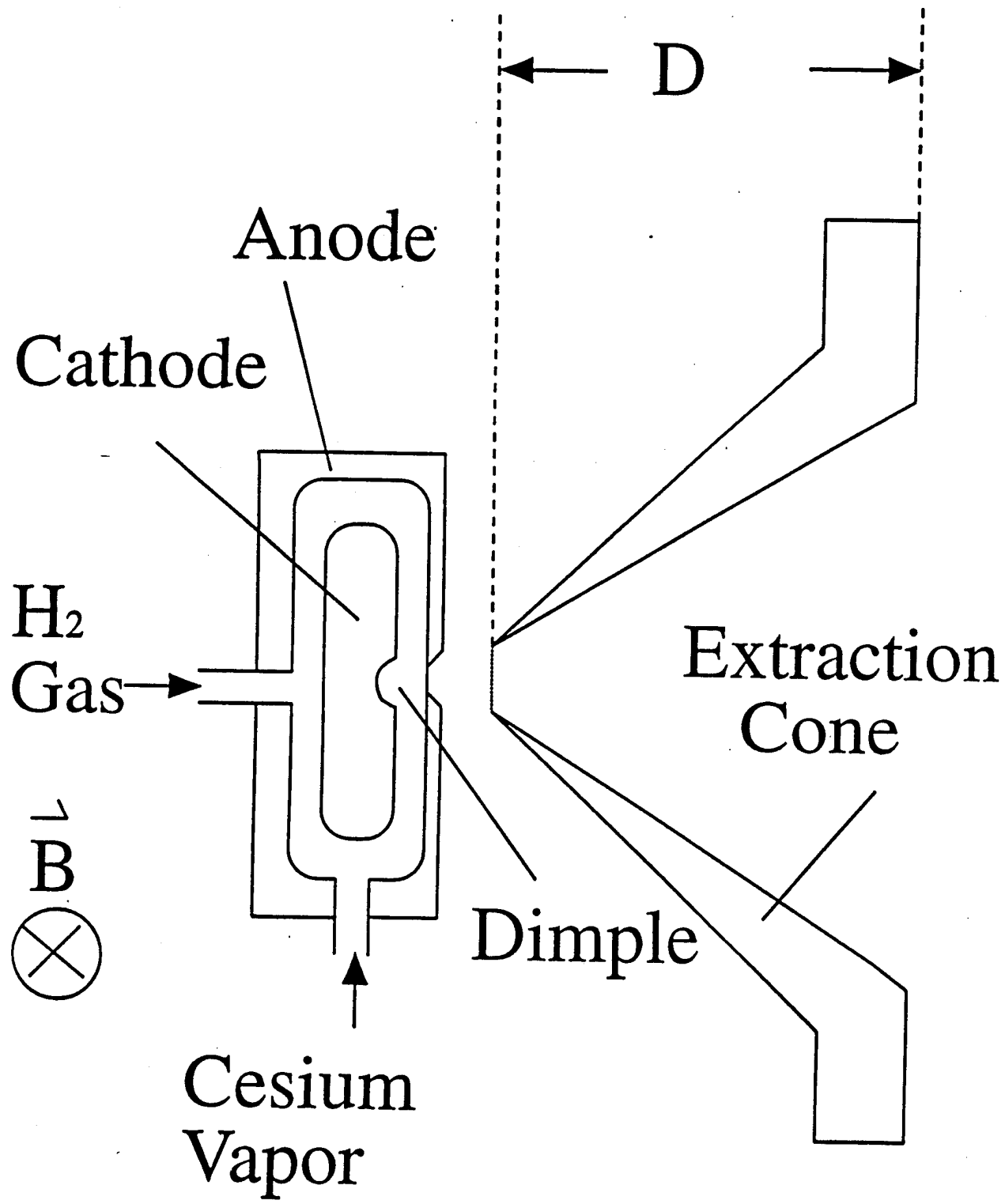


Fig. 1

ESQ ELECTRODE

GROUND PLATE

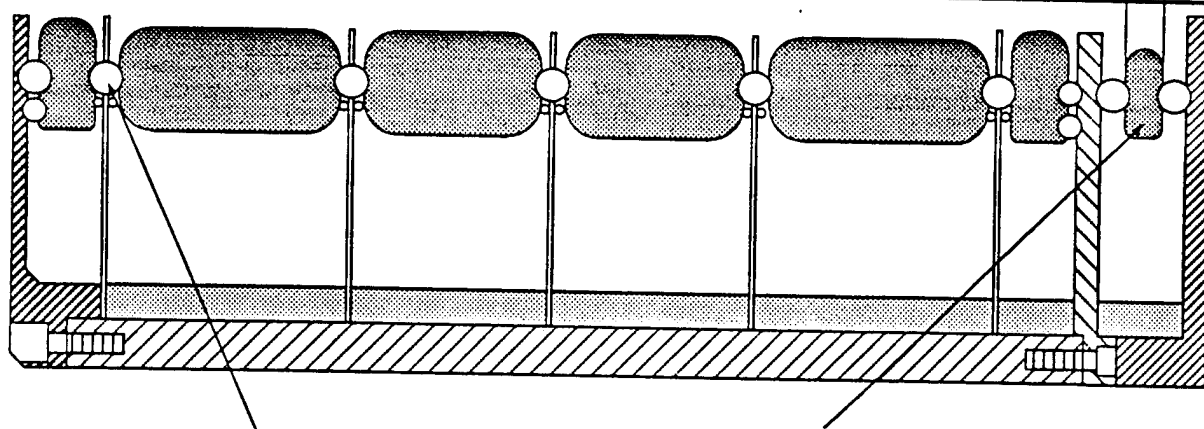
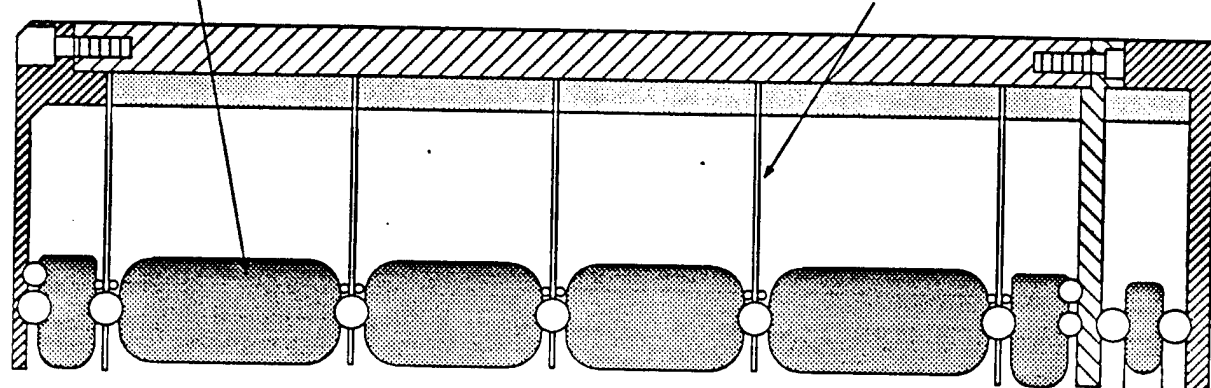


Fig. 2

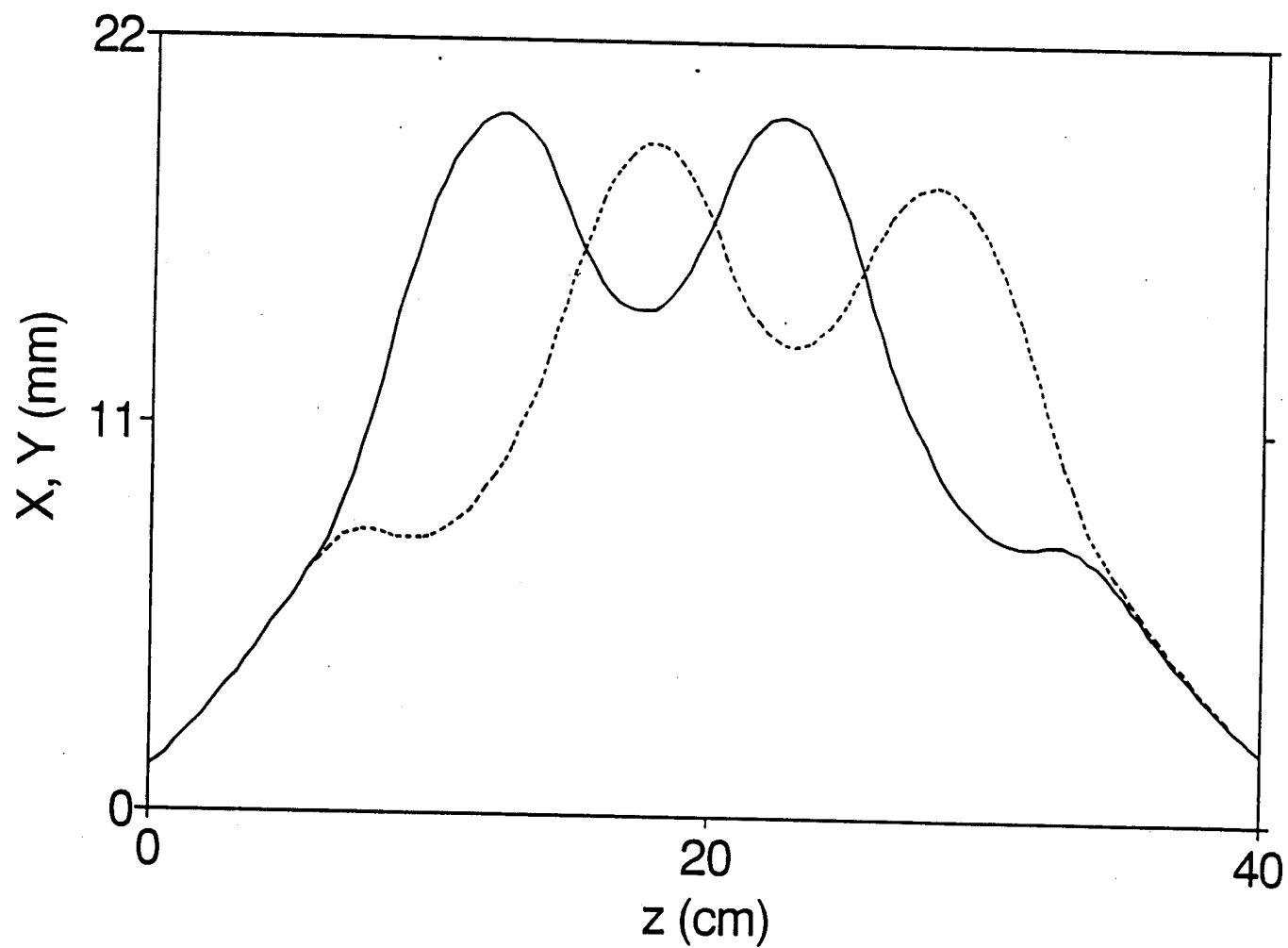


Fig. 3(a)

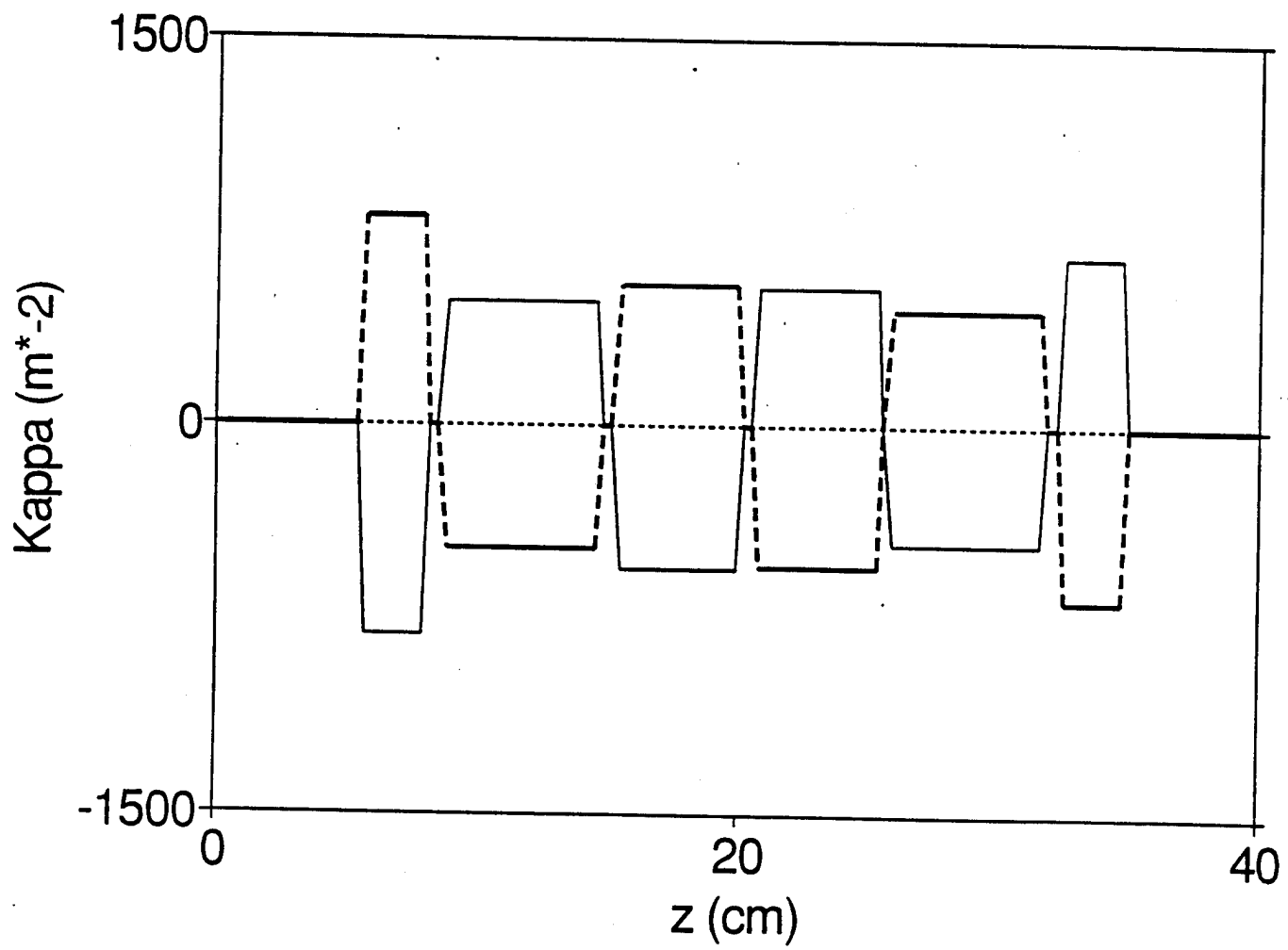


Fig. 3(b)

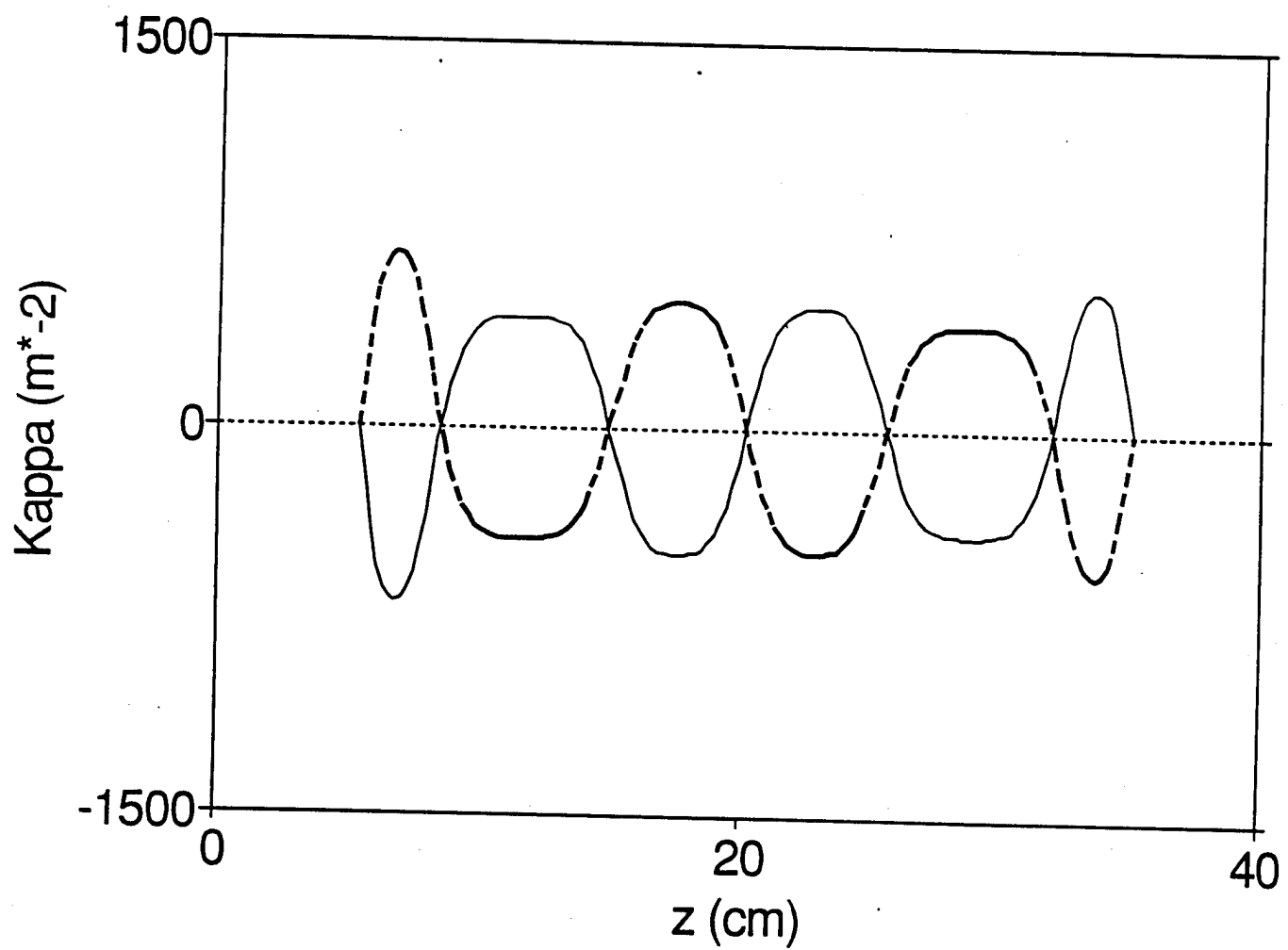


Fig. 3(c)

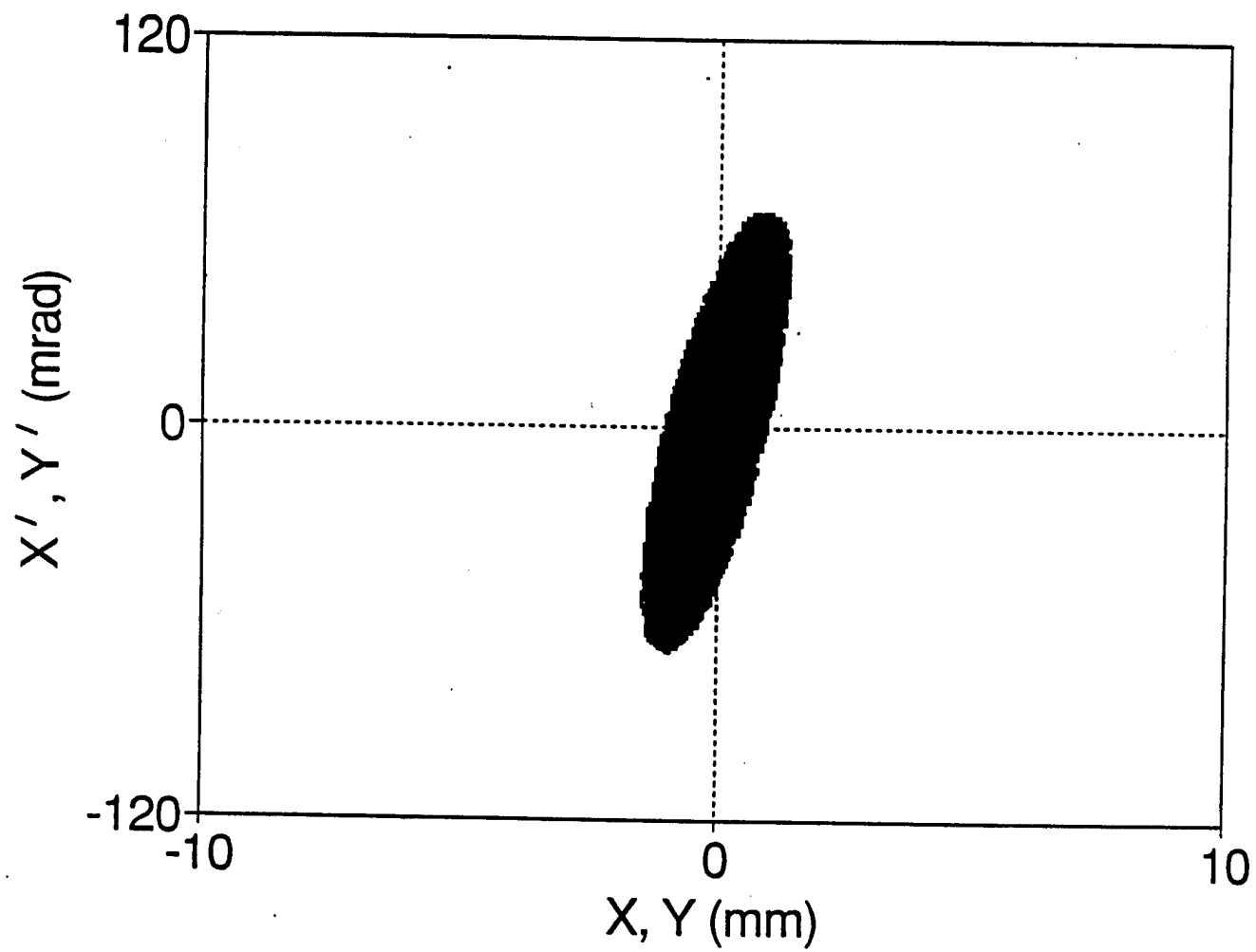


Fig. 4(a)

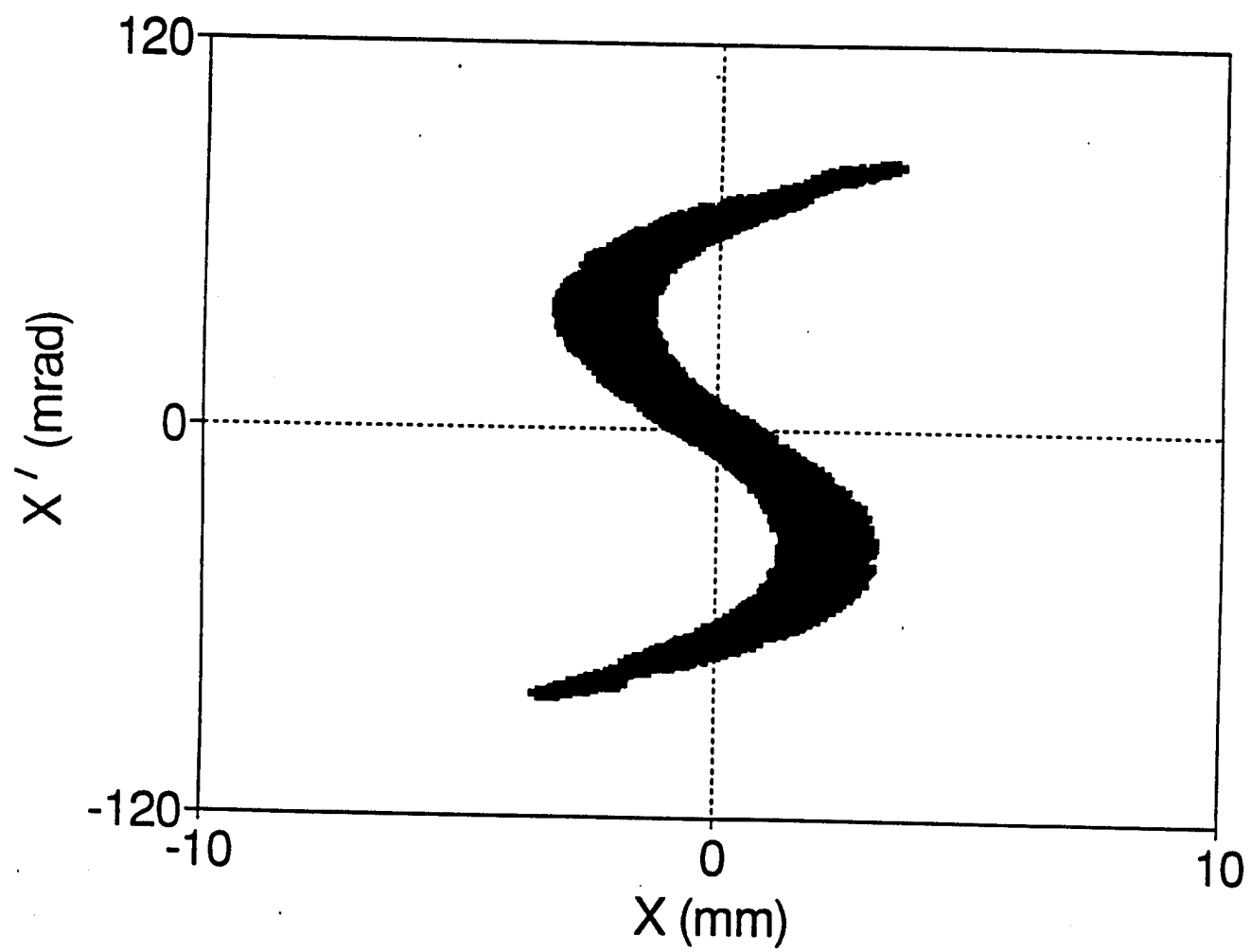


Fig. 4(b)

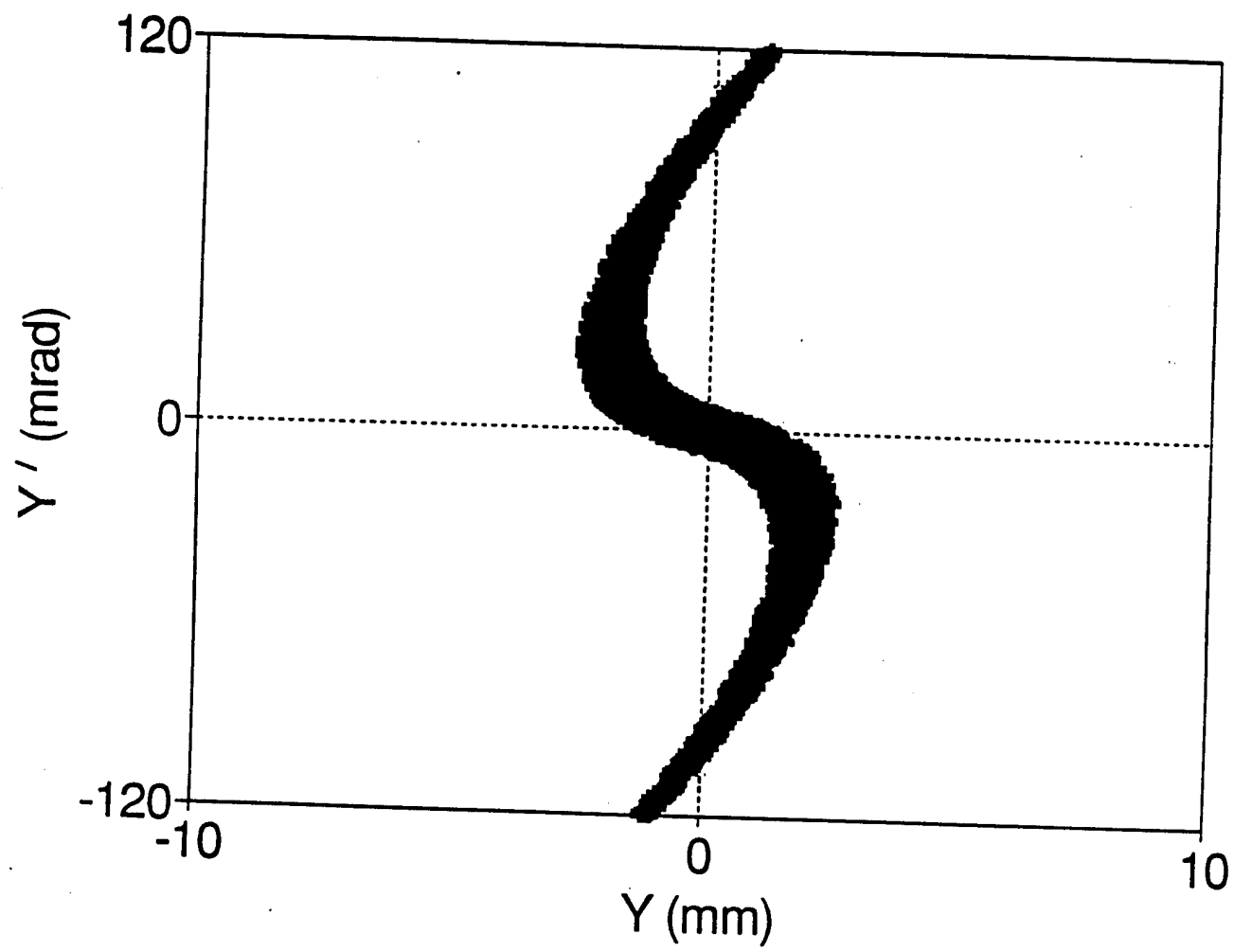


Fig. 4(c)

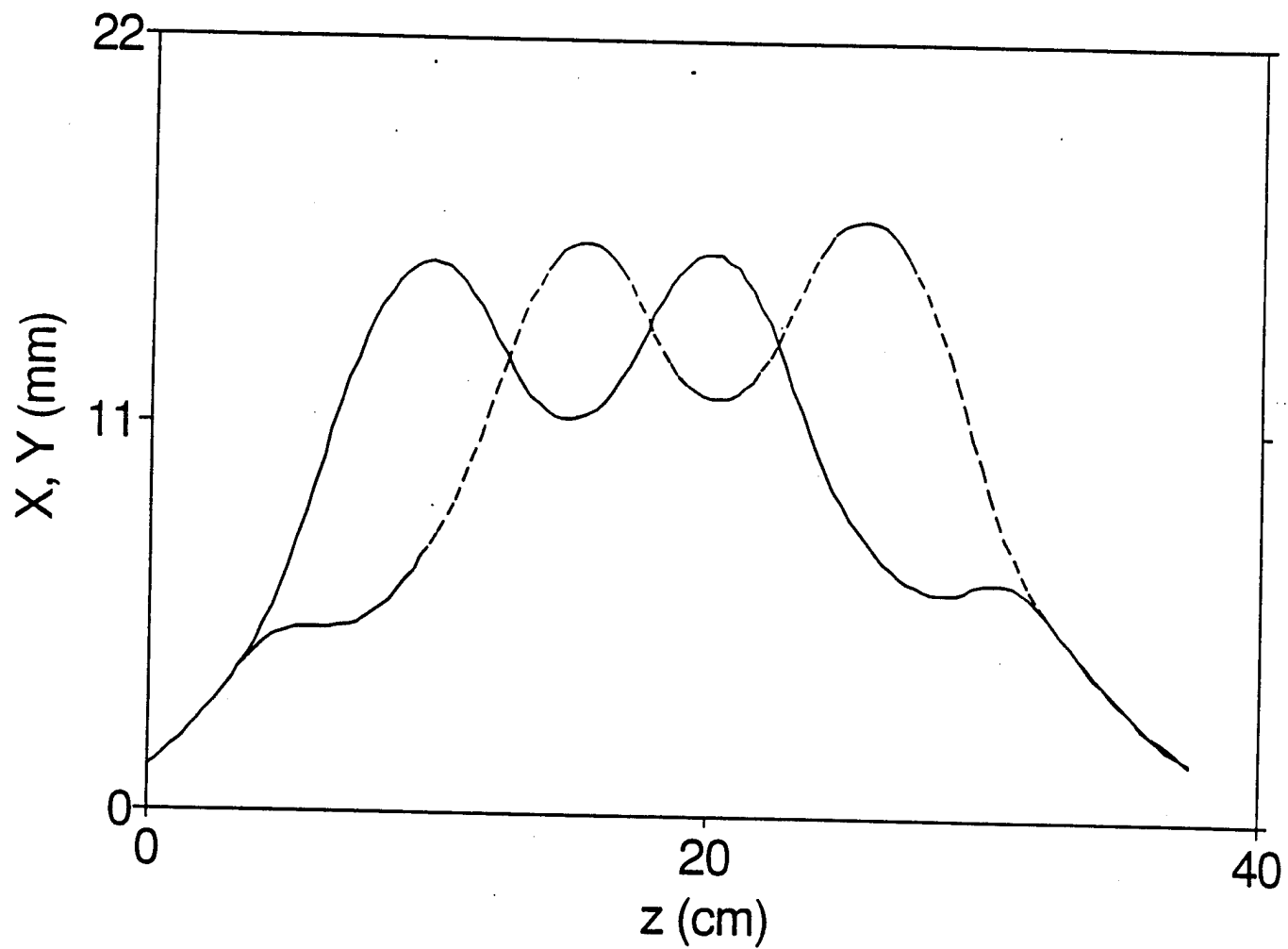


Fig. 5

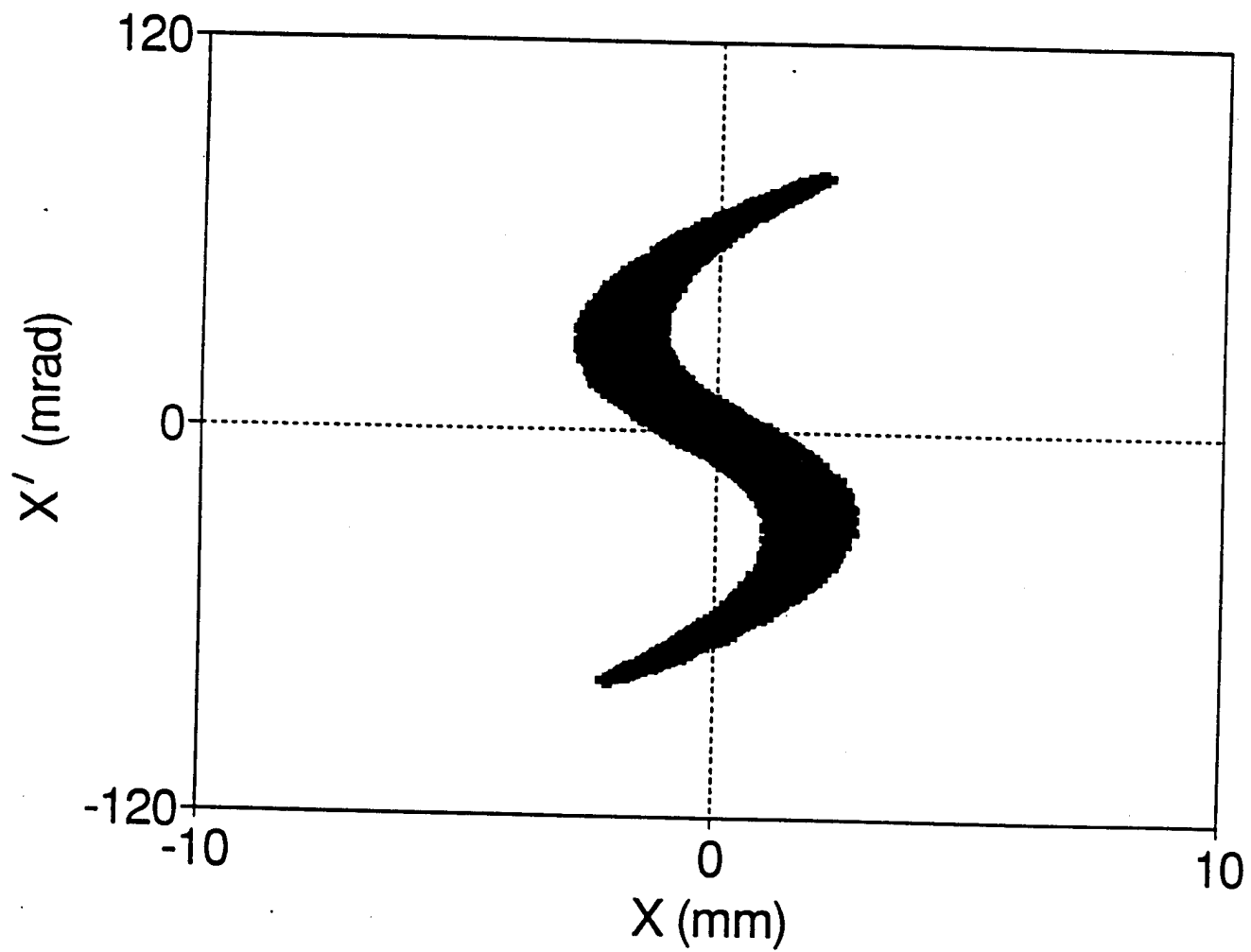


Fig. 6 (a)

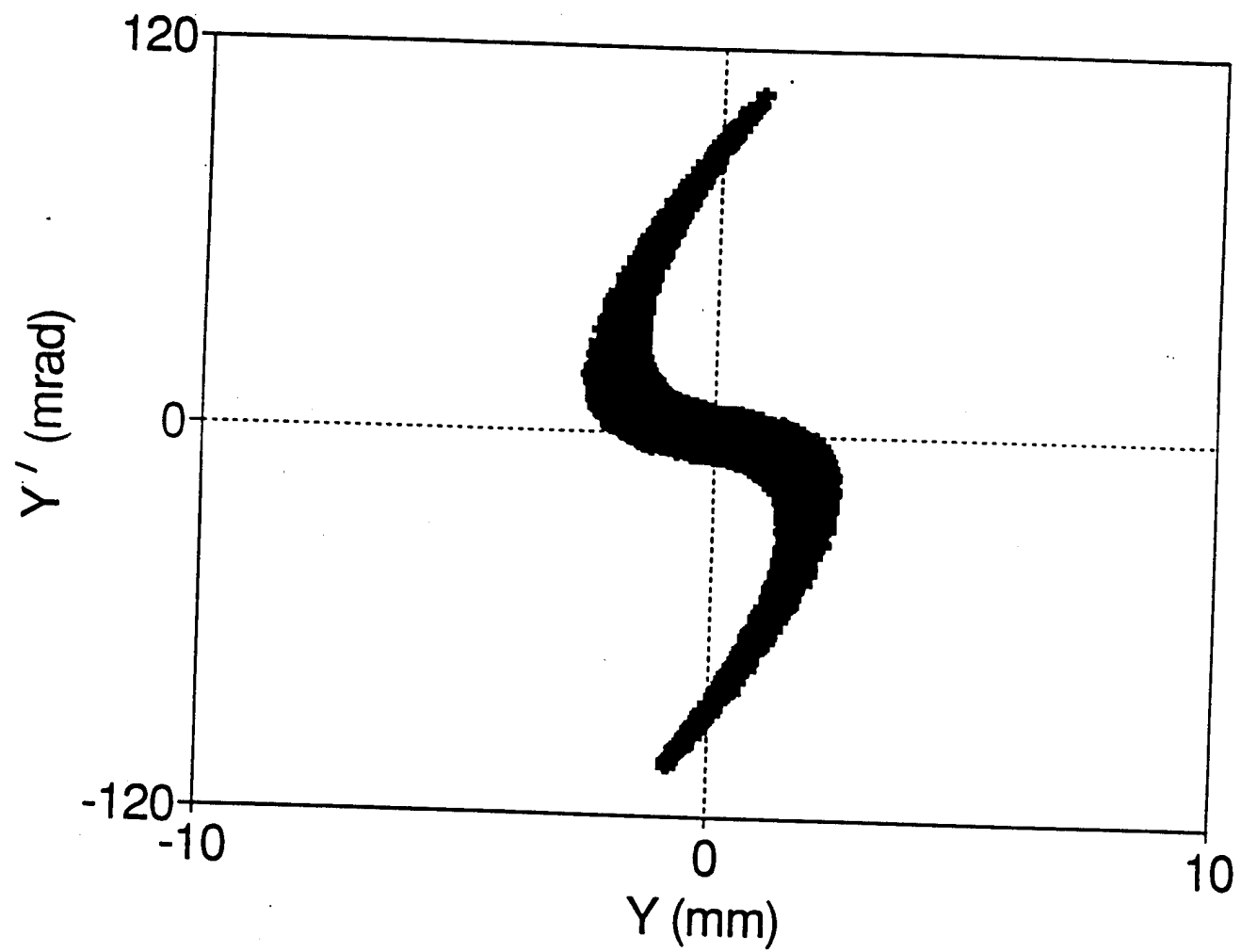


Fig. 16(5)

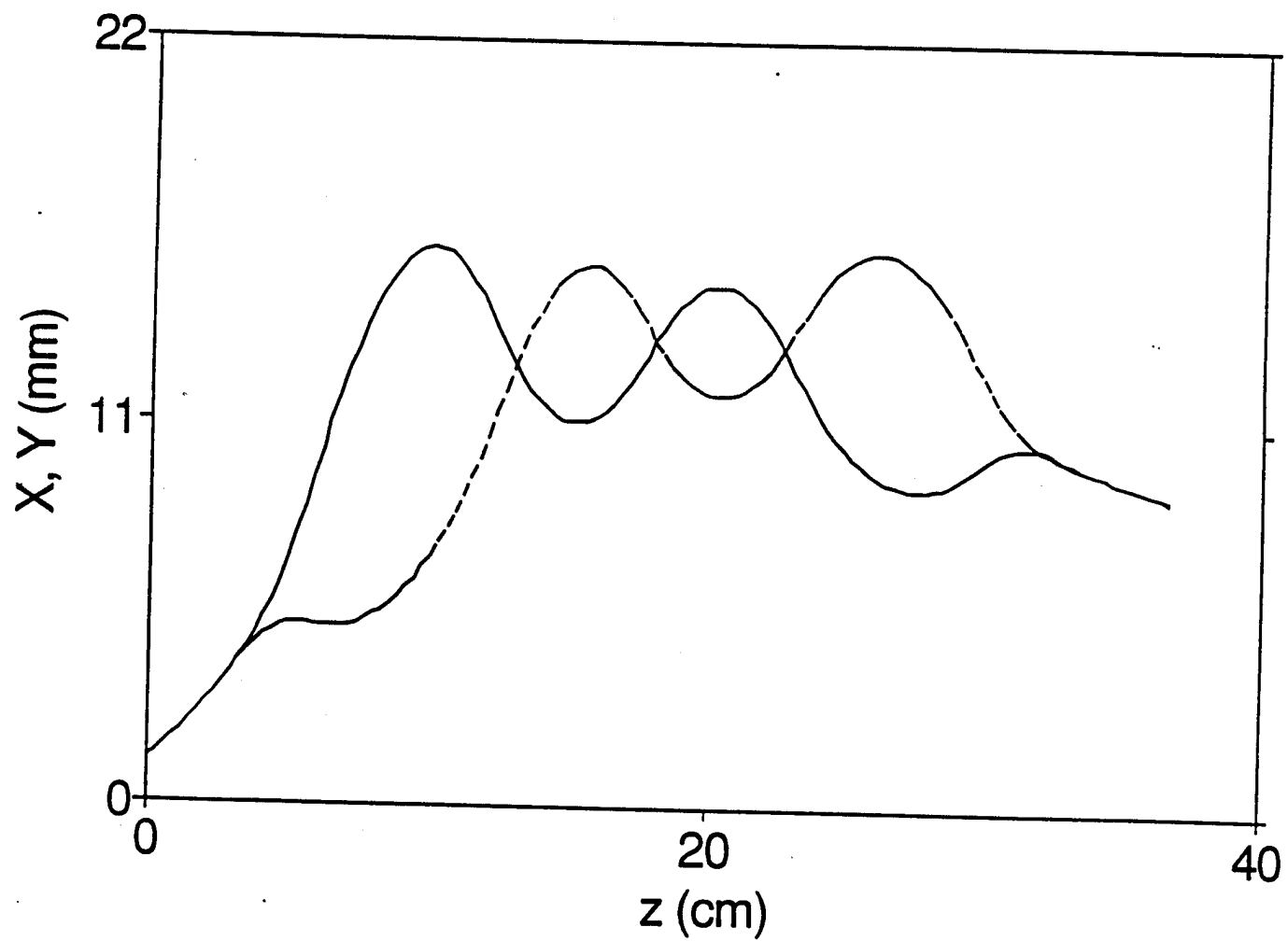
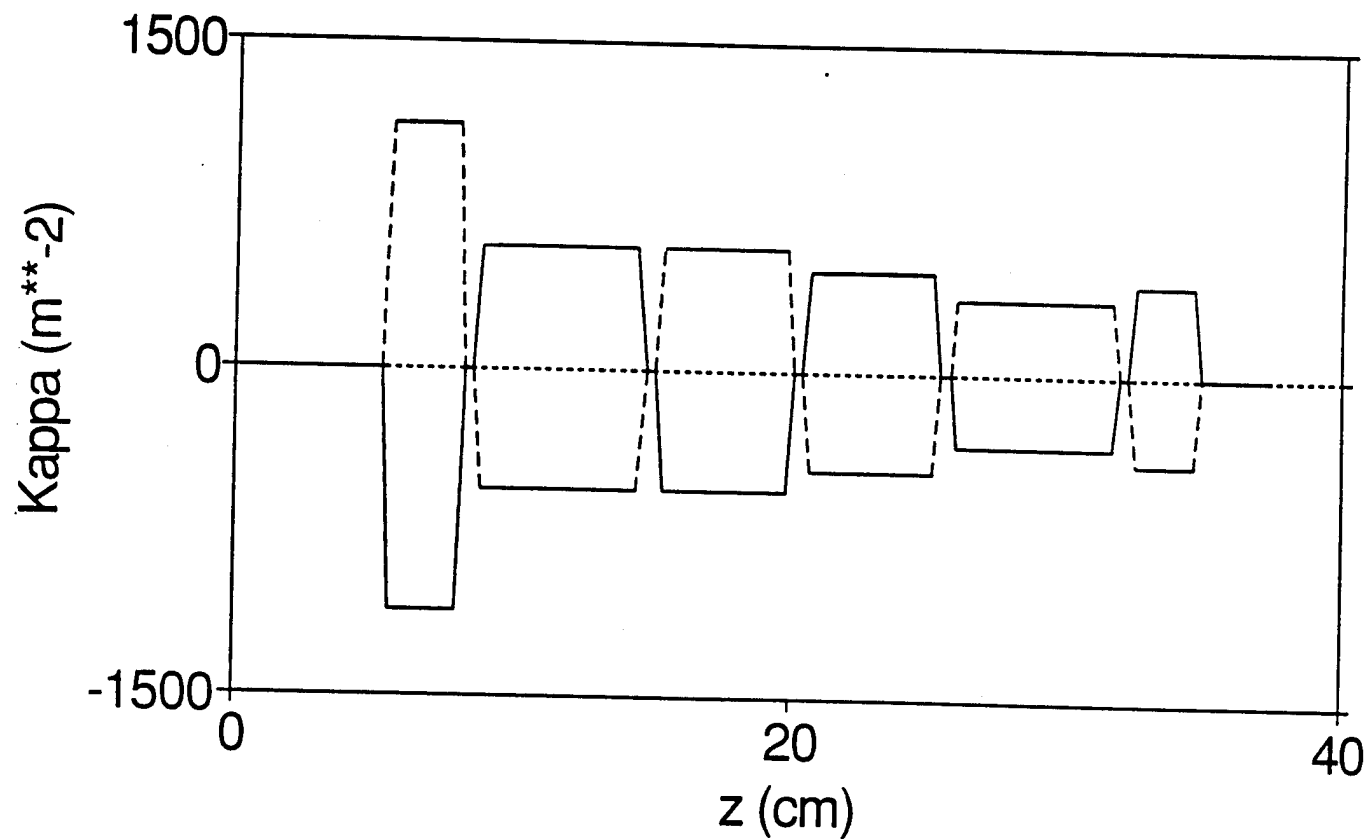


Fig. 7 (a)



— x-component ----- y-component

Fig. 7(2)

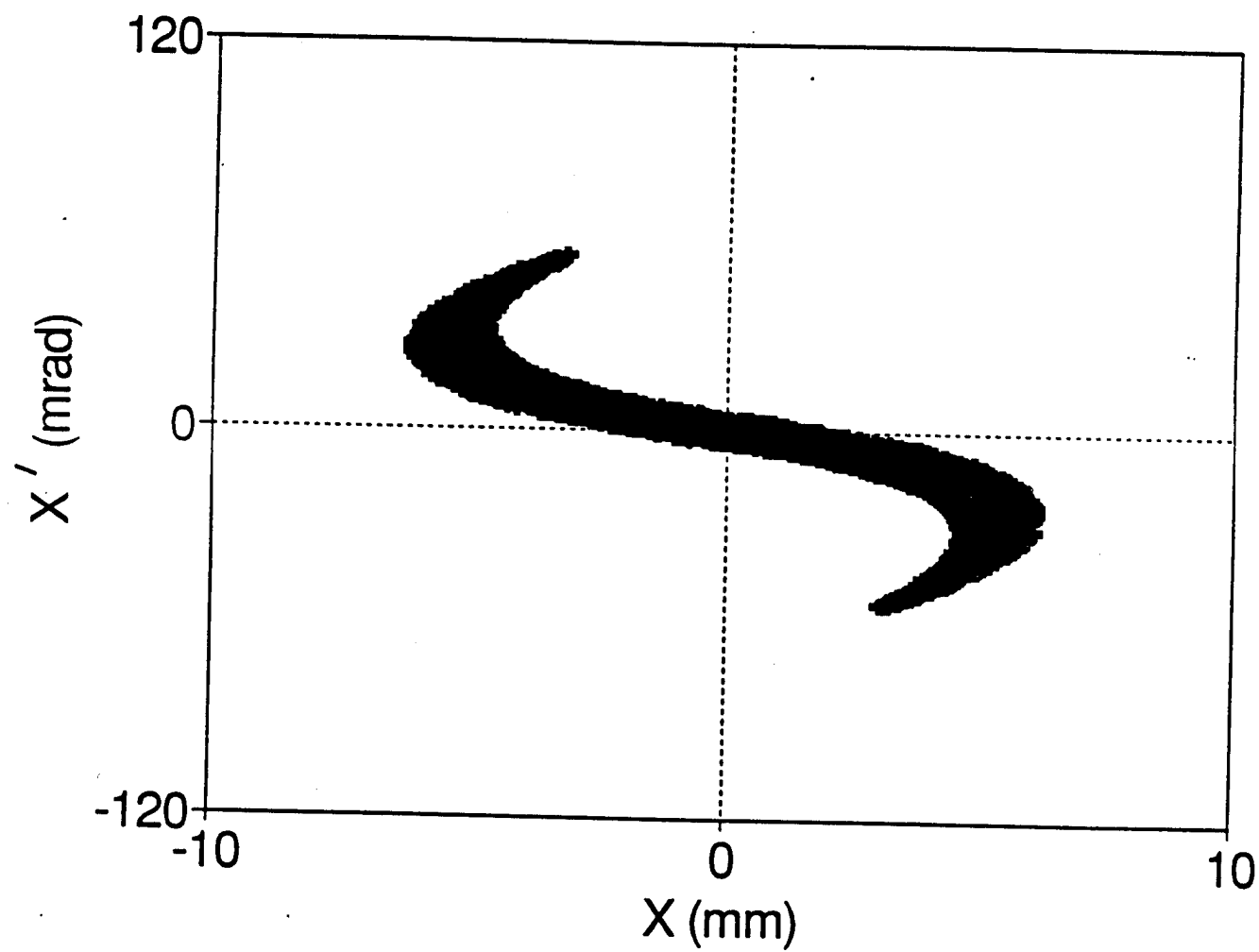


Fig. 8 (a)

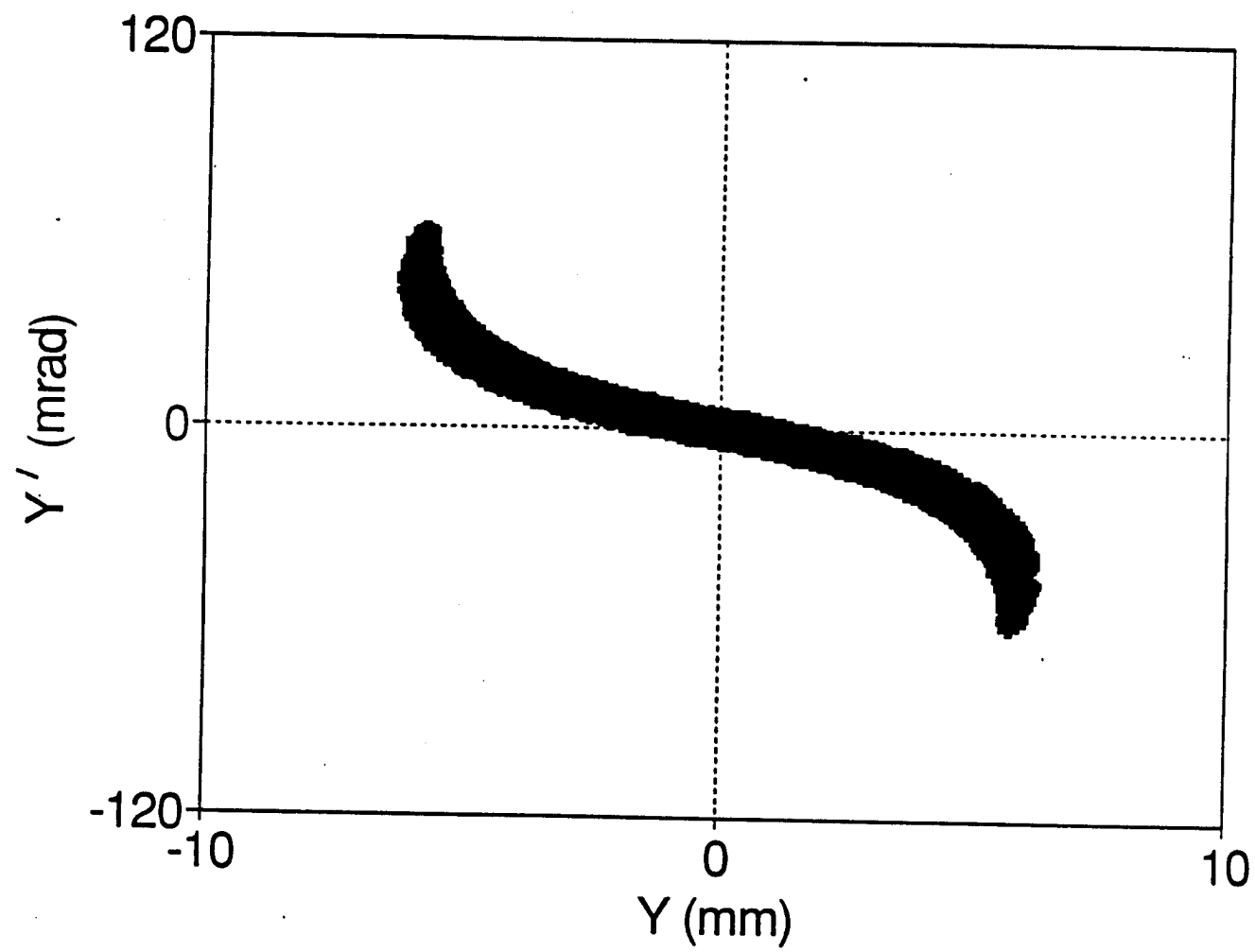


Fig. 8 (b)

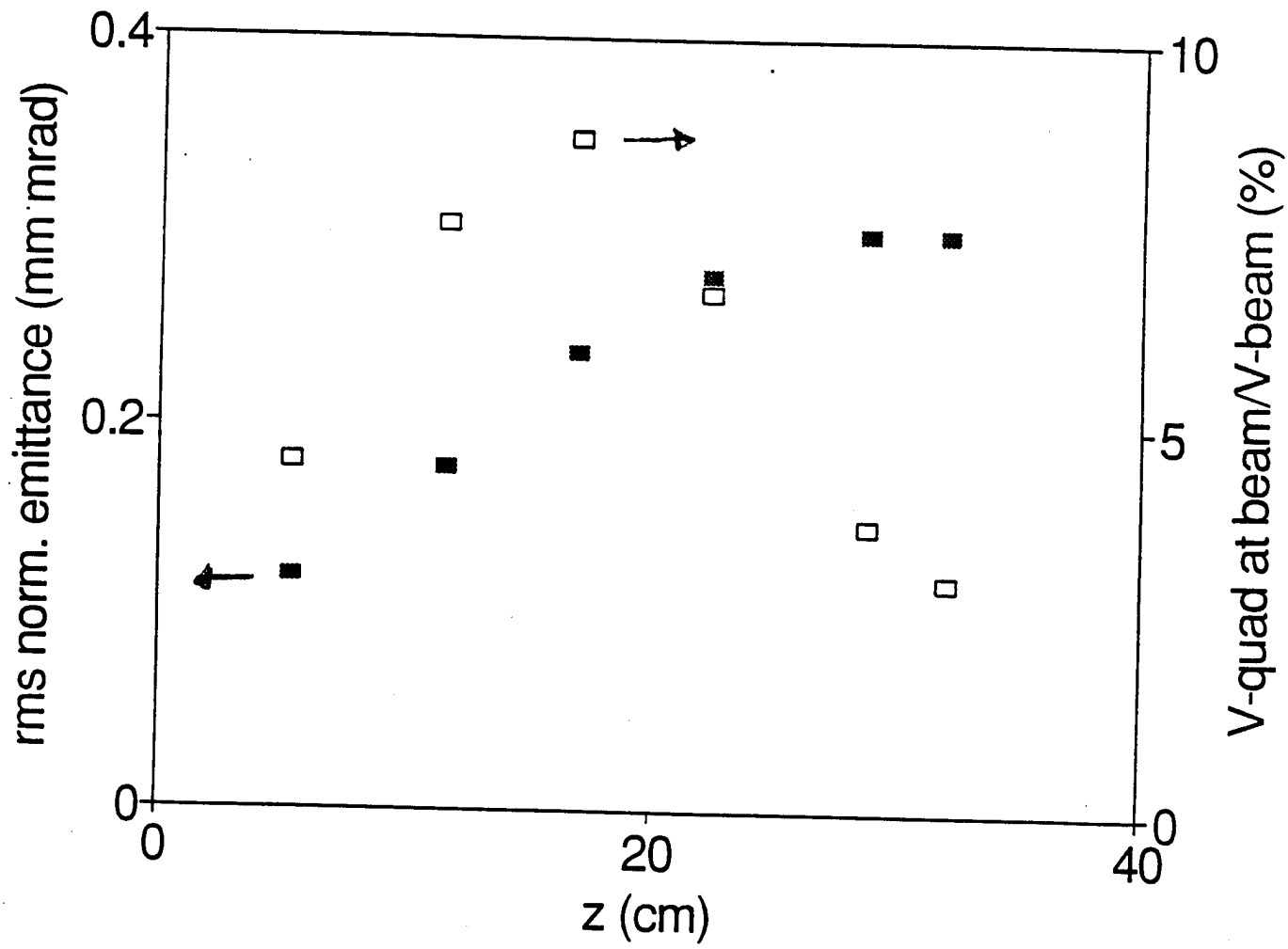


Fig. 9

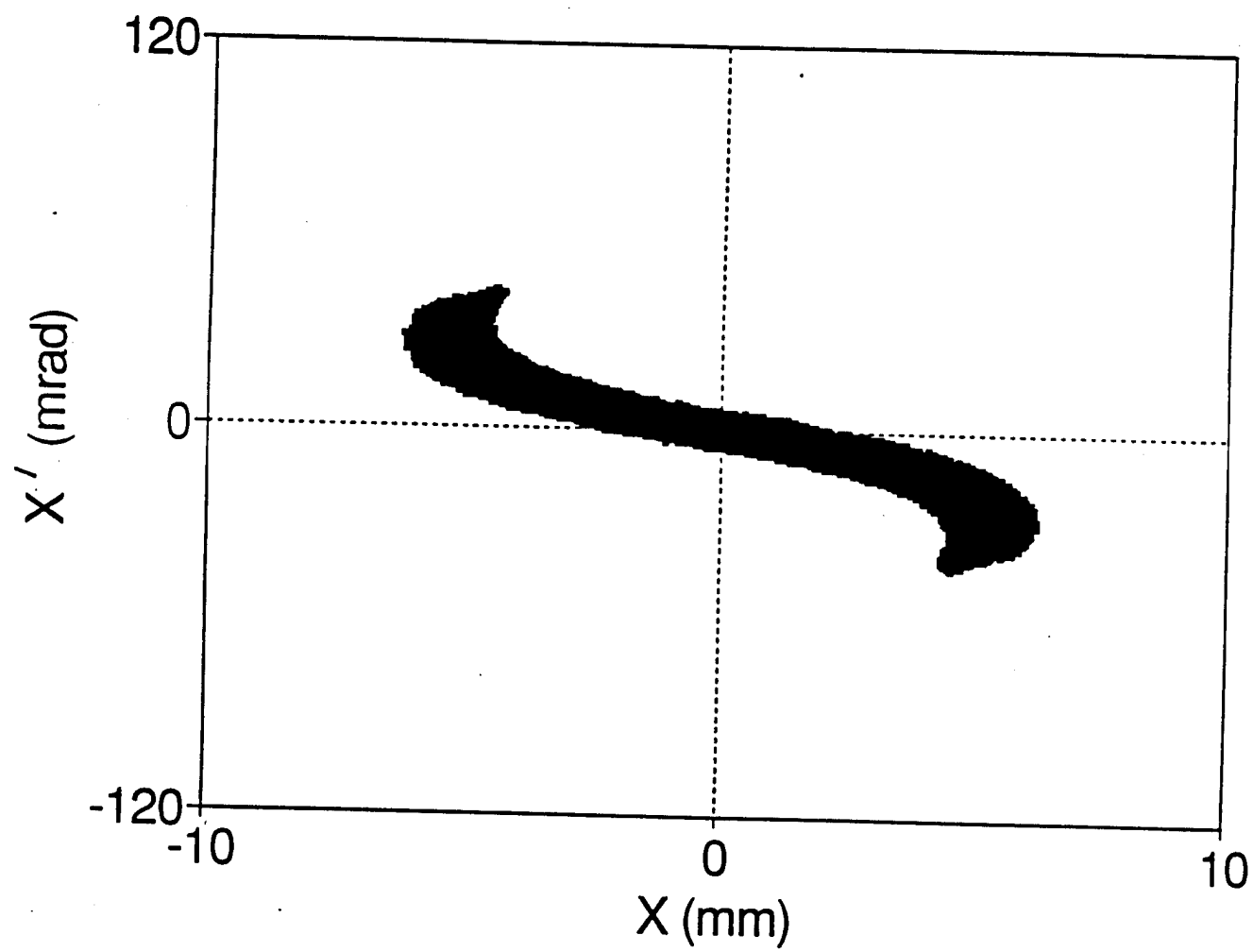


Fig. 10 (a)

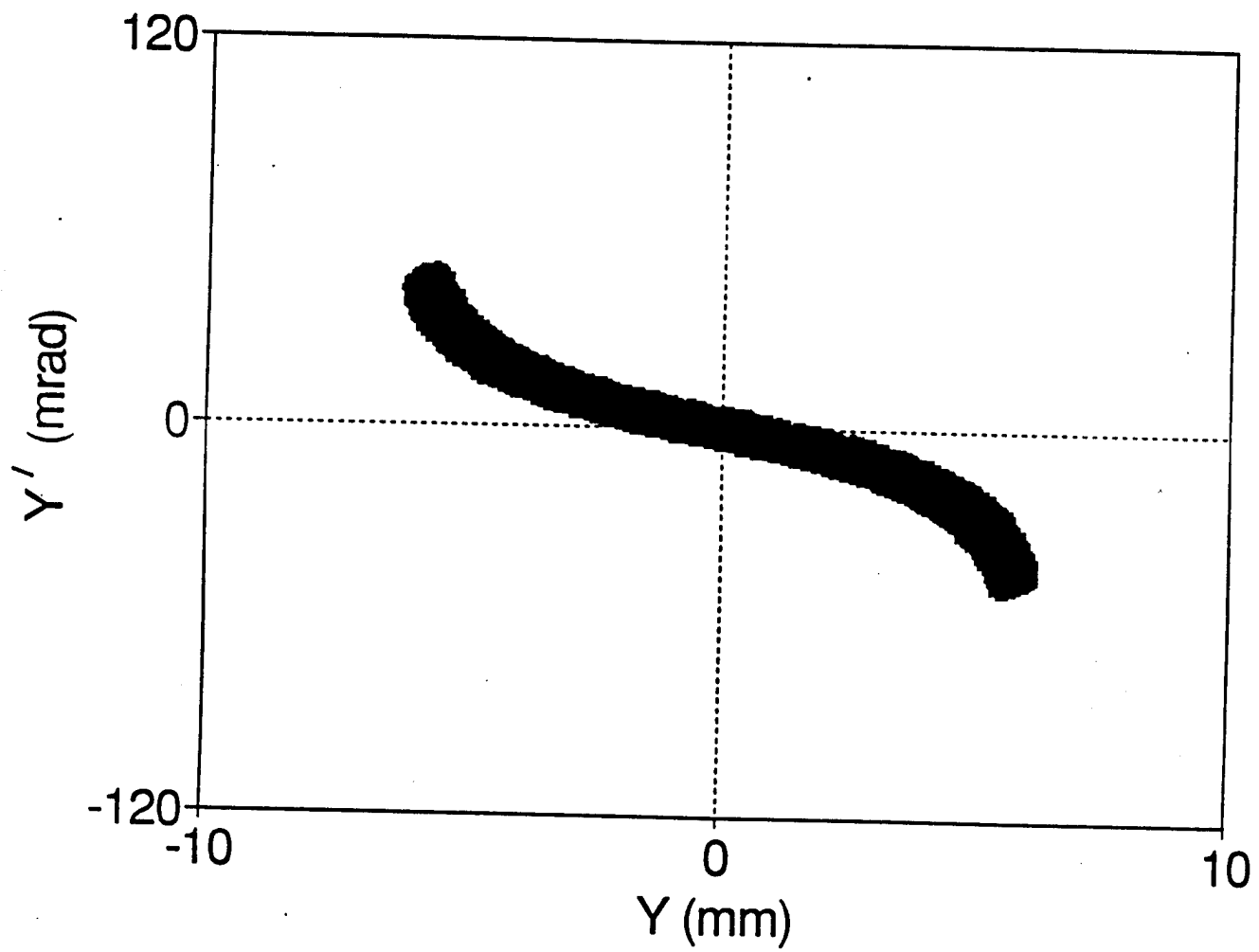


Fig. 10 (b)

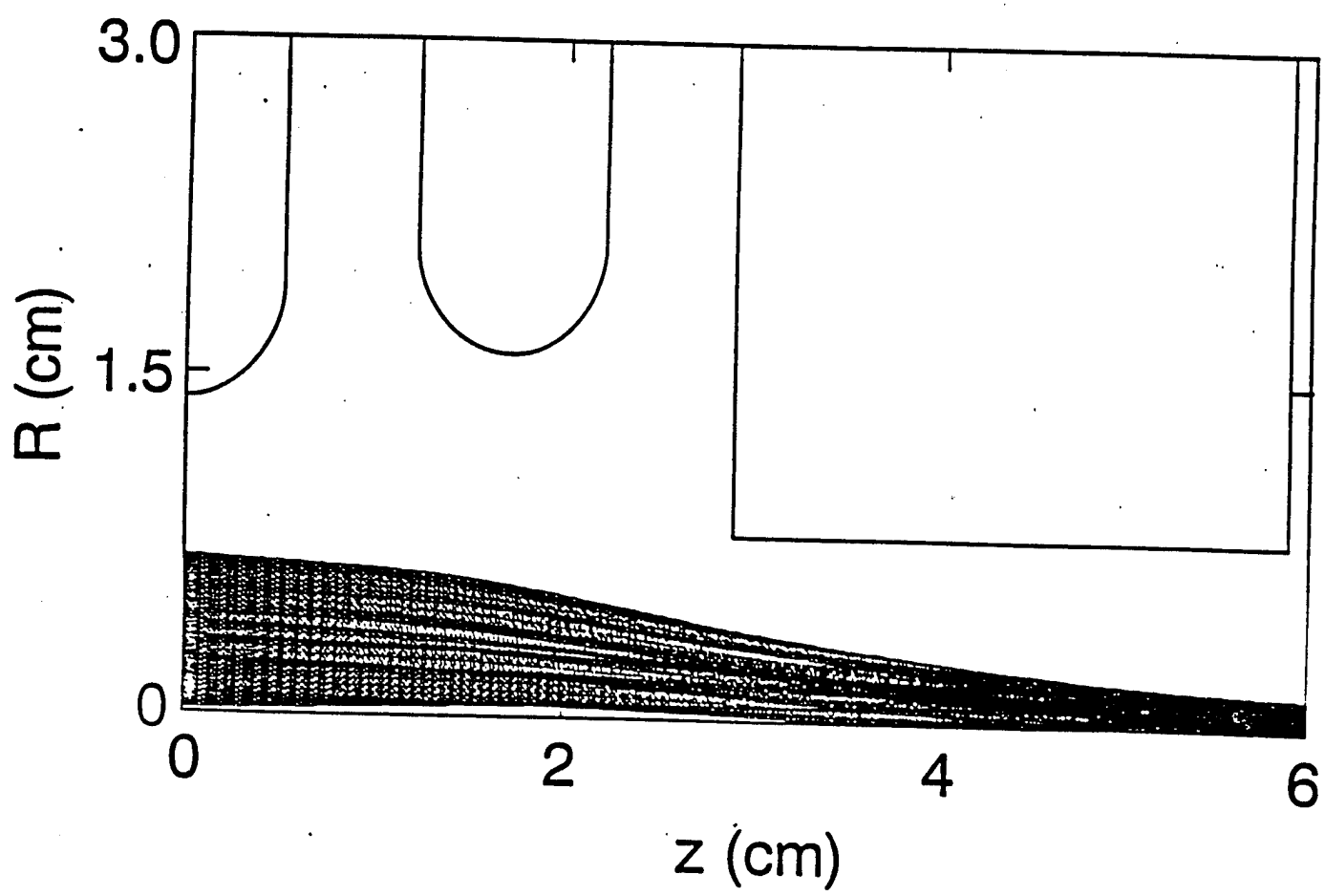


Fig. 11

# Efficient low-energy beam transport for intense, high-brightness H<sup>-</sup> beams in high energy accelerators: Perspectives and a solution using ESQ lenses<sup>a)</sup>

S. K. Guharay, C. K. Allen, and M. Reiser  
University of Maryland, College Park, Maryland 20742

K. Saadatmand and C. R. Chang  
Superconducting Super Collider Laboratory, Dallas, Texas 75712

(Received 4 September 1993; accepted for publication 4 October 1993)

The characteristics of a 30 mA, 35 kV H<sup>-</sup> beam from a volume source have been determined using emittance measurements. A low energy-beam transport (LEBT) system consisting of six electrostatic quadrupole lenses and a short (about 5 cm long) single-stage einzel lens is designed with the aim of transporting the beam over a distance of about 30 cm and focusing a clean, matched beam into a radio-frequency quadrupole accelerator of the Superconducting Super Collider. The system parameters are chosen on the basis of simulation of beam dynamics. The emittance growth in the LEBT section is within a factor of about 1.5 and this satisfies the requirement of the emittance budget. The LEBT system is designed to be mechanically rugged.

## I. INTRODUCTION

The study of intense, high-brightness H<sup>-</sup> beam transport has relevance to many modern applications, e.g., high-energy accelerators, space defense using intense neutral particle beams, ion-beam based microfabrication, etc. In this article, the system parameters and the study of the beam dynamics are focused on a specific example, namely, the Superconducting Super Collider (SSC). One of the important issues in the SSC accelerator chain is that the emittance budget is restricted; this imposes a major constraint on the ion source and the low-energy beam transport (LEBT) in the linac section. Usually the beam from the ion sources is highly diverging, and the LEBT has to transform this beam into a convergent one matching it into the very tight acceptance ellipse of the first stage of the linac, namely, a radio-frequency quadrupole (RFQ) accelerator. Typically, the rms normalized emittance of a 30 mA, 35 kV H<sup>-</sup> beam is in the range of 0.12–0.18  $\pi$  mm mrad, while the SSC RFQ requires the beam emittance at its input to be  $\leq 0.2 \pi$  mm mrad. These parameters along with experimental constraints due to the various mechanical structures often introduce some complexity in designing an efficient LEBT system. In order to achieve a satisfactory solution of this problem, the state of the art of the LEBT systems needs to be improved by means of careful simulation techniques and experimental validations of the simulation predictions.

Earlier we described the beam characteristics and beam dynamics through a LEBT for H<sup>-</sup> beams from a Penning–Dudnikov and a magnetron type source.<sup>1</sup> In recent years significant progress has been made in the performance of volume sources;<sup>2</sup> normalized beam brightness approaches about  $10^{11} \text{ A}/(\text{m rad})^2$ . This article reports the results of our study on the H<sup>-</sup> beam from the SSCL volume source. The experimental data corresponding to a 30 mA, 35 kV H<sup>-</sup> beam are

used to design a LEBT and deliver a matched beam into the SSC RFQ. The analysis of the beam dynamics through the LEBT is based on simulations wherein many important practical considerations are included. The LEBT system consists of six ESQ lenses and a short module of a single einzel lens. This design offers some flexibility to efficiently handle the input beam parameters and match the beam into the RFQ without any significant emittance dilution. The entire LEBT system is very compact and mechanically rugged.

Section II deals with the beam characterization, simulation of the beam through the LEBT, and the essential characteristics of the apparatus. Discussions and conclusions are included in Sec. III.

## II. BEAM DYNAMICS AND THE LEBT APPARATUS

### A. H<sup>-</sup> beam from the SSCL volume source

A 30 mA, 35 kV H<sup>-</sup> beam has been extracted from the SSCL volume source through an aperture of radius 4 mm in the test stand facility of the SSCL linac injector. The H<sup>-</sup> beam is measured at 10.13 cm downstream using an emittance diagnostic device; the electrons are deflected away from the extracted beam current by a 10-cm-long magnetic trap (initial electron-to-ion current ratio at the extractor  $\sim 40$ ). The contour plots showing the phase-space distribution of the beam are given in Fig. 1. A relative flattening of the distribution in the upper half is possibly caused by the space-charge force due to the electrons deflected upward. The beam parameters at  $z = 10.13$  cm are: beam size  $D = 2.38$  cm, full divergence  $\Delta\theta = 260$  mrad; normalized rms emittance  $\pi\bar{\epsilon}_n = 0.1537 \pi$  mm mrad. (Note that the beam divergence in this article is always quoted at the maximum envelope excursion unless otherwise specified.) These data are used in an envelope simulation code that solves the well-known Kapchinskij–Vladimirskij (KV) envelope equations, and the beam characteristics at the extraction electrode are estimated. The space-charge effect due to the electron swarm in the initial 10-cm-long magnetic trap is modeled assuming

<sup>a)</sup>The abstract for this paper appears in the Proceedings of the 5th International Conference on Ion Sources in Part II, Rev. Sci. Instrum. 65, 1427 (1994).

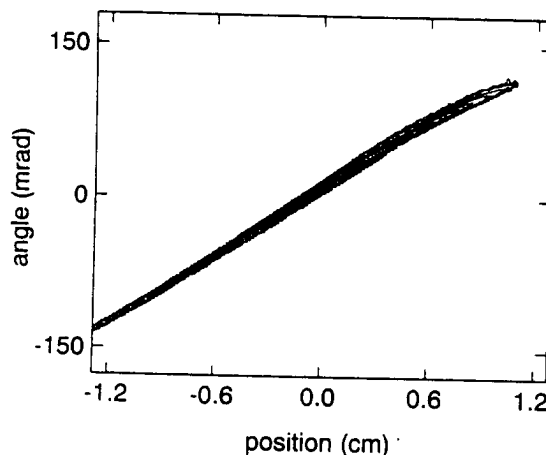


FIG. 1. Contour plot of the beam distribution at  $z = 10.13$  cm.

an exponential fall-off of the electron population downstream from the extraction electrode. This analysis suggests that a beamwaist is formed near the extraction electrode when the beam size is close to the aperture of the extractor; the beam blows up downstream afterwards.

### B. Beam dynamics and the design of a LEBT

The design of the LEBT is mainly dictated by the beam parameters at two locations: first, at the end of the electron suppression system and second, at the tip of the RFQ vane; the LEBT is located between these two components. After detailed simulation studies it is concluded that the drift space at either of the above two ends of the LEBT should be maintained as short as possible to ensure a proper matching with the RFQ. In recent experiments on the SSC test stand a 5-cm-long electron suppressor is used.<sup>3</sup> Assuming the mode of operation of the ion source to be the same as what has been described in Sec. II A, the beam parameters at the end of the shorter (5-cm-long) electron suppressor are estimated: beam size  $D = 1.2$  cm and beam divergence  $\Delta\theta = 126$  mrad. Measured data at this location showed a somewhat higher value of both  $D$  and  $\Delta\theta$ ,<sup>3</sup> the ion source parameters were not optimized in this case.

The SSC RFQ acceptance for a 30 mA, 35 kV  $H^-$  beam is given by the Twiss parameters:  $\alpha = 1.26$ ,  $\beta = 1.86$  cm/rad,  $\pi\epsilon_n = 0.2 \pi$  mm mrad. Thus the matching condition dictates that the beam parameters at the tip of the RFQ vane should be beam radius = 1.3 mm and the corresponding slope of the beam envelope = -89 mrad. The match point is located at about 3 cm downstream from the front wall of the SSC RFQ; this poses a big challenge to match the full beam current (30 mA) into the RFQ acceptance ellipse.

With the above knowledge of the beam parameters at the input as well as at the output of the LEBT, the lens elements are set up—the key point is that the emittance growth in the LEBT should not exceed a factor of about 1.5. We have concluded from the numerous simulation studies of the beam dynamics that a combination of a set of six ESQ lenses and a single-stage short einzel lens module at the end will create a very flexible environment to deliver a satisfactory solution. The ESQ lenses gradually transform the divergent beam

TABLE I. ESQ lens parameters. The spacing corresponds to the gap between the lens electrode and its neighboring ground plate. The voltage on a lens is of opposite polarity with respect to its immediate neighboring ones.

Lens No.	Aperture radius (mm)	Electrode radius (mm)	Length (mm)	Spacing (mm)	Voltage (kV)
1 & 6	15.0	17.2	25.0	2.0	5.0
2 & 5	22.0	25.2	59.0	2.0	7.8
3 & 4	22.0	25.2	47.0	2.0	9.8

from the source into a moderately convergent one creating almost a mirror image of the input beam. The einzel lens can then efficiently handle this beam to match it into the RFQ. In order to satisfy the initial emittance requirement, the beam envelope through the ESQ lenses is kept within about 75% of the quadrupole aperture, and it is maintained within about 50% of the aperture of the einzel lens.

The design of the ESQ lenses follows a simulation tree threading three codes; details about the code have been reported elsewhere.<sup>4</sup> First, a linear beam optics code solves the KV envelope equations for a given set of input beam parameters; the external focusing force due to the quadrupoles is assumed to be of hard-edge type. Second, a 3D LAPLACE solver is used to map the field of the ESQ lens system. Finally, the results from these two steps are used in the modified PARMILA,<sup>5</sup> a particle simulation code, to evaluate the distribution of the beam particles through the ESQ LEBT. A loop through the three codes is manually generated to optimize the lens parameters.

The essential parameters of the ESQ lens system are given in Table I. Figure 2 shows the KV envelope solution. Note that the output beam is almost of the same size as the input beam, while the slope is of opposite sign. The lens geometry is then included in the 3D LAPLACE solver to evaluate the fringe fields. The evolution of the phase-space distribution of the beam particles, as they propagate through the ESQ LEBT, is evaluated by the modified PARMILA code. This is a  $2\frac{1}{2}$ D code where 3D external field and 2D space-charge (each charge element is considered as a ring) field have been used. Figure 3 shows the beam distribution at the input and output of the ESQ LEBT; the input beam (30 mA) is represented by a group of 5000 macroparticles with a KV type distribution. The distortions in the output beam are very modest, and the emittance growth is about a factor of 1.5. The estimated output beam parameters at a distance of 7 mm downstream from the end of the sixth lens are: beam excursions in the  $x$  and  $y$  directions are  $X = 7.2$  mm and  $Y = 7.3$  mm, respectively; the corresponding slopes are  $X' = -51$  mrad and  $Y' = -51$  mrad. The emittance growth

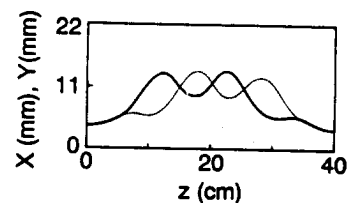


FIG. 2. Beam envelopes in  $x$  and  $y$  directions through the ESQ LEBT assuming a hard-edge focusing function.

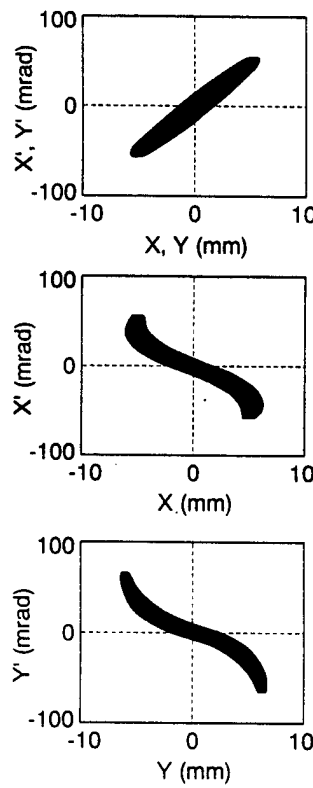


FIG. 3. Particle distribution in phase space: at the input of the ESQ LEBT (top); at 7 mm downstream from the sixth lens of the ESQ LEBT (middle and bottom).

is reduced to a factor of about 1.2, if the energy of all the particles across any cross section of the beam through the LEBT is held constant numerically; this shows that a significant fraction of beam distortions is due to the chromatic aberration.

The beam from the ESQ LEBT is coupled to an einzel lens for final focusing. The einzel lens is designed using the SNOW-2D code.<sup>6</sup> The particle trajectory through the einzel lens is shown in Fig. 4; the lens parameters are given in Table II. The Twiss parameters describing the effective ellipse from the output beam from the ESQ LEBT (Fig. 3, middle and bottom) are used to generate the input beam parameters for the einzel lens. The beam distributions at the input (center of the first grounded electrode) and the output (approximate location of the tip of the RFQ vane) are shown

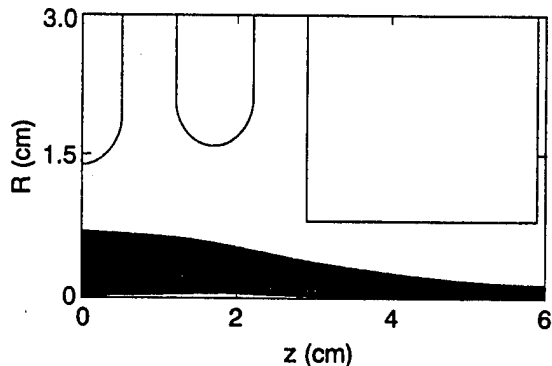


FIG. 4. Particle trajectory through the einzel lens section.

TABLE II. Einzel lens parameters.

Aperture radius of the center electrode (mm)	Thickness of the center electrode (mm)	Spacing <sup>a</sup> (mm)	Voltage (kV)
17.0	10.0	7.0	-26.0

<sup>a</sup>The spacing corresponds to the gap between the center electrode and the neighboring ground electrodes.

in Fig. 5. The matching of the beam appears to be quite good; the einzel lens does not yield any noticeable distortions of the beam.

### III. DISCUSSIONS AND CONCLUSIONS

This article addresses some keypoints to develop an efficient LEBT system using detailed simulation of the beam dynamics when many practical features have been considered in the light of a planned experiment at the SSCL injector test stand. Emittance measurements of a 30 mA, 35 kV H<sup>-</sup> beam from the SSCL volume source have been studied to characterize the beam from the source and thus reliably set up the input parameters in the design. The system parameters have been chosen so that the external focusing force acts on the beam envelope almost adiabatically and the phase of the envelope changes very smoothly; this procedure allows to control the emittance growth. By cascading two types of focusing elements, an ESQ section and a short einzel lens, we have been able to obtain a satisfactory solution of the particular problem. The emittance growth in the entire LEBT system for 30 mA, 35 kV beam is kept within a factor of about 1.5. In order to avoid too many control parameters in the experiment, the ESQ LEBT section is so designed that the electrodes of the six lenses are stacked one above the other and the entire system is self-aligned mechanically. This requires a very high level of precision in the fabrication of each component as well as in assembling them together. A prototype ESQ LEBT has been made and its mechanical characteristics have been described earlier;<sup>1</sup> the same principle is being followed in developing the LEBT system described in this article.

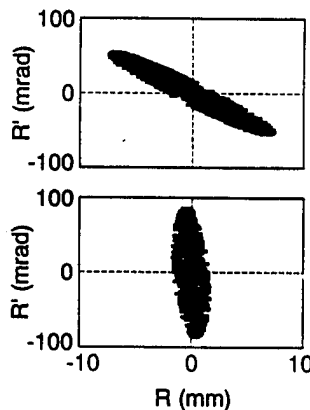


FIG. 5. Particle distribution at the input (top) and output (bottom) of the einzel lens.

## ACKNOWLEDGMENTS

This work is supported by the Office of Naval Research and the U.S. Department of Energy.

<sup>1</sup>S. K. Guharay, C. K. Allen, and M. Reiser, in *Proceedings of High-Brightness Beams for Advanced Accelerator Applications*, edited by W. W. Destler and S. K. Guharay (American Institute of Physics, New York, 1992), AIP Conf. Proc. No. 253, p. 67; S. K. Guharay, C. K. Allen, M. Reiser, K. Saadatmand, and C. R. Chang, Proceedings of the Sixth International Symposium on the Production and Neutralization of Negative Ions and Beams, Brookhaven National Lab., Nov. 9-13, 1992 (to be published in the AIP Conf. Proc. No. 287).

<sup>2</sup>K. N. Leung, Proceedings of the Sixth International Symposium on the Production and Neutralization of Negative Ions and Beams, Brookhaven National Lab., Nov. 9-13, 1992 (to be published in the AIP Conf. Proc.

No. 287); J. G. Alessi, D. McCafferty, and K. Prelec, *ibid.*

<sup>3</sup>J. Lenz, K. Saadatmand, D. Raparia, J. Hebert, and N. Okay, Proceedings 1993 Particle Accelerator Conf., Washington, D.C., May 17-20, 1993 (to be published).

<sup>4</sup>S. K. Guharay, C. K. Allen, and M. Reiser, *Proceedings on Intense Microwave and Particle Beams II*, Los Angeles, January 1991 (Society of Photo-Optical Instrumentation Engineers, Washington), Vol. 1407, p. 610, and references therein.

<sup>5</sup>G. P. Boicourt, Proceedings Linear Accelerator and Beam Optics Codes, edited by C. R. Eminhizer (American Institute of Physics, New York, 1988), AIP Conf. Proc. No. 177, p. 1; C. R. Chang, E. Horowitz, and M. Reiser, *Proceedings on Intense Microwave and Particle Beams*, Los Angeles, January 1990 (Society of Photo-Optical Instrumentation Engineers, Washington), Vol. 1226, p. 483.

<sup>6</sup>J. E. Boers, Sandia National Lab. Report No. SAND 79-1027, 1980.

10<sup>th</sup>  
International  
Conference  
on High Power  
Particle Beams

BEAMS '94

June 20-24, 1994  
San Diego, CA

# OPTIMAL CONTROL OF LOW ENERGY PARTICLE BEAMS\*

Christopher K. Allen, Samar K. Guharay, and Martin Reiser  
Institute for Plasma Research  
University of Maryland  
College Park, MD 20742

## Abstract

*The transport and matching problem for a low energy particle beam is addressed from a control theoretical viewpoint. We model the particle beam using the KV envelope equations. With this model we formulate the optimal control problem. Dynamic programming is used to solve this problem. Focusing functions are computed which satisfy the matching conditions and optimize selected design criteria. Examples and their solutions are presented.*

## 1.0 INTRODUCTION

The design of particle beam transport and matching systems has typically been accomplished in much the same way as an experiment is run<sup>1</sup>. A computer program is used to simulate the behavior of the beam in a given transport system. The knobs of this simulated system are then adjusted until a satisfactory solution is obtained. This can be a lengthy and arduous process. The progress of such a procedure relies completely upon the experience, judgement, and intuition of the designer.

It is the goal of this work to utilize the principles of optimal control theory in the design of beam transport and matching systems. We present an automated technique which determines the optimal lens strengths to match the beam envelope to a prescribed final state. In this paper, we consider an axisymmetric Low Energy Beam Transport (LEBT) section where space charge plays a dominant role.

## 2.0 THE MATHEMATICAL MODEL

We model the particle beam using the KV envelope equations. Consider the one dimensional (axisymmetric) case. The beam is centered on axis, with envelope radius given by  $R=R(z)$ ,  $z$  being the axial distance. This system may be described by the single differential equation<sup>2</sup>

$$R'' + \kappa(z)R - \frac{K}{R} - \frac{\epsilon^2}{R^3} = 0, \quad (1)$$

where the prime indicates differentiation with respect to  $z$ ,  $\kappa(z)$  is the focusing (control) function,  $K$  is the generalized beam permeance, and  $\epsilon$  is the effective emittance of the beam. In the case of a transport and matching system we are also given initial conditions at  $z=z_i$  and desired final conditions at  $z=z_f$ ,  $z_i$  and  $z_f$  being the entrance and exit locations of the LEBT, respectively. Thus, we have

$$\begin{aligned} R(z_i) &= R_i, & R(z_f) &= R_f, \\ R'(z_i) &= R'_i, & R'(z_f) &= R'_f, \end{aligned} \quad (2)$$

---

\*Supported by ONR

would be chosen by the designer). If  $R(z)$  is the actual solution to a given set of controls  $\{\kappa_n\}$ , then a plausible merit functional  $J$  for the solution trajectory  $R(z)$  is given by

$$J \equiv \int_{z_i}^{z_f} [R(z) - \bar{R}(z)]^2 dz. \quad (8)$$

Since we are concerned with a discrete system, we subsection the interval of integration to yeild a merit functional  $J_n$  for each stage,

$$J_n \equiv \int_{z_n}^{z_{n+1}} [R(z) - \bar{R}(z)]^2 dz. \quad (9)$$

Note that the state trajectory  $x(z)$  for  $z \in [z_n, z_{n+1}]$  is completely determined by  $\kappa_n$  and  $x_n$  according Eq. (6). Thus,  $J_n = J_n(x_n, \kappa_n)$  and Eq. (8) has the form

$$J = \sum_{n=0}^{N-1} J_n(x_n, \kappa_n). \quad (10)$$

We may now state the formal optimal control problem as follows: *find the sequence of controls  $\{\kappa_n\}$  which steers the system state from  $x_i$  to  $x_f$  according to the dynamics of Eq. (5) and which minimizes the merit functional of Eq. (10).*

#### 4.0 DYNAMIC PROGRAMMING

With some modification, our control problem is a suitable candidate for dynamic programming. Instead of imposing the boundary condition of Eq. (7) as a hard constraint, we create a cost functional  $\phi(x_N)$  for the final state. For example,

$$\phi(x_N) \equiv c_1(R_N - R_f)^2 + c_2(R'_N - R'_f)^2 \quad (11)$$

where  $c_1$  and  $c_2$  are real numbers to be used as tuning parameters. Now we add this functional to our merit functional of the previous section to obtain

$$J = \sum_{n=0}^{N-1} J_n(x_n, \kappa_n) + \phi(x_N) \quad (12)$$

The principle behind dynamic programming is to embed our optimal control problem in a family of problems with variable initial states  $x$  and initial times  $k$ . As such, we define the value function  $V(k, x)$  as follows:

$$V(k, x) \equiv \begin{cases} \sum_{n=k}^{N-1} J_n(x_n, \kappa_n) + \phi(x_N), & k \in \{0, \dots, N-1\} \\ \phi(x) & k=N \end{cases}$$

$$\begin{aligned} x_k &= x, \\ x_{n+1} &= f_n(x_n, \kappa_n) \quad n=k, k+1, \dots, N-1. \end{aligned} \quad (13)$$

That is,  $V(k, x)$  is the value of the merit functional starting from the initial time  $k \in \{0, \dots, N-1\}$  and with initial state  $x$ .

Dynamic programming relies upon the following fact for discrete systems<sup>5</sup>:

$$\begin{aligned} V(k, x) &= \min_{\kappa \in \Omega_k} \{J_k(x, \kappa) + V(k+1, f_k(x, \kappa))\} \\ V(N, x) &= \phi(x) \end{aligned} \quad (14)$$

where  $k \in \{0, \dots, N-1\}$  and  $\Omega_k$  is some constraint set for the control  $\kappa_k$ . We may recursively solve Eq. (14) backwards, the minimization procedure yielding the optimal control at each stage  $k$ . Since we do not know the optimal trajectory *a priori*, we must solve Eq. (14) for every feasible state  $x_n$  at each stage  $n=0, \dots, N-1$ . Consequently, the procedure is very CPU demanding.

#### 5.0 EXAMPLES

**Example 1:** Consider the transport section depicted in Figure 1. Let  $L_n = 2.5\text{cm}$  and  $l_n = 2.5\text{cm}$  for each  $n$ . The initial drift space also has length 2.5cm. Let the beam have generalized perveance  $K=0.01$  and effective emittance  $\epsilon=10^{-4}\text{m-rad}$ . The initial

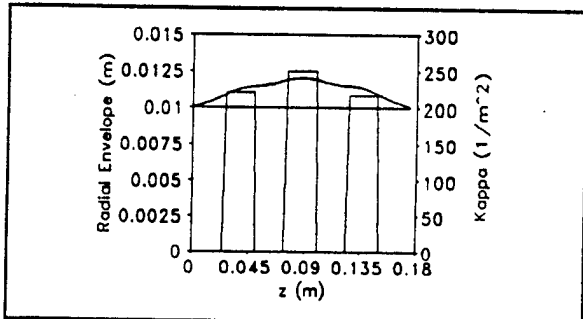


Figure 2: Example 1

envelope conditions are  $R_i=1\text{cm}$  and  $R_i'=20\text{mrad}$ . The desired final conditions are  $R_f=1\text{cm}$  and  $R_f'=20\text{mrad}$ . We use for the reference trajectory  $\bar{R}(z)=1\text{cm}$ . The optimal control sequence for this example is computed to be  $\{220, 250, 216\}$  in units of  $1/\text{m}^2$ . Fig. 2

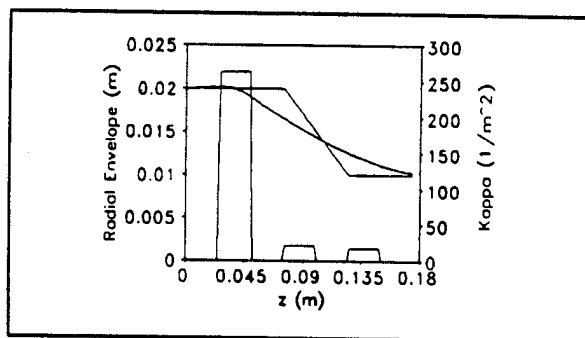


Figure 3: Example 2

plots the corresponding  $\kappa(z)$  for this set along with the resulting trajectory  $R(z)$  and reference trajectory  $\bar{R}(z)$ .

**Example 2:** In this example we keep the same geometry and beam parameters but change the initial conditions and the reference trajectory. Let  $R_i=2\text{cm}$  and  $R_i'=0\text{mrad}$ . Let the reference trajectory be the series of straight lines shown in Fig. 3. The control sequence is computed to be  $\{263, 20.5, 16.8\}$  (again in units of  $1/\text{m}^2$ ), and the corresponding solution data are depicted in Fig. 3.

## 6.0 CONCLUSION AND FUTURE WORK

The technique outlined here works well for the one-dimensional transport and matching problem. It is a fairly robust method which yields global results; however, it requires intensive computation. Our implementation was performed on an i486 CPU and ran about 15 minutes for each case. The result of this computation is essentially a map of the optimal control  $\kappa_n$  over the feasible state space. Thus, it is unnecessary to recompute the optimal controls for a change in initial conditions as long as the initial state and subsequent states lie in the feasible region.

Our current research is concerned with the transport and matching problem using quadrupole lenses. As such we use the two-dimensional coupled envelope equations as mathematical model. Due to the added dimensionality and the more complex action of the quadrupole lenses, the computational demand of dynamic programming may become prohibitively large. Thus, we will most likely need to develop an alternative procedure. We are currently considering a variation of parameters approach (continuation methods) from a linearized envelope equation.

The authors wish to thank Gilmer Blankenship for useful discussions.

## 7.0 REFERENCES

- [1] S. K. Guharay, C. K. Allen, and M. Reiser, Nucl. Instr. and Meth. in Phys. Res., A 339 (1994), pp. 429-438.
- [2] M. Reiser, *Theory and Design of Charged Particle Beams* (Wiley, 1994), Chapt. 4.
- [3] M. Vidyasagar, "Nonlinear System Analysis", (Prentice-Hall, 1978), Chapt. 1.
- [4] W. H. Press, B. P. Flannery, S. A. Teukolsky, W. T. Vetterling, "Numerical Recipes in C", (Cambridge University Press, 1988) Chapt. 15
- [5] P. P. Varaiya, "Notes on Optimization" (Van Nostrand Reinhold, 1972), Chapt. 9.



OFFICE OF THE UNDER SECRETARY OF DEFENSE (ACQUISITION)  
DEFENSE TECHNICAL INFORMATION CENTER  
CAMERON STATION  
ALEXANDRIA, VIRGINIA 22304-6145

IN REPLY  
REFER TO

DTIC-OCC

SUBJECT: Distribution Statements on Technical Documents

TO: OFFICE OF NAVAL RESEARCH  
CORPORATE PROGRAMS DIVISION  
ONR 353  
800 NORTH QUINCY STREET  
ARLINGTON, VA 22217-5660

1995 1027 001

1. Reference: DoD Directive 5230.24, Distribution Statements on Technical Documents, 18 Mar 87.
2. The Defense Technical Information Center received the enclosed report (referenced below) which is not marked in accordance with the above reference.

FINAL REPORT  
N00014-90-J1913  
TITLE: STUDY OF BRIGHTNESS AND  
CURRENT LIMITATIONS IN INTENSE  
CHARGED PARTICLE BEAMS

3. We request the appropriate distribution statement be assigned and the report returned to DTIC within 5 working days.
4. Approved distribution statements are listed on the reverse of this letter. If you have any questions regarding these statements, call DTIC's Cataloging Branch, (703) 274-6837.

FOR THE ADMINISTRATOR:

1 Encl

GOPALAKRISHNAN NAIR  
Chief, Cataloging Branch

FL-171  
Jul 93

DISTRIBUTION STATEMENT A:

APPROVED FOR PUBLIC RELEASE: DISTRIBUTION IS UNLIMITED

DISTRIBUTION STATEMENT B:

DISTRIBUTION AUTHORIZED TO U.S. GOVERNMENT AGENCIES ONLY;  
(Indicate Reason and Date Below). OTHER REQUESTS FOR THIS DOCUMENT SHALL BE REFERRED  
TO (Indicate Controlling DoD Office Below).

DISTRIBUTION STATEMENT C:

DISTRIBUTION AUTHORIZED TO U.S. GOVERNMENT AGENCIES AND THEIR CONTRACTORS;  
(Indicate Reason and Date Below). OTHER REQUESTS FOR THIS DOCUMENT SHALL BE REFERRED  
TO (Indicate Controlling DoD Office Below).

DISTRIBUTION STATEMENT D:

DISTRIBUTION AUTHORIZED TO DOD AND U.S. DOD CONTRACTORS ONLY; (Indicate Reason  
and Date Below). OTHER REQUESTS SHALL BE REFERRED TO (Indicate Controlling DoD Office Below).

DISTRIBUTION STATEMENT E:

DISTRIBUTION AUTHORIZED TO DOD COMPONENTS ONLY; (Indicate Reason and Date Below).  
OTHER REQUESTS SHALL BE REFERRED TO (Indicate Controlling DoD Office Below).

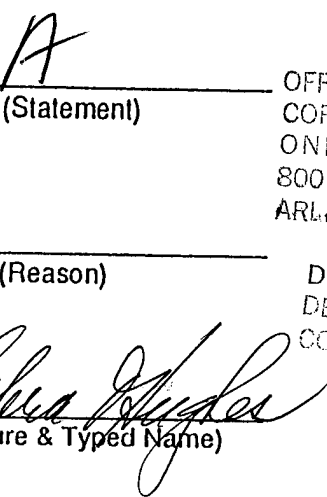
DISTRIBUTION STATEMENT F:

FURTHER DISSEMINATION ONLY AS DIRECTED BY (Indicate Controlling DoD Office and Date  
Below) or HIGHER DOD AUTHORITY.

DISTRIBUTION STATEMENT X:

DISTRIBUTION AUTHORIZED TO U.S. GOVERNMENT AGENCIES AND PRIVATE INDIVIDUALS  
OR ENTERPRISES ELIGIBLE TO OBTAIN EXPORT-CONTROLLED TECHNICAL DATA IN ACCORDANCE  
WITH DOD DIRECTIVE 5230.25, WITHHOLDING OF UNCLASSIFIED TECHNICAL DATA FROM PUBLIC  
DISCLOSURE, 6 Nov 1984 (Indicate date of determination). CONTROLLING DOD OFFICE IS (Indicate  
Controlling DoD Office).

The cited documents has been reviewed by competent authority and the following distribution statement is  
hereby authorized.

  
(Statement)

OFFICE OF NAVAL RESEARCH  
CORPORATE PROGRAMS DIVISION  
ONR 353  
800 NORTH QUINCY STREET  
ARLINGTON, VA 22217-5660

(Controlling DoD Office Name)

(Reason)

DEBRA T. HUGHES  
DEPUTY DIRECTOR  
CORPORATE PROGRAMS OFFICE

(Controlling DoD Office Address,  
City, State, Zip)

(Signature & Typed Name)

(Assigning Office)

10 SEP 1985

(Date Statement Assigned)